Scottish Government
Riaghaltas na h-Alba
gov.scot

Refining Estimates of Collision Risk for Harbour Seals and Tidal Turbines

Scottish Marine and Freshwater Science Vol 7 No 17

B Band, C Sparling, D Thompson, J Onoufriou, E San Martin and N West

marinescotland

© Crown copyright 2016

Refining Estimates of Collision Risk for Harbour Seals and Tidal Turbines

Scottish Marine and Freshwater Science Volume 7 Number 17

Bill Band, Carol Sparling, Dave Thompson, Joe Onoufriou,
Elena San Martin and Nigel West

Published by Marine Scotland Science

ISSN: 2043-7722

DOI: 10.7489/1786-1

Marine Scotland is the directorate of the Scottish Government responsible for the integrated management of Scotland's seas. Marine Scotland Science (formerly Fisheries Research Services) provides expert scientific and technical advice on marine and fisheries issues. *Scottish Marine and Freshwater Science* is a series of reports that publishes results of research and monitoring carried out by Marine Scotland Science. It also publishes the results of marine and freshwater scientific work that has been carried out under external commission. These reports are not subject to formal external peer-review.

This report publishes the results of research carried out under external commission. The work was funded through the Scottish Government's Contract Research Fund and by Scottish Natural Heritage.

© Crown copyright 2016

You may re-use this information (excluding logos and images) free of charge in any format or medium, under the terms of the Open Government Licence. To view this licence, visit: http://www.nationalarchives.gov.uk/doc/open-government-licence/version/3/ or email: psi@nationalarchives.gsi.gov.uk.

Where we have identified any third party copyright information you will need to obtain permission from the copyright holders concerned.

Contents

Tables

Figures

Refining Estimates of Collision Risk for Harbour Seals and Tidal Turbines

Bill Band[1], Carol Sparling[2], Dave Thompson[3], Joe Onoufriou[3], Elena San Martin[4] and Nigel West[4]

[1] Independent Environmental Consultant
[2] SMRU Consulting, New Technology Centre, University of St Andrews, North Haugh, St Andrews, Fife, KY16 9SR
[3] Sea Mammal Research Unit, Scottish Oceans Institute, University of St Andrews, St Andrews, Fife, KY16 8LB
[4] ABP Marine Environmental Research Ltd, Quayside Suite, Medina Chambers, Town Quay, Southampton, SO14 2AQ

1 Executive Summary

1.1 Introduction

There is currently considerable uncertainty regarding the potential for lethal and injurious interactions between marine mammals and tidal turbines. This uncertainty is particularly concerning for harbour seals in the Orkney and North Coast management unit, where the population has been undergoing a protracted decline. This has led to constraints being placed on tidal developments in this area until more information is available on the real risks presented to this species by tidal turbines.

The aim of this research project was to provide improved assessments of the level of mortality to harbour seals potentially caused by tidal turbines in the Pentland Firth and Orkney Waters region, using recently available information from a number of areas of work. These include the consequences of collision for individuals, detailed information on tidal flow, updated tidal turbine parameters and data on temporal and spatial variation of harbour seals within the water column. Specifically, this project was developed to review the assessment process to determine areas where inputs could be refined to improve estimates in the short term; and to use the outputs of these reviews to generate an updated model that is fit for use to estimate the no-avoidance collision rates between seals and tidal turbines. Finally, this updated model was applied to an agreed envelope of consented tidal energy projects in the Orkney and Pentland Firth region. This envelope consisted of two projects: the MeyGen Phase 1a array of four turbines at the Inner Sound in the Pentland Firth, and the multiberth European Marine Energy Centre (EMEC) tidal test site at the Fall of Warness, Orkney.

In this report the word ‘collision’ is used to refer to the situation in which a transit through the swept area of a turbine would be predicted to result in physical contact between the marine mammal and the turbine blade. Unless otherwise specified, this refers to ‘no-avoidance’ collision, assuming no avoidance or evasive action is taken by the animal. This is the same as the definition of the term ‘encounter’ in Wilson *et al*. (2007), however here the word collision is chosen rather than encounter (unless specifically referring to the Wilson *et al*., 2007 model) because ‘encounter’ could be interpreted as an animal coming close to the device but without actual contact whereas ‘collision’ better reflects the potential for actual physical contact between the device and the animal that is the aim of the prediction. Where the text refers to ‘collision risk’, this is the probability of collision for an animal when making a single transit through the swept area of a turbine. Once account is taken of the likely number of such transits, ‘collision rate’ is the overall number of collisions estimated within a given period (usually one year).

1.2 Model and Data Review

A review of collision risk models revealed a number of key areas where current models could be refined. The model selected for refinement was the modified Band collision risk model (Band, 2000; 2012a; Scottish Natural Heritage, 2016). The avenues identified for refinement of the model were grouped into a number of areas: 1) consideration of site specific detailed information on seal movement and behaviour, 2) the consequences of collision, i.e. relaxing the assumption that every collision would end in death for the animal, 3) evasion and avoidance behaviour in response to the turbine itself, 4) properties of individual turbines, and 5) uncertainty in input parameters. The review revealed that sufficient data were available to inform an assessment of refinements of the model for Areas 1), 2) and 4). For 5) it was concluded that, although uncertainty in some input parameters (e.g. animal density) would be relatively straight forward, explicit incorporation of all sources of uncertainty into estimates of collision and mortality rates would require more resource than was available for this project. There are currently very little empirical data to inform refinements based on 3) evasion and avoidance so all calculations presented in this report assume no avoidance or evasion, with the exception of the comparison in Table 24 in Section 10 where a range of avoidance rates are adopted to provide a comparison to previous estimates.

1.3 Examination of Site Specific Telemetry Data

To inform refinements based on site specific seal behaviour, a detailed exploration of seal telemetry data was carried out. This focused on telemetry data from the two tidal sites, MeyGen and EMEC. The most striking result from this was the observation that seals at both sites generally swam against the tide. On most dives, the seal's movement over the ground (transit) was slow, despite the often fast moving currents at those sites. These transit speeds have a direct bearing on the likelihood of being hit by a turbine blade if a seal passes through the swept area; where slow transit speeds will increase that probability. Conversely, slow transit speeds will also reduce the number of times seals will be assessed to pass through the swept areas. Interestingly, the transit speeds do not appear to be related to current speeds, nor was there any pattern in the temporal distribution of transits in relation to the current speeds – transits were distributed across all current speeds.

The distributions of swimming activity at different depths in the water column were estimated from high resolution dive depth profiles (nine depth points per dive) transmitted for each dive by the tags. These data suggest that seals spend a large proportion of each dive at the bottom of the dive, producing mostly flat bottomed, U shaped dive profiles. These patterns do not differ between flood and ebb tides and do not appear to vary with current speed. The dive depth distribution, derived from the tags, has been used to produce depth usage profiles for seals swimming in different water depths, which can be adopted in collision assessments for other sites.

1.4 Consequences of Collision

Refinement based on the consequences of collision drew on recent work carried out at the Sea Mammal Research Unit. Thompson *et al.* (2015a) assessed the damage imposed on grey seal carcasses through turbine impacts. In this investigation, adult and juvenile carcasses were subjected to collisions at various points along their bodies and at various speeds. Due to limitations in experimental design, maximum turbine speeds could not be tested and so the most severe impact conducted was at 6 m/s. No skeletal damage was observed in any of the collisions. Soft tissue results were deemed unreliable since the carcasses had been previously frozen. The freeze-thaw effects would be expected to make these organs more prone to damage, however no tears or rupture to internal organs were detected. These results suggest that over half of expected collisions, irrespective of blade dimension, would occur at blade speeds that would not be lethal. This investigation concluded that a mortality rate estimator could be included in the Collision Risk Model (CRM), such that it accounts for the likelihood of death should a collision occur. The model

function could be as simple as assuming that any closing speed greater than an empirically determined speed would be fatal, thus drawing on results of investigations such as those detailed above. Additionally a metric could be applied to the mortality function to assess the likelihood of a fatal interaction given the point of the blade which struck the animal. The formula for the risk of collision during a single transit discriminates between terms deriving from either the leading edge or the remainder of the blade striking the animal.

1.5 Model Refinements

A detailed examination of the consequences of the various proposed refinements building on the CRM in its 'basic' version, as applied to underwater turbines and marine wildlife, is described in 'Assessing collision risks between underwater turbines and marine wildlife: Guidance on using three models' (Scottish Natural Heritage, 2016). A spreadsheet distributed with that guidance facilitates the calculations required. For the purpose of exploring refinements, models were run for a single rotor, three blades, 2 m max chord width, standard profile, tip pitch 5º (degrees), rotation speed 12 rpm, minimum depth below surface 8 m; animal length 1.6 m, 0.38 m width, speed relative to rotor 1.64 m/s, body ratio 0.5.

A total of 12 individual refinements were tested. Each of the refinements adds an increment to the complexity of the CRM calculation. While some may add to the apparent accuracy of the calculation, it must be borne in mind that none of this takes into account the animals' behavioural response over which there is currently a wide margin of uncertainty. Also, collision rates scale with the density of animals, and at present there is major uncertainty over the density of harbour seals at key project sites.

The refinements which have the potential to make the most significant difference to the CRM collision and mortality estimates, in terms of the percentage change in mortality estimate resulting from the refinement, are judged to be as follows (in descending order of significance):

- Refinement 12: Density;
- Refinement 5: Mortality;
- Refinements 10 and 11: Transit speed;
- Refinement 1: Making use of a depth distribution; and
- Refinement 4: Blade thickness.

Inclusion of these refinements in the calculation of collision and mortality risk has led to four successively refined methods of calculation, described as 'CRM Basic', 'CRM Extended', 'CRM Plus' and 'CRM Plus Plus'. See Table 1 below for a summary of the progressively refined CRM methods and a summary of their differences. There was a clear trend of reduced estimates of collision risk from use of the progressively refined methods.

Table 1 Summary of the progressively refined collision risk model methods and a summary of their differences

Model	Factors Which Successive Models Treat in A More Refined Way		
	Depth Distribution	**Rotational Speed**	**Ground Speed**
CRM Basic See Section 7.1	Assumes uniform depth distribution	Risk based on single mean rotational speed	Uses fixed ground speed or resultant ground speed
CRM Extended See Refinement 1	Uses generic observed depth distribution	Risk based on single mean rotational speed	Uses fixed ground speed or resultant ground speed
CRM Plus See Refinements 8 and 9	Uses generic observed depth distribution	Risk calculated at each current/rotation speed and summed over current speed frequency distribution	Uses fixed ground speed or resultant ground speed
CRM Plus Plus See Refinement 11	Uses generic observed depth distribution	Risk calculated at each current/rotation speed and summed over current speed frequency distribution	Risk summed over observed ground speed frequency distribution
	All four models make use of blade profile and blade pitch information if provided (or use a default profile if not provided), and include a correction to allow for blade thickness (see Refinements 2 and 4).		
	All four models can estimate mortality rate as well as collision rate, based on an assumption that only collisions with a blade leading edge, above a given threshold impact speed, will lead to fatality.		
	As to animal transit speed, the first three models may be calculated for a fixed ground speed or a speed which is the resultant of swim speed and current speed (see Refinement 10). The fourth model requires a known distribution of ground speeds, obtained from studies of animal movement (see Refinement 11).		

1.6 Updated Collision Risk Model Assessment of Consented Energy Projects

The next step in the project was to apply the refined model to the current envelope of consented developments in the Orkney and North Coast seal management unit, Orkney and Pentland Firth region, MeyGen Phase 1a and EMEC Fall of Warness test site. The choice of density estimate used in the CRM clearly has a very important effect on the resulting estimates. The range of existing density estimates are described in Appendix 1.

For the purposes of this report, a single measure of seal density was adopted. This density measure was taken from the seal usage maps generated by SMRU and published in Jones *et al.* (2015), which incorporates seal telemetry data and recent population counts to scale up the behaviour of tagged animals to estimate population level usage and associated uncertainty. This density was chosen as it is the only measure for which methods were consistent and comparable across both sites. This CRM assessment assumed a threshold collision speed for mortality of 5 m/s.

For the MeyGen Phase 1a array of four turbines, based on a mean seal density of 0.4 seals/km² (95 % confidence intervals 0.17-0.64), and using the distribution of ground speeds from telemetry data, a no avoidance collision rate of 93 (40-149) per year, and a corresponding mortality rate of 69 (29-110) seals per year were calculated.

For the EMEC Fall of Warness test site, for the maximum scenario of 18 turbine rotors, based on a mean seal density of 0.6 seals/km² (95 % confidence intervals 0.12-1.00), and using the distribution of ground speeds from telemetry data, a no avoidance collision rate of 976 (201-1627) collisions per year, and a corresponding mortality rate of 689 (142-1149) seals per year were calculated.

It is important to note that the confidence intervals only represent uncertainty around the seal density estimate and do not incorporate uncertainty in other input parameters. It is equally important to note that these figures do not include any correction for avoidance or evasion.

1.7 Population Level Consequences

In order to provide context for the collision risk modelling exercise, a basic assessment of the potential population consequences of a range of mortality rates were carried out. Differences in predicted trajectories between a simulated

population with no collision-related mortality and populations experiencing a range of annual collision-related mortality were explored using a publicly available stochastic population modelling tool (a version of the interim Population Consequences of Disturbance (PCoD) framework (King *et al.,* 2015) modified to model the population consequences of collisions).

The interim PCoD framework provides, as outputs, the probability of a 1%, 2% and 5% decline in each of the un-impacted and impacted populations after each year of the simulation, and the additional risk presented as the difference between the two. Given the current status of the harbour seal population in the Orkney and North Coast management unit, both the impacted and un-impacted populations were predicted to decrease, although the difference in the probability of a 5% decline between impacted and un-impacted populations was modest for mortality rates up to 15 per year (1-3%), this increased to 9% for 150 mortalities per year. Above this level, the differential was constant or declining because the probability of a 5% decline for the impacted population reached 1 and could not increase further. Further adaptation of the iPCoD code would be required to explore this further.

1.8 Conclusions

This study has identified, tested and implemented a range of refinements to an existing Collision Risk Model (Scottish Natural Heritage, 2016).

The refinements included covered a range of areas, falling into four main categories:

- More detailed and device specific information from turbine manufacturers (shape of rotors and relationships between current and rotor speed);
- More detailed understanding of tidal currents;
- A better understanding of seal behaviour in tidal areas in relation to tide; and
- A developing understanding of the consequences of collisions between seals and rotors and the likelihood of mortality.

The parameters most influencing the magnitude of predicted collision rates are (in descending order):

- Seal density;
- Incorporation of a threshold speed for mortality;
- Incorporation of telemetry derived estimates of transit speed;
- Incorporation of telemetry derived depth distribution; and
- Incorporation of a blade thickness parameter.

This assessment has not included the application of avoidance/evasion rates, primarily because there is currently not enough empirical evidence on which to base the quantification of these. However, no-avoidance collision and mortality rates can be converted into estimates of the actual number of collisions and mortalities taking avoidance into account by expressing them assuming a range of potential avoidance rates.

The refined model presented here uses site specific and turbine specific data. It is therefore not likely to be generally applicable and will need to be revised for use in other locations and with different turbines.

2 Introduction

The Scottish Government has set a target for the equivalent of 100% of Scottish energy demand from renewable energy sources by 2020, by creating a balanced portfolio of both onshore and offshore technologies. Wave and tidal energy are emerging industries, with many technologies at an early development stage. The Scottish Government is actively working with key stakeholders, such as industry, local authorities and the Crown Estate, to harness the wave and tidal energy resource in a sustainable manner.

In 2010, the Scottish Government introduced the use of Potential Biological Removal (PBR) to determine the number of seals that could be removed under licence from regional management units without affecting the long term status of the population. For harbour seals in the Orkney and North Coast management unit, the PBR is small and is reducing, due to the protracted decline in this population. This has led to constraints being placed on tidal developments in this area until more information is available on the real risks presented to this species by tidal turbines. A key element of Environmental Impact Assessments (EIAs) for assessing collision risk is the production of a model to estimate the number of individuals of different species that might collide with the turbines. Early models assumed equal distribution of animals through the water column and at different times of tide, day and season, although recent modelling in support of project applications have incorporated depth distribution information. Initially, models generally assume no avoiding action is taken by animals. This is dealt with at a later stage where a judgement is made to determine an overall avoidance rate. Models have also assumed that all collisions are fatal, irrespective of the blade speed, which varies with tidal speed.

The aim of this research project was to provide more realistic assessments of the level of mortality resulting from collisions between harbour seals and tidal turbines in the Pentland Firth and Orkney Waters region, using recently available information from a number of areas of work. These include the consequences of collision for individuals, detailed information on tidal flow, updated tidal turbine parameters and data on temporal and spatial variation of harbour seals within the water column.

This work had the following specific objectives:

- Review the collision risk assessment process to determine areas where inputs could be refined to make estimates more realistic in the short term; and

- Use the outputs of these reviews to inform refinements to collision risk models and generate an updated model fit for use in estimating collision rates between seals and tidal turbines.

Apply this updated model to an agreed envelope of consented tidal energy projects in the Pentland Firth and Orkney Waters strategic area.

In this report the word ‘collision’ is used to refer to the situation in which a transit through the swept area of a turbine would be predicted to result in physical contact between the marine mammal and the turbine blade. Unless otherwise specified, this refers to ‘no-avoidance’ collision, assuming no avoidance or evasive action is taken by the animal. This is the same as the definition of the term ‘encounter’ in Wilson *et al*. (2007), however the word collision has been chosen rather than encounter (unless specifically referring to the Wilson *et al*., 2007 model) because ‘encounter’ could be interpreted as coming close to but without actual contact whereas ‘collision’ better reflects the potential for actual physical contact between the device and the animal that is the aim of the prediction. Where the text refers to ‘collision risk’, this is the probability of collision for an animal when making a single transit through the swept area of a turbine. Once account is taken of the likely number of such transits, ‘collision rate’ is the overall number of collisions estimated within a given period (usually, one year).

3 Review of Collision Risk Models and Datasets to Identify Parameters for Refinement

3.1 Background

This section provides a review of the currently available and commonly used models for predicting the risk of collision between tidal energy devices and marine animals. This review has primarily focused on the two existing blade strike models to estimate collisions between marine mammals and tidal turbines: 1) the Scottish Association for Marine Science (SAMS) Research Services Limited (SRSL) Encounter Rate Model (Wilson *et al*., 2007) which estimates the overall rate of collisions between animals and turbines using an adaptation to a predator-prey model by Gerritsen and Strickler (1977), and 2) the modified Band collision risk model (Band, 2000; 2012b; Scottish Natural Heritage, 2016) which estimates the risk posed to individual seals during each set of a discrete number of transits through a simulated device. In addition, the Exposure-Time Model developed by Grant *et al.* (2014) will be described. Other models currently available to assess the potential of impacts between anthropogenic devices and wildlife were considered (e.g. Baudin *et al*., 2013; Stantec, 2015; Parrot *et al.*, 2010) in the initial research process, but were not considered in this final review. This was predominantly due to their application for predicting the risk of co-occurrence of marine mammals and mobile threats (e.g. ship traffic) compared to collision risk models with the objective of predicting the probability of contact between the moving parts of a device in a fixed position. Furthermore, the models outlined below have all previously been adapted to specifically address the issue of potential impacts between tidal turbines and marine mammals.

3.2 Model Review

The following section discusses the principles of each approach. Assumptions and simplifications of each model are identified, including where they overlap, and an overview of case studies where they have been applied is outlined.

3.3 The SRSL Encounter Rate Model (Wilson *et al*., 2007)

This model has been used in assessments at several sites where renewable energy developers have a specific concern as to the interactions between their turbine arrays and marine mammals. Specifically this method has been utilised for examining the impact of the MeyGen development in the Pentland Firth, the details

of which can be found in Batty *et al.* (2012), Band (2012b) and Scottish Natural Heritage (2016).

The output of this model, the overall collision rate of a population, is generated as the product of three parameters:

- The local population density, D;
- The effective cross-sectional area A of approaching blades (the 'predator'), taking account of the effective radius of the animals ('the prey') if animals are to clear the blades; and
- The mean speed of the turbine blades relative to the animal, V.

The simple equation which is derived from the predator-prey model (Gerritsen and Strickler, 1977) is as follows:

$$C_{ERM} = D \times A \times V \quad (1)$$

This equation can be expanded to include all the computable terms as follows:

$$\mathrm{C_{ERM}} = \mathrm{D} \times \mathrm{Bb(w + 2r)(R + r)} \times \mathrm{v}\left(1 + \left({}^{\mathrm{u}^2}/_{3\mathrm{v}^2}\right)\right) \quad (2)$$

Where:

B = number of rotors;
b = number of blades;
w = width of a turbine blade;
R = turbine blade length;
r = 'effective radius' which is the clearance required (from the centre of mass) due to the body size of the animal;
v = blade speed relative to the water which combines tangential speed and current speed (the blade speed is assumed to be faster than the animal speed relative to the water current, in this case); and
u = animal's swim speed relative to the water.

The model acknowledges that a behavioural metric is also needed to take account of the probability that an animal will avoid a device or, if not avoided, evades its blades.

This equation carries many assumptions including independent movement of both the turbine and the animal, where animals will approach the turbine in random swim

directions, and that marine animals, notwithstanding their long and narrow shapes, can have an assumed equivalence to a sphere of a single effective radius. The first assumption is intuitively unlikely given the likely influence of water speed and state of tide on both the animal's speed and direction, that marine animals when at risk depth are most likely to be diving or surfacing, and on the speed and orientation of the operating turbine i.e. if an animal is drifting passively and upstream of an operating turbine the probability of a collision is still high.

The term describing density D also comprises simplifications and apparent errors which could be circumvented with more detailed modelling. D is estimated as a product of the proportion of animals within the operating depth of the turbine rotor (P) and twice the blade length (R_b), to account for approach at any point in the circumference of the blade sweep zone) divided by the mean water depth (H) across the array site:

$$D = \frac{P2R_b}{H} \quad (3)$$

Lonergan and Thompson (2015) comment that this equation appears incomplete as it omits the abundance of animals per square metre of water surface, N, and therefore should be modified as follows:

$$D = \frac{NP}{(2R_b)} \quad (4)$$

However this assumes that P means the proportion of animals within the range of blade swept depths and that the animals are distributed uniformly within this volume.

To arrive at an encounter rate, the operational time within a given period must finally be factored into the equation for C_{ERM}, as turbines are not always moving (such as during slack tides or scheduled maintenance).

3.3.1 Modified Band Collision Risk Model (Band 2000; Davies and Thompson, 2011 and Updates in Band, 2012a; Scottish Natural Heritage, 2016)

This model has been used to assess the collision risk to marine mammals at the proposed Scottish Power Renewables tidal project in the Sound of Islay and the EMEC test site at the Fall of Warness. It was developed as a modification to the CRM by Band (2000) which sought to estimate the number of birds expected to collide with onshore wind farms. Its output is the estimated risk of a marine mammal colliding with a turbine blade during a set of discrete transits through the 'danger

area'. This is estimated by calculating the product of the number of transits per year, assuming the animals are unaware of the turbine, the probability of collision during a transit, the proportion of time the turbine is operational and a correction factor to represent the animals' avoidance behaviour. The number of transits per year is reliant on information on the density of a species for the area encompassing the turbine(s).

The density of seals cannot be estimated by taking a snapshot observation at the surface as at any given time a proportion of the local population will be underwater. Band (2014) describes how to make allowance for animals underwater, having regard for the duration of watch of any area of the sea surface. The underwater collision model requires observed density to be divided by the proportion of time animals are visible at the surface to produce the estimate of true density per unit area of sea surface.

Three-dimensional (3-D) movement behaviour can be derived empirically from telemetry deployments and operational information is calculable using hydrodynamic models of the study area coupled with the turbine specifications and information provided by developers on scheduled maintenance and expected operational periods. The information on 3-D movement information is not always available for the sites under assessment however, and so inferences and generalisations across species and sites are often necessary. Consequently, these estimates would be less reliable than estimates based on site specific behaviour data due to the higher levels of uncertainty surrounding parameter estimates.

When considering benthic foragers such as seals, the transits through turbines are treated as directed and without serious deviations away from a straight line route. However, contrary to the original model, Davies and Thompson (2011) adapted the approach to model discrete transits as being a series of dives in which both the descent and ascent phases are potentially susceptible to collision. However, the collision risk estimate still assumes all motion as being parallel to the axis of the turbine. The model proceeds with this assumption by multiplying the estimated number of animals in the area of the device by twice the number of expected dives over a given-time period. Under the assumption that the animals are diving at a constant, vertical speed, the number of animals at risk depth (between the shallowest and deepest parts of the rotor) can be estimated. This enables the number of transits which pass through a turbine to be estimated. If empirical data existed to inform the transit rate through an area this could be substituted for this estimation step. This is then scaled by the parameters of speed of transit and length

of the animal and under the assumption that the animals are moving at a constant, vertical speed.

In the updated iteration of the model (Scottish Natural Heritage, 2016) it was recommended that empirically derived depth distributions are used to estimate the proportion of time seals are at risk depths. When looking at depth distributions of seals from the Pentland Firth, it was noted by Thompson (2015) that frequency histograms of time at depth indicated more activity in midwater than would be expected if seals swam directly to the sea bed on all dives, suggesting time at risk depths could be higher than previously assumed. This is only a factor for seals below the surface as all individuals at the surface are presumed to be out of risk depth as turbine minimum depth is assumed to be greater than one animal body length deep.

The number of transits through a turbine may then be multiplied by the mean probability of collision during transit, calculated from rotor and animal parameters. Collision risk estimates are calculated separately for a set of concentric circles emanating from the centre of the device. Each turbine blade is considered to be a twisted lamina surface with length equal to rotor radius R, a variable chord width c and a pitch relative to the rotor plane which may vary along blade length. The point of passage of the animal through the lamina is taken as the radius r from the axis and the angle φ measured from the vertical i.e. the deviation away from a transit directly above the rotor hub. One can then calculate collision probability for a transit at radius, r. This is a geometrical exercise, best done by viewing the animal in a frame which moves with the animal, while the blades move both across the animal's swim direction and – in this moving frame - towards the animal. A crucial parameter is the ratio of the speed of the animal to the blade speed, as the latter increases with distance from turbine hub. The result of this calculation is the collision probability p(r) at the radius of the point of transit: given the assumption that a marine animal is circularly symmetric around its axis, this probability is the same at all points of radius r. Finally, the mean of all these values is taken over the entire rotor disk area to provide the eventual risk of collision.

In the original model developed for bird transits, Band (2000) had to account for the two states a bird in transit could be in: flapping or gliding. In the adapted model, marine mammals are modelled simply as two equally long cones attached base to base with the axis of transit along the centre line.

The Band model yields different risks for animals travelling upstream and downstream, as a result of the pitch of the blades in different orientations, assuming animal speed relative to the ground is the same. However, much more substantial differences are likely to be due to differing upstream and downstream transit speeds as a result of swimming with or against the tide. The calculations made by Marine Scotland during the assessment of the collision risk posed to harbour seals at the Sound of Islay demonstrated underestimation of collision risk by approximately 10% when compared to results which averaged upstream and downstream movement using the same speed over ground (Lonergan and Thompson, 2015). This increase in risk is a function of the intuitive notion that while upstream movement is more energetically demanding and therefore much more likely at low flow speeds, the slower animal speed over ground results in an increased collision rate with the turbine during those transits. It has also been recently noted from observations of telemetered harbour seals in Kyle Rhea, and from observations in the Inner Sound (see Section 6), that harbour seals do often travel against the direction of flow at peak flow speeds. In this case, the model would predict high collision rates as blade rotation would be at maximum speed with relatively slow target approach speeds.

Similarly to the SRSL model, the modified Band model uses a simple multiplier to account for avoidance in the absence of any data which could inform this parameter. This is arguably the most important source of uncertainty for this and other collision risk models as it is very possible that, due to the perceived threat posed by these devices, animals could exhibit significant avoidance behaviour. Alternatively however, there could also be the potential for attraction to structures if they serve as fish aggregating devices and lead to enhanced foraging opportunities, such as has been seen for other marine infrastructure (Russell *et al.,* 2014). Field observations indicate that fish aggregation around devices occurs mainly at slack water (e.g. Broadhurst *et al.,* 2014), therefore this may not add to collision risk.

3.3.2 Exposure-Time Model for Tidal Turbines and Seabirds (Grant *et al.,* 2014)

In an attempt to determine potentially detrimental effects of collisions at a population level Grant *et al.* (2014) developed an exposure-time model which produces a collision rate derived from estimation of ‘acceptable thresholds of additional mortality’. This model accounts for the potential time each individual within a population is at risk of collision and is based on a simple population model which predicts age structure from survival and population size estimates. Collision risk is not explicitly calculated in the method. However, the collision risk which would be associated with a given level of mortality is estimated. In fundamental terms, it uses a reverse approach to the CRM and Encounter Rate Models in that it attempts to

predict whether a detrimental level of mortality at the population level is likely given the population modelling results and considering the effects of potentially high levels of avoidance.

The underlying model of host-parasitoid population dynamics which drives this method was developed by Nicholson and Bailey (1935). In simple terms, it predicts the number of deaths, D, as a result of collisions with turbines as a function of population size, N, collision rate, $\propto$, and length of time spent exposed to a turbine array, T:

$$D = N \propto T \quad (5)$$

This equation can therefore be rearranged to provide a target collision rate based on a given level of 'acceptable mortality'. The underlying assumptions of the model are consequently and justifiably conservative as they assume that collision rate and probability of collision are equal and remain equal throughout the estimated period. This is based on the assumption that collision rate will be relatively low when compared to population size. A further assumption of this model ignores the effect of additional mortality affecting further collision rates in successive time-steps (analogous to sampling with replacement). While conservative, this assumption is counter-intuitive as collision rate is based largely on population size and therefore density. When applied to a large population, the effect of this assumption is low. However, when dealing with smaller, declining populations, such as with local sub populations of harbour seals in the Pentland Firth and Orkney waters, the removal of a small number of animals could have a relatively large effect on future predicted collision rate.

The exposure time parameter is tricky to estimate as it is informed by observation data which carries with it additional uncertainty. Foraging trip number, number of trips within a danger area, number of dives per trip, mean length of time during each foraging trip spent at vulnerable depths and the proportion of the water at vulnerable depths occupied by the device are all required to be measured or estimated to accurately calculate exposure time. This can be informed reasonably confidently using telemetry data and fine-scale movement behaviour. However, similarly to the Encounter Rate Model and CRM models, in lieu of these data, density estimates from surface observations with associated large confidence intervals have to suffice.

Ultimately, the population modelling element of the exposure-time model determines the probability of a decline at various mortality levels rather than just determining whether an additional estimated mortality as a result of collisions is estimated to lead

to decline. This relies heavily on demographic data, which define the reliability of the derived acceptable thresholds. This is problematic as demographic parameters are poorly understood for many populations and are consequently very difficult to estimate. This results in the need for accurate estimates to be drawn from well-studied populations and inferences to be made about the relatedness between different populations of the same species. A large amount of uncertainty is associated with this method of parameter estimation and this is compounded by the fact that not all components of the parameter estimates carry an equal and proportional weighting, so slight changes in single components can have significant effects on exposure time.

3.3.3 Review Summary

There are difficulties associated with the assumptions underlying each of the reviewed models. While it is not possible to conclude which model is 'more correct', a brief overview of the use of the models and their adaptability would suggest that the Band CRM model is more flexible. As noted by Lonergan and Thompson (2015), the Band CRM model could be more easily adapted to incorporate a more realistic relationship between movement metrics of marine mammals and turbine speed than the other models. For example, with the appropriate data, it would appear relatively simple to build in a mortality function alongside an integration of depth distributions to provide a deeper insight into (a) the amount of time spent at risk depths and (b) the proportion of turbine blade collisions which are fatal.

Due to the increased adaptability of the Band model when compared with the SRSL Encounter Rate Model approach, and the apparent use of the Exposure-Time Population Model being restricted to estimating detrimental collision rates with regard to populations, the rest of this section will focus on possible adaptations which could be made to the Band CRM approach. Refinement options are detailed along with their potential to improve collision rate estimates.

4 Options for Model Improvement/Refinement

This section identifies potential improvements and refinements to models and describes existing datasets which can be used to inform these improvements.

4.1 Telemetry Derived Empirical Estimates of Transit Rate

Where sufficient data are available to describe the patterns of seal movements through proposed turbine deployment sites, it may be possible to combine the observed passage rates with information on the expected turbine array structure and the operational characteristics of the turbines to estimate the potential collision rate for the tagged animals. This can then be combined with estimates of the size of the relevant, at-risk population to estimate a predicted no-avoidance collision rate.

The advantage of such a calculation is that it does not require assumptions about the behaviour and movement patterns of the study species other than assuming the data to be representative of the population. It will automatically take into account any local distribution features. As with CRM described in Section 3, the estimates do not incorporate any information on avoidance or evasion behaviour. Where data are available, it may be possible to propagate the uncertainty in input parameters through the calculations to produce appropriate confidence intervals for the mean collision rate estimates.

Thompson *et al.* (2015b) estimated the expected number of collisions between harbour seals and turbines at an array in the Pentland Firth based on details of their movements relative to the locations of hypothetical tidal turbine blades, assuming that seals are oblivious to the presence of devices (i.e. show no avoidance and take no evasive action).

The observed behaviour patterns were derived from targeted telemetry tracking studies and the size of the population at risk of collision was based on recent population survey data. GPS location fixes recorded during surface breathing periods and depth measurements recorded during dives were used to estimate the 3-D positions of the seals. Linear interpolation between data points was used to estimate the locations of all tagged animals at all times and to estimate the number of times tagged seals would have passed through the swept area of individual turbines in a hypothetical turbine array within the site. The same data were used to estimate the frequency distribution of transit speeds and approach angles for seals passing through the swept area of each turbine to estimate the probability of collision for each event.

Telemetry data from seals tagged at various sites in the Pentland Firth and throughout the Orkney Islands were used to determine the geographical extent of the population that could be considered at risk of interacting with the hypothetical array. This was combined with the most recent aerial survey data for the population which was itself scaled up to provide a total, at-risk population estimate. Finally, the estimated number of possible collisions was scaled by the duration of the telemetry deployments and the estimated size of the at-risk population to derive a potential annual no-avoidance collision rate for the hypothetical turbine array.

The resulting estimate was approximately 15% of the equivalent estimate from a CRM for the same site (Thompson *et al*., 2015b).

These telemetry based estimates provide an alternative method of estimating collision rates and may be preferable in situations where local data exist and can be used to assess the performance of CRM or ERM. In the case of the Pentland Firth analysis, it appears that the major factor that differs between the CRM derived estimate and the telemetry data derived estimate of collision risk is the fine scale distribution of seals within the Inner Sound. Using similar methods at other sites will allow similar comparisons with model derived estimates. This will help to identify the local features that should be taken into account to refine model estimates.

4.2 Consequences of Collision

All of the models currently available for determining collision risk between renewable energy devices and animals assume each collision results in mortality and therefore removal from the population. This is unlikely to be true as mortality will vary as a function of collision speed which in turn will vary as a result of the position along the blade and on the position in the tidal cycle.

There are two distinct types of potential impact. The most likely case involves an animal being struck by the leading edge of a blade while transiting through the swept area of the turbine. The likelihood of such an impact being lethal is discussed in detail below. In addition, it is also considered possible that marine mammals may collide with the sides/trailing edge of the blade. At present, it is assumed that any such collisions would also be fatal. However, it is not clear how likely it is that marine mammals would collide with the side/trailing edge of a turbine blade. Collision with the side or trailing edge requires that the marine mammal swims directly into the blade. While avoiding the leading edge may require a rapid change of direction that may be beyond the capabilities of some animals, avoiding a head-

first collision with a passing blade should only require an animal to turn its head away in the direction of travel of the blade. It might be expected that in most cases a conscious, alert marine mammal should avoid such collisions. If a trailing edge collision were to occur at the tip of the blade where the pitch angle is shallowest, the maximum speed of impact would be very close to the speed of the animal over the ground. The force of this impact would decrease with increasing blade pitch as the animal would be deflected rather than experience a direct blunt force impact. However, the speed of impact when colliding with an angled surface then becomes a factor of effective blade speed and approach speed. The effective blade speed is scaled down as a factor of how acute the angle is (a more acute angle results in a slower effective blade speed) however it is a parameter which must still be accounted for.

For a collision with the side/trailing edge of a blade, the highest impact speed would be encountered in the case of an animal swimming in the same direction as the current at maximum flow. In general, seals and cetaceans swim at around their minimum cost of transport speeds (e.g. Feldkamp, 1987; Hindell and Lea, 1998) which are generally below 2.5 m/s. Combined with a flowing tide of 3 m/s this would produce a maximum collision speed with the blade whilst travelling at ~5.5 m/s. In the unlikely situation that the animal makes no attempt to avoid the collision, this would potentially cause injury. However, the maximum collision speed would be similar to the maximum effective speeds of blade edge collisions tested in the trials described below that did not cause skeletal damage. The fact that the contact point would be on a relatively wide flat surface rather than a narrow blade like edge would suggest that skeletal damage is unlikely.

Further research is underway to address the assumption that all collisions will be fatal by assessing the characteristics of vulnerable animals and how they respond to impacts similar to a turbine impact. Two distinct approaches have been employed for marine mammals, a theoretical modelling approach (Carlson *et al.,* 2014) and a simple experimental approach (Thompson *et al.,* 2015a).

As part of the OpenHydro project in Puget Sound, WA, USA, Carlson *et al*. (2014) conducted finite element analysis which focussed on how killer whale tissue would be expected to react to turbine blade impacts. Although the OpenHydro device is somewhat different to the typical open rotor horizontal axis design, the impact of the leading edge of the annular blades striking an animal was still of concern. The study used information on the turbine array such as number, location, shape, blade angle, leading edge dimensions, blade mass and operating characteristics to calculate peak loads imposed during a theoretical collision with a killer whale. As a conservative

approach, they used these peak-load values to predict all further reactions. The blades were assumed to be moving at maximum operating velocity and the impact was taken as being as close to the tip of the blade as possible. Testing the worst case scenario by calculating the effects of the most severe collision is a logical approach. If the worst case is determined to not be lethal, all other collisions can be assumed to be non-lethal.

The biomechanical properties of a neonatal and juvenile killer whale were then ascertained by testing the tensile and compression strength of blubber and skin samples. These stress characteristics were used in the collision model to estimate the force which would be exerted by the blade at the impact point. If the tissues did not experience tissue failure as predicted by the tensile and compression tests, tissue damage was not expected to be at a detrimental level.

The results of the worst case encounter rate scenario in which the OpenHydro blade struck the top of the whale's skull and melon at maximum force were considered "unlikely to be transferred deep into the animal's body, based on knowledge of forces required to break the jaw of larger whales" (Carlson *et al.,* 2014). While difficult to extend these results to smaller, physiologically dissimilar marine mammals, it provides an important indicator that blubber can provide significant protection to the vital organs. Strikes of a similar force from the leading edges of the blades of an open bladed design would likely yield similar results (although the probability of strike may be different due to the very different turbine design). Furthermore, it provides a useful framework from which to work from and adapt to more species. It also informs some sources of uncertainty with regards to the severity of injury for turbine blade strikes.

Thompson *et al.* (2015a) investigated the same issue; by assessing the damage imposed on grey seal carcasses through turbine impacts. The leading edge of the outer 1 metre of a turbine blade was modelled and welded to the hull of a jet drive boat. The boat was then driven at tethered floating seal carcasses at a range of speeds to simulate the impact of blade strikes. Adult and juvenile carcasses were subjected to collisions at various points along their bodies and at various speeds. Due to limitations in boat speed and angle of attack of the blade, maximum potential turbine blade speeds could not be tested and the most severe impact conducted was at 6 m/s. No skeletal damage was observed in any of the collisions. In contrast to Carlson *et al.* (2014), the primary goal was to assess skeletal damage. Soft tissue results were deemed unreliable due to the freeze-thaw process. The freeze thaw effects would be expected to make these organs more prone to damage however, no

tears or rupture to internal organs were detected. These results suggest that over half of expected collisions would occur at blade speeds that would not be lethal.

Neither investigation could assess all physiological ramifications of impacts to their particular study species. Potential fatalities due to conditions such as concussion or unconsciousness would be very difficult to ascertain under any experimental conditions. However, results from both studies suggested that although actual damage could not be assessed with certainty, there would likely be no damage at the speeds tested for either species. Studies of hydropower turbines and fish have identified thresholds at which particular types of damage occur and this has been adopted into prediction methods (e.g. Turnpenny *et al*., 2000) and this approach has been assessed here.

The model function could be as simple as assuming that any closing speed greater than an empirically determined speed would be fatal, thus drawing on results of investigations such as those detailed above.

Additionally a metric could be applied to the mortality function to assess the likelihood of a fatal interaction given the point of the blade which struck the animal. The formula for the risk of collision during a single transit discriminates between terms deriving from either the leading edge or the remainder of the blade striking the animal. It may be beneficial to discriminate between these scenarios within the mortality function if experimental data could be generated to inform this. This would reflect the particular risks associated with the sharp radius of curvature of the leading edge of a turbine blade.

Intuitively it seems likely that collision with parts of a turbine blade other than its leading edge – the 'trailing blade' - would be less damaging for two reasons. The effective collision speed will be a function of the closing speed (equal to the square root of the sum of the squares of swim speed and blade speed) and the angle of the blade relative to the plane of rotation. For example close to the tip, the blade presents a relatively flat surface almost in line with the plane of rotation. Further down the blade it will be a rounder surface that is to a greater extent perpendicular to the rotor plane and the seal will be subject to a side-swipe from the moving blade. Thus the blade speed of concern is $r\Omega \tan \gamma$ where γ is the pitch of the blade relative to the rotor plane. The effective pitch of the blade will differ with distance from the centre of rotation. At the tip where speeds are highest, the pitch angle will be small, typically of the order of 4°, and the blade profile will be relatively flat so impact with the trailing surface will be predominantly a function of the swimming speed. Closer to the centre, the blade is twisted to maintain a constant angle of attack and is also

thicker so the effect of blade speed on trailing edge collisions will be more important. However blade speed decreases linearly with distance from the tip, so such collisions are less likely to be damaging.

Secondly, a collision with the trailing blade would represent a comparatively large surface area and therefore the force of the impact would be spread across a larger proportion of the animal resulting in a decrease in energy transmission to the subcutaneous layers, resulting in a decreased chance of muscle and organ damage.

4.3 Evasion/Avoidance

Encounter rates are calculated assuming that animals will not react to the presence of a device. This is clearly unreasonable in many, if not most circumstances. Converting no-avoidance collision rates into actual predicted collision rates requires the application of an avoidance/evasion factor. Seals have good vision both above and below water and in low light levels. They also have highly sensitive vibrissae, capable of sensing movements in the water generated by swimming fish (Hanke *et al.,* 2013). Perhaps more importantly, they have excellent underwater hearing at the frequencies of sound generated by tidal turbines. It is therefore unlikely that seals will be able to approach an operational turbine without detecting it. Seals are active predators evolved to hunt fast moving, highly reactive and highly manoeuvrable fish prey. As such, they clearly have the capabilities required to avoid and/or evade collisions with turbines.

Evasion may also be dependent on the behavioural and physiological traits associated with different life stages. For example, seal pups which are inexperienced in the water could produce less of an avoidance response than adult seals (Wilson *et al.,* 2007). Furthermore, seals are also inquisitive of foreign objects placed in their marine environment and so curiosity around a new tidal turbine device could also influence encounter rates and ultimately collision (Wilson *et al*., 2007), although this is extremely difficult to parameterise.

At present there are no reliable data to allow calculation of an evasion factor for seals or other marine mammals. Only one tidal turbine has been monitored with sufficient effort and appropriate technology to assess avoidance behaviour; the SeaGen device operating in Strangford Narrows, Northern Ireland (NI). Results of GPS telemetry tracking of harbour seals in the channel at Strangford indicated that seal transits past the turbine were reduced by on average 20% during turbine operations suggesting some degree of avoidance (Savidge *et al*., 2014). Further analyses of these data suggested that the density of seal locations within 200 m of

the turbine were 66% lower after installation and commissioning of the turbine compared to baseline, although a different sample of animals were tagged in each time period so comparison is complicated by high inter-individual variation. However, the mitigation requirements at the Strangford site required that the turbine be stopped whenever a suspected marine mammal came within 50 m of the device. The operation of the device therefore provided no information on fine scale, near field evasion behaviour.

Ongoing work on behavioural responses of seals to playback of simulated turbine noise appears to show reduction in seal activity close to the source indicating a low level but significant avoidance (Hastie *et al*., in review). Work on captive seals suggests that they may alter their foraging behaviour in response to playback of the same simulated turbine noise (Hastie *et al*., in review). Again, this work does not provide information on close range evasion. Plans are in place to monitor the close range behaviour of marine mammals around operating turbines at the first Scottish arrays and this information will be incorporated into predictions of collision risk (see Sparling *et al*., 2016).

A model developed to estimate the probability of fish evading collision (Batty and Wilson, 2010) has been proposed as the basis for evasion estimates for marine mammals. The model uses information on the visual, behavioural and swimming capabilities of fish to predict the probability of evasion in response to visual cues from approaching turbine blades. The model predicts that blade speed is critical, with more than 50% of fish failing to evade collision with blades moving faster than 6 m/s. Blade width was also important in blade detection range with later detection, and therefore less evasion, of narrower blades. The authors note that this work could be extended to include responses to auditory cues.

Batty *et al*. (2012) also list a set of reasons why, or circumstances when, a marine mammal may not respond appropriately to cues from a turbine, including detection failure, diving constraints, attraction, confusion, distraction or an unexplained inappropriate response. There is currently little or no information to assess the importance of these issues.

At present the evasion rates for marine mammals have been extrapolated from observations on behaviour of birds interacting with wind turbines. In those situations, avoidance rates can be derived from comparisons between predicted mortality rates, based on an assumption of no-avoidance, with direct observation of collisions and/or counts of carcasses. Avoidance rate estimates for most bird species are still not known with accuracy, but where data exist they suggest that avoidance/evasion

factors for most species are very high (Cook *et al*., 2014), with most species estimates in excess of 98%.

It is not clear how these estimates relate to marine mammals. Manoeuvrability, reaction times, acceleration capabilities, turbine visibility and sensory abilities/detection ranges etc. and turbine visibility differ significantly. This should be a major research priority as the evasion factors currently employed for seals are high and speculative and therefore open to debate. Currently, it is common practice to present an illustration of the effect of a range of avoidance/evasion factors on collision risk estimates. Such an approach is recommended until empirical data is generated to support the choice of correction factor. As discussed above, plans are in place to gather empirical data at the first array projects that will allow collision risk estimates to be modified to take account of avoidance and evasion.

4.4 Uncertainty

A significant limitation of published models for marine mammals is their lack of accounting for uncertainty, with results producing mean estimates with no associated confidence intervals. Sources of uncertainty lie in the sparse or absent data for informing parameter estimates and without incorporating statistical techniques to account for the fact that these estimates often carry with them large confidence-intervals, it is not possible to assess the degree of confidence one should place in the point estimates. Whilst the relationships between turbine characteristics and tidal parameters are very well known, less well known parameters include the behaviour of animals (swim speed and direction in relation to the tide) and the density of animals (particularly in relation to the tidal cycle).

4.5 Turbine Operation and Structural Characteristics

The operational characteristics of a turbine may differ from the predicted/expected patterns. For example, the Strangford Lough, SeaGen device tip-speed ratios (ratio between tangential speed of the turbine blade tip and the water flow speed) were calculated to be 5.1:1 rather than the model assumed 6:1 (Wood *et al*., 2016). With slower than assumed tip-speeds the model would generate a lower collision rate, provided the other assumptions remained constant. If the relevant information is available it will provide a more reliable collision risk estimate with less associated uncertainty and so should be included wherever possible.

Information on the operational profiles showing detailed rotational speeds at a range of flow speeds, feathering profiles at various flow speeds (alteration of blade pitch to present less surface area to the incoming flow at high flow speeds), flow speeds resulting in cessation of rotation and scheduled maintenance shut-downs can all be factored in to provide a detailed model which accounts for temporal variability. Additionally, structural characteristics such as blade width profile and blade pitch irrespective of feathering should be included as an increase in surface area will lead to an increase in collision rate, especially when considering collisions with the trailing edge of the blades (see Section 4.2).

Ideally these data would require supporting hydrodynamic data from the area of interest to determine the flow speed profiles (both tidal speed and direction). This would help generate the operational parameters and be used to indicate periods of non-operation as a result of cut-off speeds being reached. These data would also provide support for the behavioural parameters in that more accurate approach speeds could be calculated for both upstream and downstream transits enabling particular physical aspects which affect the likelihood of a collision to be discerned.

4.6 Target Species Biology

Biological characteristics are also an important source of uncertainty in the models and variation in these could have a significant effect on collision risk. The key characteristics are described further below.

4.6.1 Animal Distribution

Depth Distribution

The adapted Band model is limited by lack of information to inform assumptions regarding animal behaviour, not least due to the possibility that certain behavioural characteristics such as foraging may be site-specific. Separate populations may have to adapt their foraging tactics as a result of different prey distribution and behaviour, and differences in oceanographic characteristics of tidal regions such as eddies, boils and current speed (Benjamins *et al.,* 2015). Consequently, there are simplifications and assumptions inherent in the Band model which may have significant effects on the resulting collision estimates.

One such assumption relates to the depth distribution of animals. The Band model starts with the equation for the potential collision rate C_{CRM} arising from a set of B rotors, a rotor being a single set of rotating blades:

$$C_{CRM} = D \times A \times v \times pcoll \quad (6)$$

where

D	is the mean animal density in the risk depth range;
A	is the combined area $B\pi R^2$ of *B* rotors each of radius *R*;
v	is animal speed relative to the rotor;
D x *A* x *v*	represents the number of transits per second through the swept area of these rotors;
pcoll	is the average risk of collision during a single transit through a rotor, calculated by averaging the risk of collision at a particular radius; and
p(r),	over the area of the rotor.

In the basic Band model, it is assumed that the proportion of animals within the depth range of the turbines is uniformly distributed across that range, and can be represented by the mean density *D*.

Thus:

$$C_{CRM} = B\pi R^2 \times D \times v \times \frac{\iint p(r)dA}{\iint dA} \quad (7)$$

The Band CRM has been extended to take account of details of flight height distribution for calculating collision risk to birds for offshore windfarms. The model used for wind farms can be modified for tidal turbine applications, replacing height by depth, where the correct data are available for the site under assessment. This can be achieved by simply including animal density D(y) at each depth y into the integration of p(r) over the rotor area:

$$C_{CRM} = B\pi R^2 \times v \times \iint D(y) \times p(r)dA / \iint dA \quad (8)$$

Depth distribution data derived from time-depth recorders are available for harbour seals at various tidally energetic sites around the UK including the Pentland Firth, Strangford Lough and The Sound of Islay). Differences in bathymetry at the sites make it difficult to generalise, but at each site dives are mainly to depths consistent with diving to the sea bed, but with a variable proportion of mid water dives. Site specific dive data should therefore be used wherever it is available.

Scaling Distributions/Density to Population Level

Since telemetry data (used to inform site density) represents data from a sample of all the individuals using a particular area, scaling exercises must be undertaken to produce likely densities as a function of local population size which themselves carry inherent uncertainty.

Surveying of harbour seal populations is conducted during the major haul-out periods of breeding and moulting which span the summer months and into early autumn (May to September). Consequently seasonal trends in haul out abundance and distribution cannot be confidently estimated and periods outside surveying have to be assumed to be similar to summer.

3-D distributions are also assumed to be constant in time as well as space, which again appears to be an oversimplification when viewing the available data. Animals may spend different amounts of time in different parts of the water column depending on behaviour (e.g. foraging vs. travelling vs. resting) which will have different implications for risk of collision.

Currently, the published Band model (Scottish Natural Heritage, 2016) for estimating collision risk to marine mammals requires the use of a mean operational turbine speed (outside times where the device is non-operational), and a mean speed of approach relative to the turbine, taken as the mean current speed (any swim speed relative to the water is assumed to be in an upwards or downwards direction, not affecting the speed of approach). Use of mean values for current and operational turbine speeds in this way are simplifications which may have a significant effect on overall collision rate estimates, as they do not take into account the non-linear variation of collision rate with current and turbine speeds over the tidal cycle, nor the behaviour of species in tidal environments at differing current speeds (see Section 6 for detailed discussion of seal behaviour).

Tidally dominated areas are believed to be important foraging areas for marine predators. The distribution of seals in these areas is likely to be heavily influenced by prey density which in turn is assumed to be influenced by the state of tide (Zamon, 2003). Any variations in prey availability over the tidal cycle will have resulting implications for collision risk. However there are likely be site specific differences in this pattern; recent studies in Orkney around a tidal device have shown that prey availability may be higher at slack tide (Fraser *et al*., in review). In contrast, a recent study in Kyle Rhea on the west coast of Scotland demonstrated

that seal density was highest over the peak flood tide which is thought to be related to prey availability (Hastie *et al*., in review).

To circumvent this, one might integrate information over one or more tidal cycles as v and Ω are not independent and both a function of time; combining current speed from tidal data and animal swim speed to estimate speed of approach relative to the rotor. One could then use turbine manufacturer's data to calculate rotation speed as a function of current speed and include manufacturer's information to determine periods of non-operation.

We therefore recommend that the temporal as well as spatial elements of 3D distribution are important refinements to collision risk modelling in order to produce more reliable estimates. However, caution should be exercised when generalising these distribution parameters as hydrodynamic differences between sites are likely to affect the behaviour of animals in these areas of interest (See Section 6, and Hastie *et al.,* in review).

4.6.2 Animal Shape

Currently the Band CRM uses two conical shapes connected base-to-base, with swim direction along the axes of the cones, as the marine animal model (Figure 1). It is possible that a more complicated animal modelling framework would change the resulting collision risk estimates due to the dimensional ratios moving position on the animal. Additionally if the dimensions changed then significant changes in the collision rate may result. For example, a larger seal would have a greater surface area susceptible to collision. Seal length is currently a fixed input in the CRM.

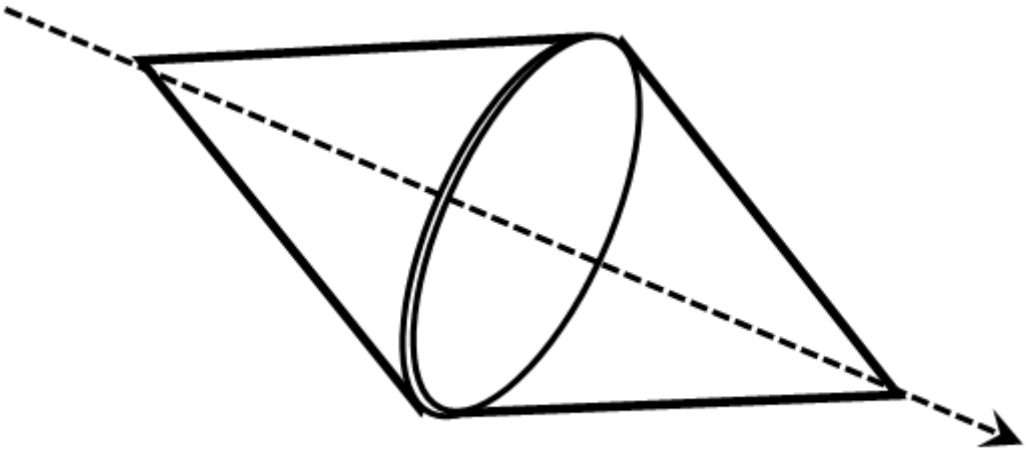

Figure 1 The two-cone shape used in the Band CRM to represent a marine mammal

It is important to note that the angle of approach is a key factor when considering the sensitivity of model estimates to animal shape. For example, when the approach angle is 90˚ to the blade sweep angle, the collision risk is predominantly affected by the length of the animal (Figure 2a). However when the angle of approach is altered, differently dimensioned animals with identical length will be exposed to the blade sweep zone for different spans of time (Figure 2b). Figure 2 demonstrates the different levels of exposure to the blade sweep zone to animals of equal length and width but different shapes. The further the axial girth moves towards the apex of the animal, the greater time it will be exposed to the leading edge of the turbine blades. This is demonstrated in refinement 3 of the CRM (below), but is to some extent counteracted by the fact that when the maximum axial girth is further forward, towards the apex, then the taper at the rear of the seal is more gradual so it will be subject to reduced risk. This partially explains why the collision rates are so insensitive to the body-ratio factor μ.

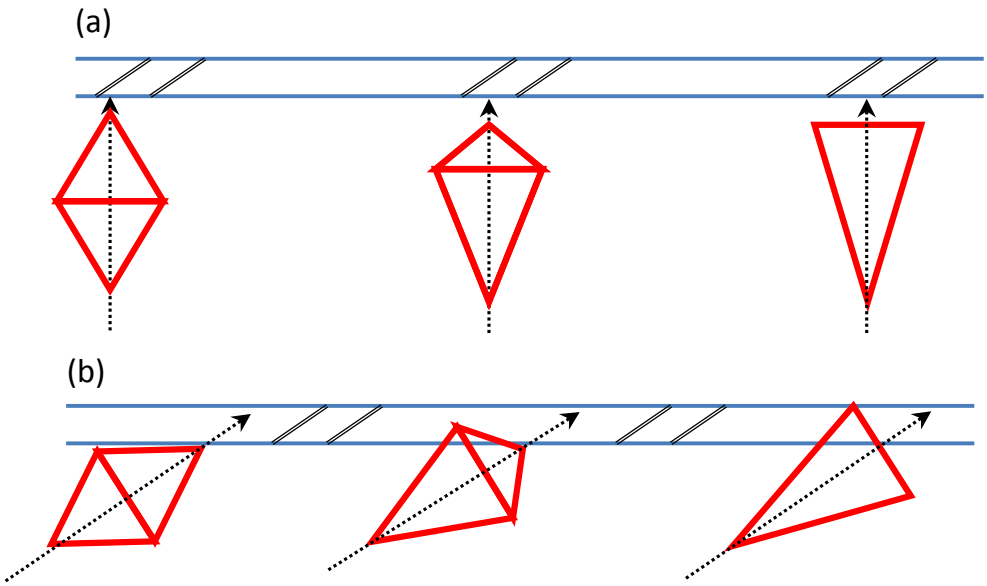

Note: Difference in level of exposure before the central apex reaches the zone between the animals in 2(b). The blade sweep zone is highlighted by the blue lines with distance between the lines indicating the depth of the sweep zone

Figure 2 The passage of three differently shaped animals with equal length and girth approaching the blade sweep zone (a) a 90˚ angle and (b) a 45˚ angle

Figure 3 demonstrates the extreme case of an animal crossing the blade sweep zone where the axial girth is at the front apex. In this case, an additional 0.03 m² of the animal is vulnerable to collision before the centre point of the apex comes into contact with the blade sweep zone. After this point, the animal would have an additional exposure period equal to the total amount of time taken for an infinitely thin animal of equal length to pass through the blade sweep zone.

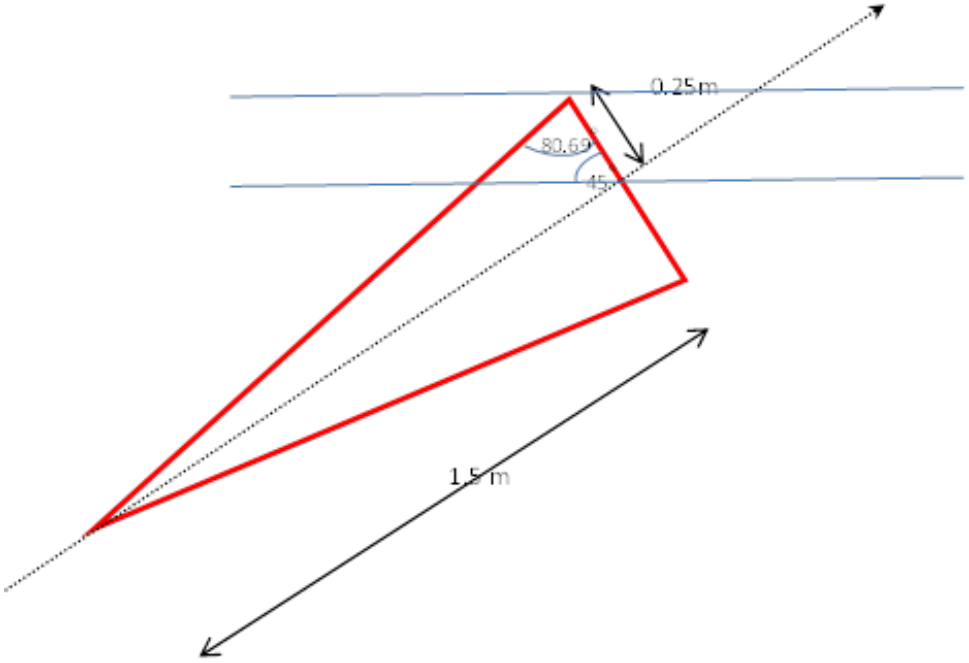

Note: The 45˚ approach angle results in an additional 0.03 m² of the animal being exposed before its central apex reaches the blade sweep zone. This results in an increase period of collision risk when compared with an approach angle of 90˚

Figure 3 Extreme case of an animal with length 1.5 metres, with axial girth of 0.5 m at the apex of its body

It must also be noted that the relative positions of a passing blade and an approaching animal are also temporally variable and are subject to approach speed and rotation rate. If the blade were to rotate past the apex of an animal but the animal continued to move forward it would still be at risk of collision with the trailing edge of the blade. The level of this risk would be dependent on the angle of approach as well as the shape of the animal, with an animal with its axial girth further towards its apex more susceptible to trailing edge collision (Figure 4b). Equally, an approach angle more parallel with the angle of the blade will lessen the probability of a trailing edge collision (Figure 4).

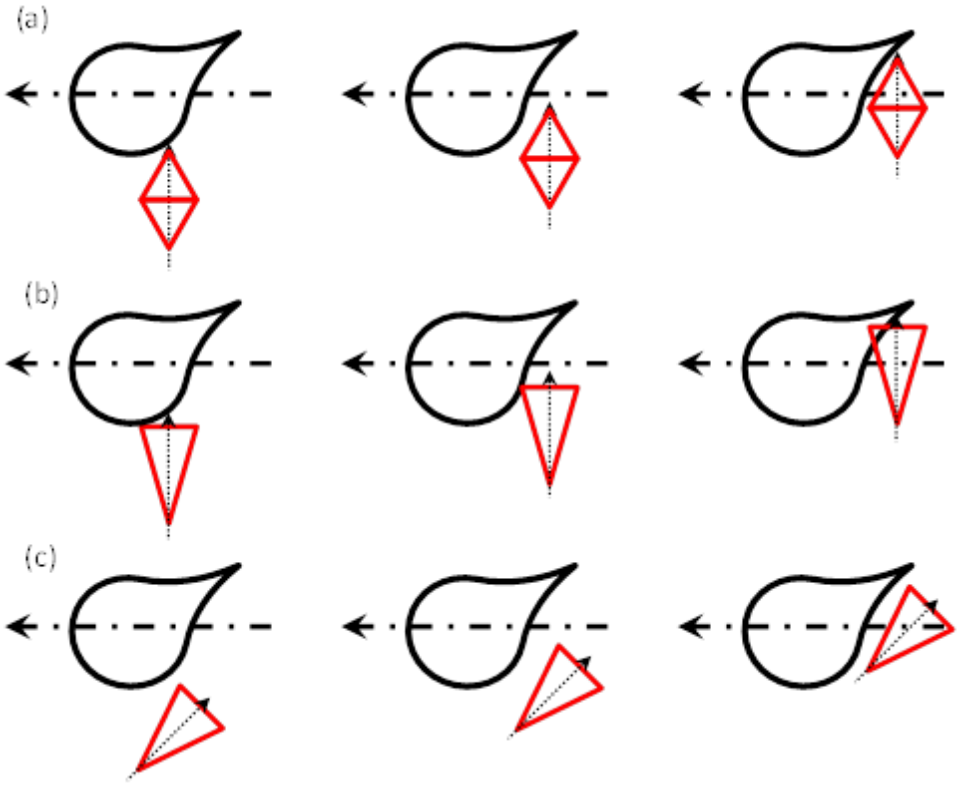

Note: The absence of an impact in figures (a) and (c) and trailing edge impact in the final time-step of (b). Each figure shows three iterative time-steps of equal length with blade speed and approach speed equal in all cases

Figure 4 Examples of an approach to a section of turbine blade angled at 35˚ from the blade sweep zone of (a) an animal with a central axial girth approaching the blade at a 90˚ to the blade sweep zone (b) an animal with an axial girth at its apex approaching at a 90˚ angle to the blade sweep zone and (c) an animal with axial girth at its apex approaching at a 45˚ angle to the blade sweep zone

5 Recommendations for Re-assessing Collision Risk in the Pentland Firth and Orkney Waters Area

The uncertainty associated with some of the input parameters to existing collision risk estimates (Section 4.4) can be minimised with the use of high resolution empirical data (e.g. for seal density) to produce narrower confidence intervals. Of the economically important sites which have been identified as potential locations for tidal energy development, the harbour seal population of the Pentland Firth is one of the most intensely studied. High resolution telemetry data providing information on 3-D movement behaviour is available from deployment of fourteen tags in 2011. There is consequently, a large amount of baseline movement and dive data for this area. Additionally, there is an existing hydrodynamic model for the Pentland Firth and Orkney area (ABPmer, 2012) which provides detailed information on the flow patterns (flow speed and direction). This model covers the MeyGen site where the first tidal array will be situated. These data, in combination with operational and mechanical data from the turbine operators, will allow a full suite of parameters to be modelled which would account for much of the uncertainty inherent in previous collision risk estimates.

With collision rate estimates already available for this site, it would be useful to incorporate the site-specific density and movement patterns into an updated CRM and compare the outputs of the updated predictions with existing predictions.

While this approach focuses on a site with an abundance of data to inform the currently uncertain parameter estimates, generic applications of these refinements may also be appropriate and will be explored to enable the updated CRM to be applied to other sites. The amount and resolution of available data are important considerations when assessing the relevance of these refinements. This should be done on a case by case basis, however certain refinements will be intended to be ubiquitous. Mortality rate as a function of impact severity and mean body shape and dimensions can be assumed to be consistent across species from different sites. However, foraging behaviour can show marked differences between different tidally dominated sites and turbine tip-speed ratios will differ with different structural characteristics. It is therefore advised that caution is exercised when adapting the refinements made to depth distributions, transit rates, approach speeds and turbine speeds to sites without a full suite of supporting field data.

6 Detailed Examination of Harbour Seal Behaviour in the Pentland Firth and Orkney Area

6.1 Introduction

This section of the report describes relevant aspects of the diving and movement patterns of harbour seals in and around the potential tidal array site in the Inner Sound between Stroma and the Scottish mainland, and in and around the tidal turbine test array site at the Fall of Warness off the south west coast of Eday in Orkney. These two sites were the focus for this examination because one of the objectives of this work was to refine collision risk estimates in these areas specifically to inform future tidal energy consenting in the Orkney and North coast harbour seal management unit (Figure 5).

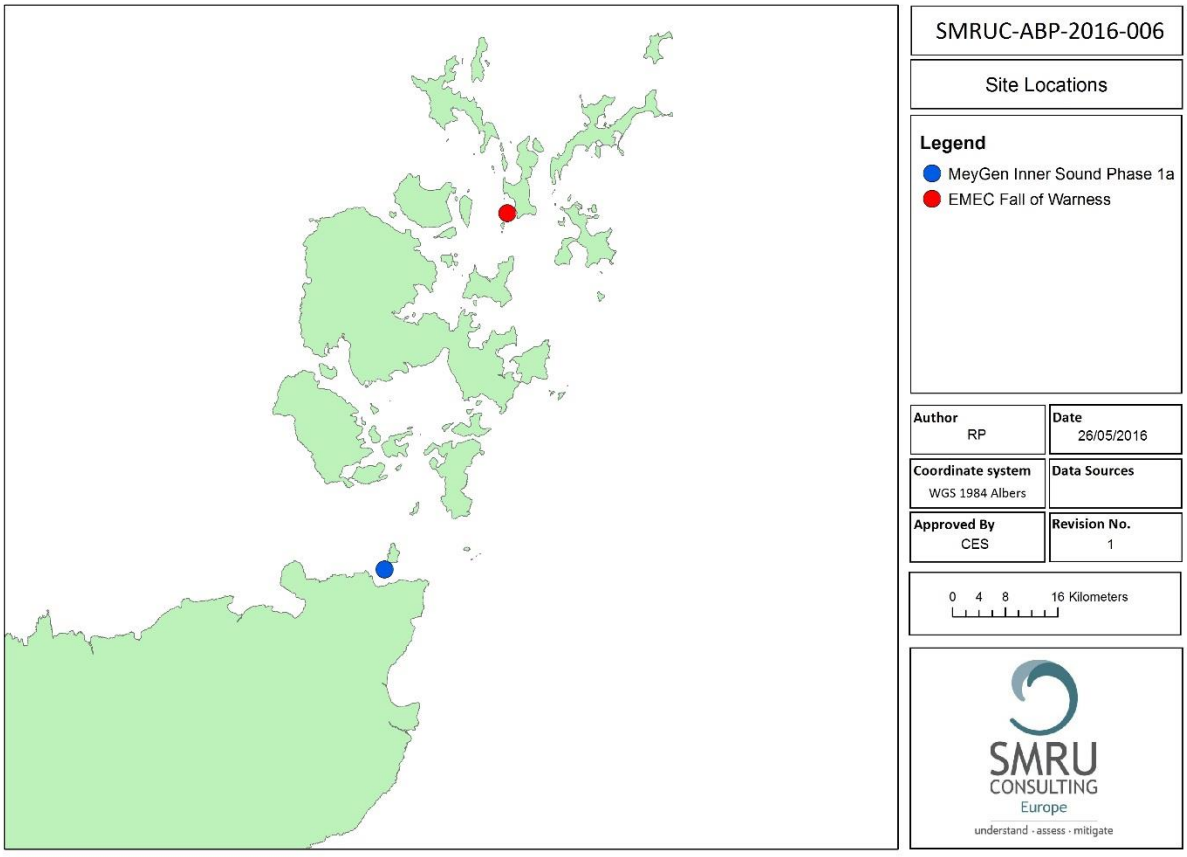

Figure 5 Map showing the two tidal energy sites which were the focus for the detailed examination of seal telemetry data

GPS location fixes from purpose built telemetry tags fitted to a sample of harbour seals at each site were used to estimate their latitude and longitude positions at the start and end of any dives recorded in the vicinity of the two test sites. These data

were then used to generate descriptors for movements with respect to tidal flows derived from a depth averaged high resolution hydrodynamic model developed by ABP Marine Environmental Research Ltd (ABPmer, 2012).

6.2 Data Collection

Tide related behavioural descriptors and metrics were derived from the observed swimming and diving behaviours of a sample of 12 adult and two sub-adult harbour seals caught at haulout sites in the Inner Sound (between Stroma and the Scottish mainland), close to the MeyGen tidal site in March and September 2011. In addition, ten adult harbour seals were caught at haulout sites around south and west Eday, close to the Fall of Warness EMEC tidal test site; eight in June and two in October 2012. These data were collected as part of a Scotland wide baseline study funded by Marine Scotland and Scottish Natural Heritage (SNH) with additional funding from the Natural Environment Research Council (NERC) for studies in Orkney.

In order to study the movement and dive patterns of seals at an appropriately fine scale, used SMRU/Fastloc GPS/GSM Phone Tags are used, which combine GPS quality locations (usually better than 10 m accuracy, but restricted to inter-dive surface periods) with efficient data transfer using the GSM mobile phone network. The tags provide locations at a user controlled rate, together with complete and detailed individual dive and haul-out records. Tags incorporate a pressure sensor and relay dive depth data in the form of nine depth records evenly spread through each dive.

The tags are small, weighing 370 g, which is less than 0.5% of the average mass of harbour seals in this study. Data are relayed via the mobile phone network when the animal is within GSM coverage. The data derived from these devices represent the highest resolution, combined movement and diving behaviour information available at present.

Due to limited battery capacity, there is a direct trade-off between the temporal resolution of the location data and the life of the transmitter. In order to produce location data for the entire period from the tagging date to the moult, when tags are expected to fall off, the tags were set to collect a GPS location fix at eight minute intervals. In practice this rate is not achieved because of the intermittent surfacing patterns of seals and the failure of the tag to make a successful connection to the GPS satellites on some surfacing's.

The eight seals tagged at Eday in June 2012 were fitted with SMRU satellite transmitters equipped with Fastloc GPS loggers. These transmitted similar quality location data, but at a lower rate so that the time between position fixes and therefore the potential error due to interpolating dive locations was greater. Data from these tags have been used only in calculating transit rates at the EMEC site.

Seals were caught using a combination of rush and grab techniques and tangle nets. Seals were anaesthetised with an intravenous dose of a Tiletamine-Zolazepam mixture (Zoletil, Virbac, France) at a dosage of 0.05 mg/kg and tags were glued to cleaned, dried fur on the back of the neck using a cyano-acrylate contact adhesive (Loctite 422, Henkel Ltd, Hemel Hempstead, UK). Seals were released and left to recover on shore close to their capture site. Eight harbour seals were caught at haul out sites in Gills Bay, the haulout sites closest to the proposed MeyGen tidal turbine array site in the Inner Sound, between 29 and 31 March 2011 and six were caught between the 24 and 26 September 2011 (Table 2).

Table 2 Tagging data and morphometrics for harbour seals used to derive the tide related behaviour metrics

Seal ID	Date	Tagging Location	Sex	Age Class	Mass (kg)	Length (cm)	Girth (cm)
pv24-165-11	30/03/2011	Inner Sound, Pentland Firth	M	Adult	90.6	143	112
pv24-541-11	30/03/2011	Inner Sound, Pentland Firth	M	Adult	96.8	153	118
pv24-x625-11	31/03/2011	Inner Sound, Pentland Firth	M	Adult	98.6	151	114
pv24-622-11	31/03/2011	Inner Sound, Pentland Firth	M	Adult	91.4	150.5	111
pv24-394-11	30/03/2011	Inner Sound, Pentland Firth	M	Juv	49.6	128	89.5
pv24-590-11	30/03/2011	Inner Sound, Pentland Firth	M	Juv	49.8	133	92
pv24-598-11	29/03/2011	Inner Sound, Pentland Firth	F	Adult	84.6	136	113.5
pv24-580-11	29/03/2011	Inner Sound, Pentland Firth	F	Adult	89	146	114
pv24-148-11	24/09/2011	Inner Sound, Pentland Firth	M	Adult	76.2	143	126
pv24-153-11	26/09/2011	Inner Sound, Pentland Firth	F	Adult	72	144	100
pv24-150-11	26/09/2011	Inner Sound, Pentland Firth	F	Adult	86.6	136	119
pv24-112-11	24/09/2011	Inner Sound, Pentland Firth	M	Adult	92.8	156	122
pv24-155-11	24/09/2011	Inner Sound, Pentland Firth	M	Adult	95	154	109
pv24-151-11	25/09/2011	Inner Sound, Pentland Firth	M	Adult	84.8	140	117
pv44-007-12	14/06/2012	Seal Skerry, Eday	F	Adult	97.6	136	116
pv44-021-12	14/06/2012	Seal Skerry, Eday	F	Adult	100	137	106

Seal ID	Date	Tagging Location	Sex	Age Class	Mass (kg)	Length (cm)	Girth (cm)
pv44-020-12	16/06/2012	Seal Skerry, Eday	F	Adult	67.8	137	100
pv44-017-12	16/06/2012	Seal Skerry, Eday	F	Adult	73	136	100
pv44-018-12	16/06/2012	Seal Skerry, Eday	F	Adult	80.2	151	103
pv44-003-12	18/06/2012	South coast of Eday	M	Adult	99	148	110
pv47-539-12	18/06/2012	South coast of Eday	M	Adult	110	153	120
pv47-585-12	18/06/2012	Seal Skerry, Eday	F	Adult	92.8	144	96
pv44-007-12	09/10/2012	South coast of Eday	M	Adult	93	142	115
pv44-021-12	09/10/2012	South coast of Eday	M	Adult	64.8	133	100
pv44-007-12	14/06/2012	Seal Skerry, Eday	F	Adult	97.6	136	116

6.3 Tidal Current Estimates

ABPmer provided estimates of tidal currents associated with each dive for a subset of the telemetry data in 2011 from their depth averaged flow model for the Pentland Firth and Orkney waters. To extrapolate to the entire telemetry data set, estimates were derived for the tidal current vectors for each dive within the tidal array site from estimates of current speed and direction at 15 minute intervals for a complete (but different) year for three locations along the centre east-west axis of the MeyGen array site and four individual turbine sites in the Fall of Warness turbine test site (locations of tide reference points are shown in Figures 41 and 42).

To ensure that the tidal cycles were synchronised with those for the tagging dates in 2011 the 2011 times and tidal heights of high and low water for a tide station on the south side of Stroma, adjacent to the proposed turbine array, were extracted from POLTIPS (NERC POL) digital tide table package. A smoothed line was fitted to those data and overlaid a plot of the estimated current speeds from the tidal flow model. The timing of the tidal flow data was adjusted and the apparent fit of the two time series was examined (Figure 6).

The similarity of the patterns was assessed by eye and the timings were adjusted so that maximum and minimum amplitude periods coincided in the two data sets. The times of high and low water were then estimated from the flow model data and the timing of the model adjusted to produce the minimum sum of squares fit to the times of high and low water for the Stroma tide station data, using the Solver routine in Excel. The resulting fit is shown in Figures 6 and 7. This results in a set of flow estimates that may differ slightly from reality in terms of current speed, but should

represent an accurate current direction. A similar process was carried out for the model output data for the Fall of Warness site using the mean times of the two closest tide stations at Rapness on Westray and Kettletoft on Sanday as the reference point for the tide times in late 2012 and early 2013.

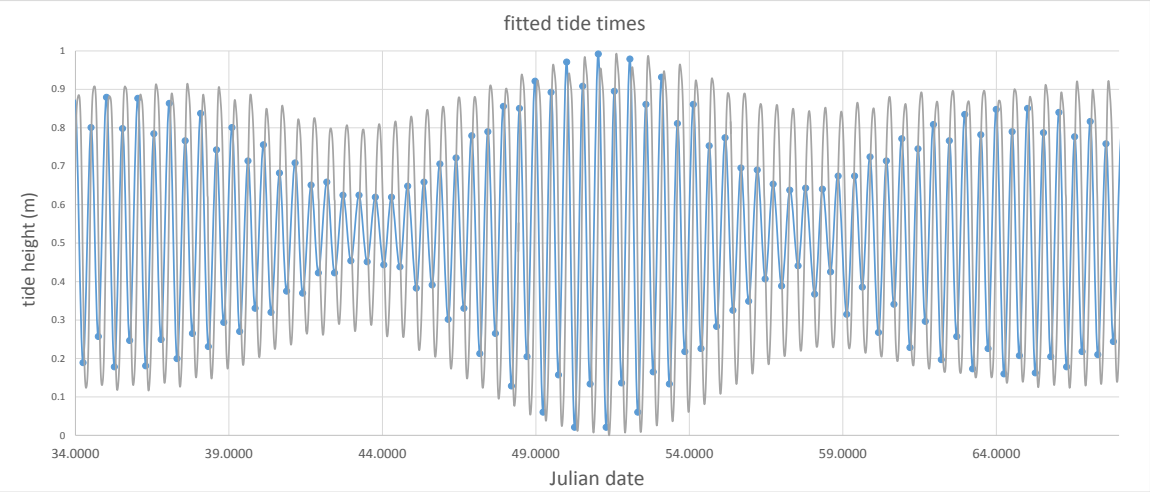

Note: Current speed is +ve for all values in the direction of the flood tide, i.e. flowing generally east and –ve for ebb tide. The plot shows the matching of the amplitudes of the current speeds and tidal heights during flood/neap cycles

Figure 6 Tidal heights at times of high and low water at a reference site on Stroma (blue) and current speeds (grey) at the western-most reference point on the centre east-west line of the MeyGen array site, for a 35 day period

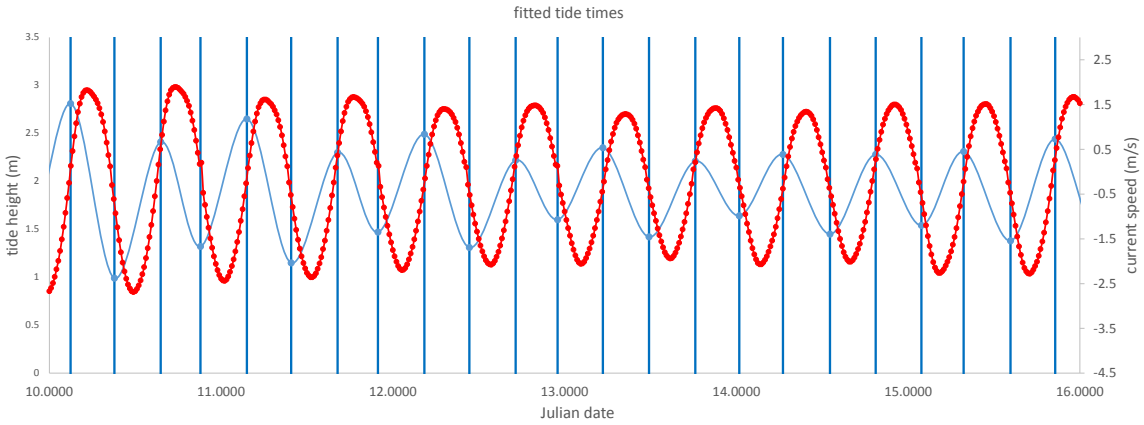

Figure 7 An expanded section of Figure 6 showing the final fit of the two tidal prediction data sets achieved by matching minimum absolute speed values to times of high and low water

6.4 Dive Selection

At both the Inner Sound and Eday sites, the majority of the swimming and foraging behaviour recorded by the tags occurred out with the sites themselves. In order to derive descriptors of dive and movement patterns relevant to the turbine sites, only dives occurring in close proximity to those sites were used (described below). A limited number of dives occurred at the turbine locations, so in order to include sufficient dives to provide robust estimates of movement parameters extended areas were assessed at both sites. Around the Inner Sound all dives that started or ended within an area including the proposed tidal array site and a 500 m buffer around the site were extracted. This produced a total of 2,711 dives from eight of the 14 tagged seals. The turbine test site at the Fall of Warness is closer to land, and a similar area would have included very shallow water close to the shore and an area around a haulout site. In that case, dives were extracted from a rectangular area bounding the four tidal data points provided from the ABPmer model (ABPmer, 2012), shown on Figure 42. This produced a total of 1,224 dives from four seals, although almost 85% of those were performed by one individual, which is a source of uncertainty in the degree to which the data are representative of the local population.

6.5 Assigning Current Vectors

A current bearing (direction of flow) and current speed were assigned to each dive. In each case, the location of the closest tide data point was assessed and a bearing and current speed value was derived from the model estimates by linearly interpolating in time between the bearing and speed estimates for the preceding and succeeding model estimate. Linear interpolation was justifiable here because the flow model estimates are provided at 15 minute intervals and therefore the frequency of location fixes was higher than that of the tidal data.

6.6 Dive Parameters

The GPS/GSM transmitters provide information on dive duration and post dive surface duration. The pressure sensors on the tags provided a 9 point depth profile for each dive with an accuracy of ± 1m. The tags also transmitted the start and end times of each dive and the maximum depth attained. The location and depth of each seal at any time could then be estimated by linearly interpolating in space the XY position and linearly interpolating in time between successive time depth records, assuming direct straight line movement between position fixes.

Two different dive shape descriptors were derived. A dive squareness index was calculated as the area under the time depth profile expressed as a proportion of the area of a rectangle given by maximum depth multiplied by the dive duration. In such an index a V shaped or spike dive will score around 0.5 while a flat bottomed dive will score close to 1, although this value will decrease in deeper dives. The proportion of time on each dive that was spent below a depth equal to a specified proportion of the maximum depth for that dive was estimated. Finally, the estimated frequency distribution of time spent at different depths in the water column was presented.

The depth of water at each dive site was extracted from the Sea-Zone TruDepth bathymetry data set using the latitude and longitude estimates for the start of each dive using the Manifold GIS package. For each dive, the maximum dive depth was expressed as a proportion of the estimated water column depth.

The tags were set to sample GPS only when at the surface and in order to conserve battery power and provide a useful tag life they were further restricted to sampling at intervals of at least 8 minutes. Not all surfacing events produced successful GPS fixes, and the combination of these restrictions produced a sampling rate of approximately one successful GPS fix every 13 minutes but with 57% of gaps being between 8 and 11 minutes. This leads to some error in the locations of the dives and that will be translated into error in the estimated seabed depth associated with the individual dives.

6.7 Seal Density Estimates

A density estimate can be derived directly from the telemetry data used to describe seal behaviour within the Inner Sound array site. The behavioural analysis is based on 2,711 dives which started or ended within an extended array site, taken as a rectangle that incorporated the tidal array plus a 500 m buffer (extended array site). Information on the duration of each of these dives and the subsequent surface interval is available.

Using the assumption of straight line movement between location fixes, the proportion of the dive plus surface duration that was spent within the extended array site was calculated; i.e. for dives both starting and ending within the extended array site 100% of dive plus surface duration was included. For dives which either started or ended within the array site + 500 m buffer, the proportion of the dive plus surface duration spent within the extended array site was included. The same calculations were also carried out for a smaller rectangular area of 0.8 km² that incorporated the expected locations of the phase 1 turbines plus a 250 m buffer zone.

The total dive time calculated as above provides a measure of seal occupancy (number of seconds in which any tagged seal occupied the site). Thompson *et al*. (2015b) reported that the total tracking time for the 14 tagged seals was 3.57 seal years. Dividing the occupancy time by the total tracking time provides an estimate of the proportion of the population present in the study site on average. The seal density is then simply the product of the proportion of seals present and the population estimate. Thompson *et al*. (2015b) estimated the size of the population at risk based on a 2013 harbour seal population survey and telemetry data from harbour seals tagged at sites throughout Orkney and the North Coast. Movement data from seals tagged at sites north of Orkney Mainland and within Scapa Flow suggested little or no movement into the study site. A population estimate based on the number of seals using haulout sites within a 10 km radius of the turbine array was selected as representing the population at risk. This was estimated to be 75 seals (95% confidence interval 61-100).The total time spent by the tagged seals in the large area, encompassing the entire array and a 500 m buffer zone, was 639,345 s, or 177.6 hr. Scaling this estimate by total tracking time of 3.57 yrs. and a seal population estimate of 75 and accounting for the area of the rectangle, 4.401 km² produces a density estimate of 0.097 seals/km². This estimate is based on the behaviour of 14 tagged seals. Only eight of these animals spent time in the study site and the amount of time varied widely between seals. Bootstrap estimate 95% confidence interval for the density estimate was 0.008 to 0.251 seals/km² were calculated by using the distribution of times spent in the study area by individual seals as the sample units and drawing 1,000 random samples of 14 values from that distribution

The same calculations for the smaller area, which encompasses the first phase of the MeyGen array development and consists of four turbines, and a 250 m buffer zone around the four turbines gives a tagged seal occupancy of 63,555 s or 17.6 hr. Scaling this estimate by total tracking time of 3.57 yrs. and a seal population estimate of 75 and accounting for the area of the rectangle, 0.802 km² produces a density estimate of 0.053 seals/km². Again this estimate was based on the observed behaviour of 14 seals, however only six of them spent any time in the smaller test area. Bootstrap estimate 95% confidence interval for the density estimate was 0.004 to 0.138 seals/km².

The discrepancy between these two density estimates is the result of fine scale differences in levels of seal activity within the array site. These small scale differences can have major effects. For example, moving the small area south by 500 m and 1,000 m produced estimates of 0.24 and 0.66 seals/km² respectively.

These density estimates are compared to other existing density estimates in Section 7.2.12 and are explored in more detail in Appendix 1.

The distribution of harbour seal haulout sites in the Pentland Firth allowed us to define a discrete local population to be used to scale up the seal occupancy estimates to produce a density estimate. At the Fall of Warness site, there are less telemetry data and there is no clear gap /separation in the distribution of haulout sites to allow us to define a discrete local population. In this case, there is no sensible alternative other than to use the seal usage maps (Jones *et al*., 2015) that incorporate telemetry and population count data for all sites that may be contributing to the seal density at the Fall of Warness.

6.8 Movement Estimates

For each dive, the locations of the start and end points were estimated by linearly interpolating between the preceding and following GPS location fixes, assuming constant speed movement in a straight line between GPS position fixes.

These estimated dive start and end points and the associated start and end times of the dive together with the model generated current speeds and directions were used to generate three vectors for each dive:

- A transit vector describing the track or course over the ground (speed and bearing of the measured horizontal displacement during a dive);
- A current vector describing the speed and direction over the ground of the current (this would be the expected transit vector for an object passively floating in the current); and
- An estimated swim vector, describing the horizontal component of swim speed and heading of a seal relative to the water, (this would be the expected transit vector for a swimming seal if there were no current).

The transit vector may be thought of as the resultant of adding the swim vector and the current vector. In practice it is the transit vector which was observed, and the current vector is modelled, so the swim vector is estimated by subtracting the current vector from the transit vector.

6.9 Transit Speeds

For each dive in the data set, the position at the start of the dive and the end of the dive and at the start of the next dive was estimated. The dive start and dive end

positions were used to estimate horizontal displacement during the dive and then divided by dive duration to estimate the speed over the ground or transit speed. The frequency distribution of transit speeds was heavily skewed to the left (Figure 8), i.e. the majority of estimates of speed over the ground were below 0.5 m/s. This is in clear contrast to the tidal current speed estimates for those same dives derived from the ABPmer flow model (Figure 9) which indicates that tidal current speeds are distributed as a skewed normal distribution with a peak at around 1.8 m/s

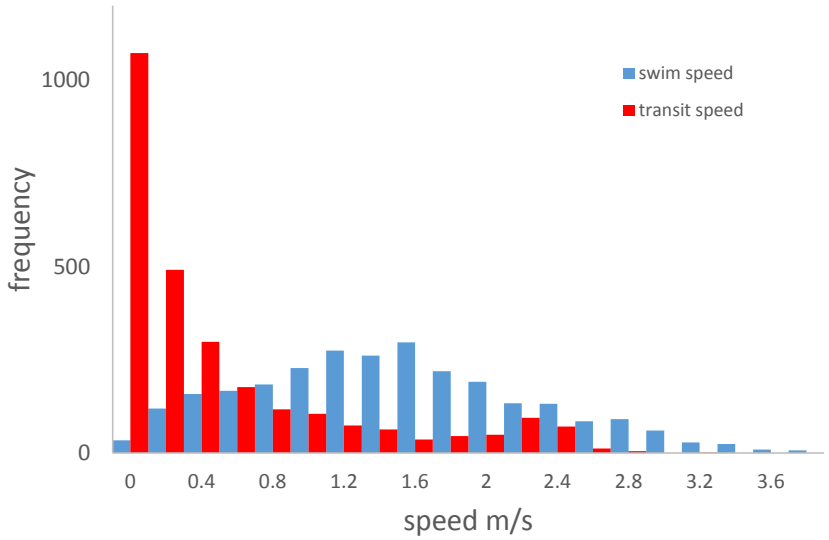

Figure 8 **Swim speed (transit speed minus current speed) and transit speed (speed across ground) estimates for 2711 dives by harbour seals in the vicinity of the proposed tidal array in the Inner Sound**

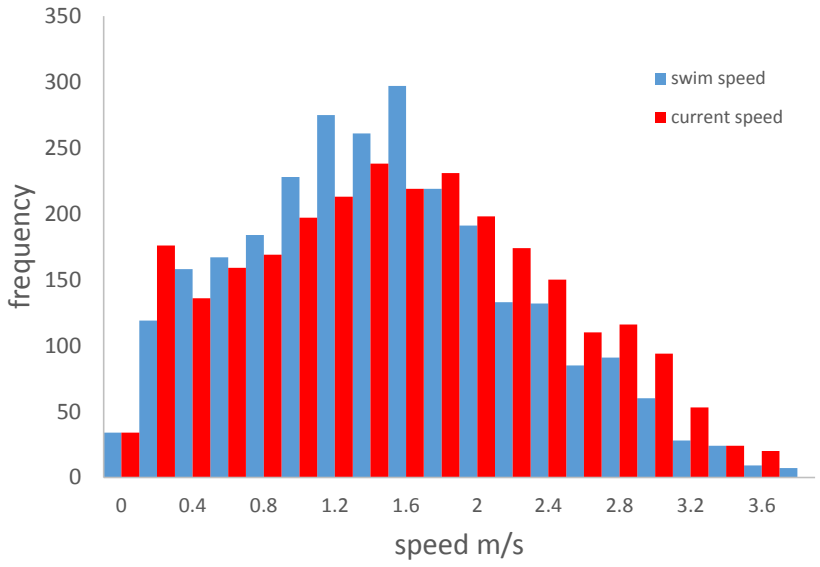

Figure 9 **Estimated swim speeds and current speeds derived from ABPmer tidal flow model for 2711 dives by harbour seals in the vicinity of the proposed tidal array in the Inner Sound**

These dives all occurred in open water, so the seals were presumably subject to those currents. Subtracting the current vector from the transit vector produces an estimate of the horizontal component of the swim speed and the heading of the seal.

As these values were based on the movements of seals calculated by linear interpolation between GPS fixes there is likely to be some error. However, the majority of that error would come from the lack of information on tracks between locations. At present there is no robust method available for determining the magnitude of this error.

The fact that the distribution of swim speed estimates so closely follows the frequency distribution of current speeds (Figure 9, Figure 10) is a consequence of the fact that transit speeds are generally slow (Figure 8) and current speeds are generally much greater. The seals are in open water and therefore presumably subject to the current. In order for the speed of movement over the ground to be less than the speed of the current the seals must be swimming into the flow. In most cases, the speed over the ground was slow, suggesting that seals were swimming directly into the current on most dives, or had the ability to exploit local small scale eddies to avoid the current.

Apparent swim speed estimates and swimming headings are estimated by subtracting the current vector from the transit vector. To compare the seals' swimming heading to the current bearing one is simply subtracted from the other. Figure 11 shows that in the majority of dives the seals were apparently swimming against the current.

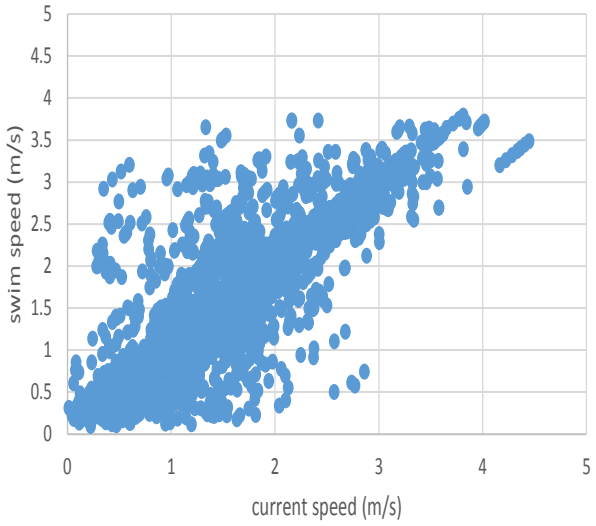

Figure 10 Estimated swim speed plotted against the estimated current speed for each dive

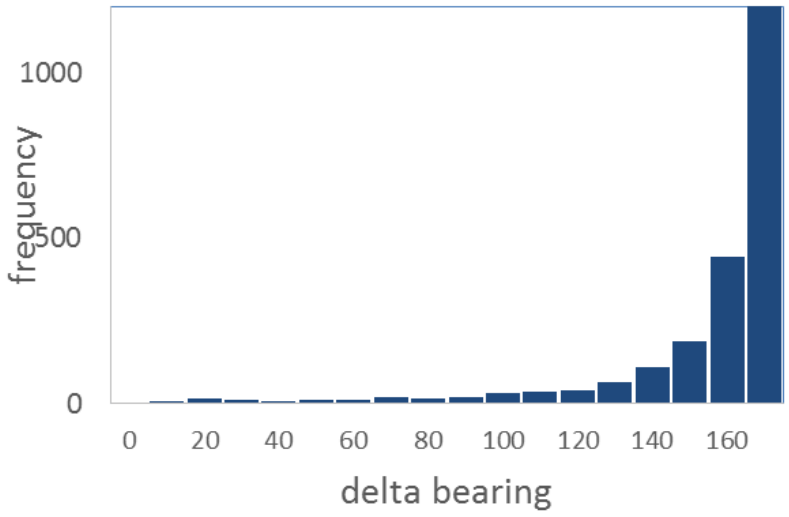

Note: Delta bearings are the differences between current bearing and seal swimming heading

Figure 11 Frequency histogram of delta bearings for individual dives in the vicinity of the tidal array site

A corollary of the data in Figure 12 is that the transit movements are in general aligned with the current. Figure 13 shows that the transits are generally orientated along an east-west axis on both the flood (flowing east) and ebb (flowing west) tides. However, the estimated swimming headings show that in most cases the seals are swimming directly against the prevailing current (Figure 11) with the seal heading west on most dives during flood tides and swimming east on most dives during ebb tides.

Figure 14 presents examples of dives by five different seals with the dive depth profiles for each dive. In all but two of these dives, the seal appears to have swum against the current and in the remaining two examples it swam across the current at approximately 90° to the direction of flow.

The dive depth profiles in Figure 14 are consistent with the limited or even apparent lack of movement across the sea bed in dives with swimming against the current. Seals generally swam direct to the maximum depth and show little vertical movement until swimming directly back to the surface at the end of the dive. This is consistent with seals holding station, against the current, at or close to the sea bed.

(a)

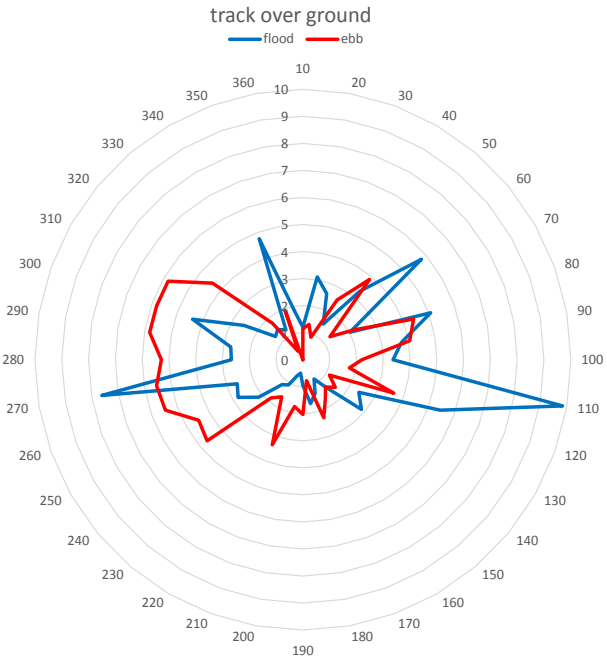

(b)

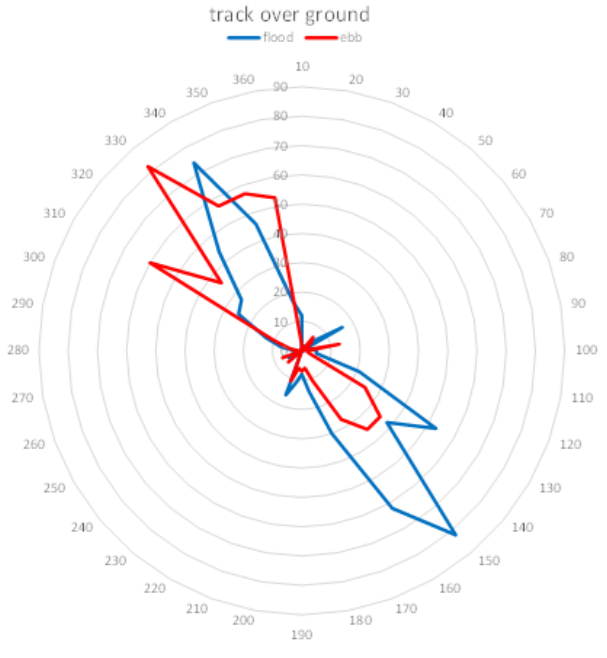

Note: Direction of the track over the ground for seals diving in the vicinity of the tidal array site, during flood (blue) and ebb (red) tides; a) MeyGen site; b) Fall of Warness Frequency of occurrence at each bearing is represented by distance from the centre

Figure 12 Frequency distribution of transit bearings

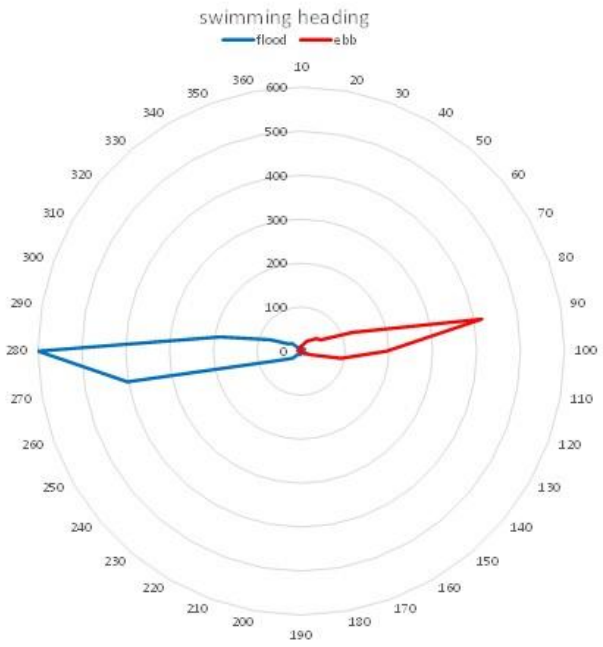

Note: Flood tides flow west to east and ebb tides flow east to west at the site. The data suggest that seals are swimming against the current in almost all dives. Frequency of occurrence at each bearing is represented by distance from the centre

Figure 13 Frequency distribution of swimming headings for seals diving in the vicinity of the MeyGen tidal array site, during flood (blue) and ebb (red) tides

Care should be taken in interpreting these data. The swim speed estimates are derived from the current flow data and assumes that the seals are in a water column that is moving at that speed. However, the ABPmer tidal flow model is a depth averaged model providing predictions of the movement of the entire water column. It uses the simplifying assumption that the flow rates and directions are constant with respect to depth in the water column. In reality, flow rates will be lower close to the sea bed. In addition, it is likely that irregularities in the sea bed will lead to significant eddies and areas of reduced flow downstream of topographical features. There will also be small scale irregularities in flow patterns that are not captured by the model. If seals are able to exploit such features, they may be able to effectively reduce the swimming effort required to maintain station against the flow..

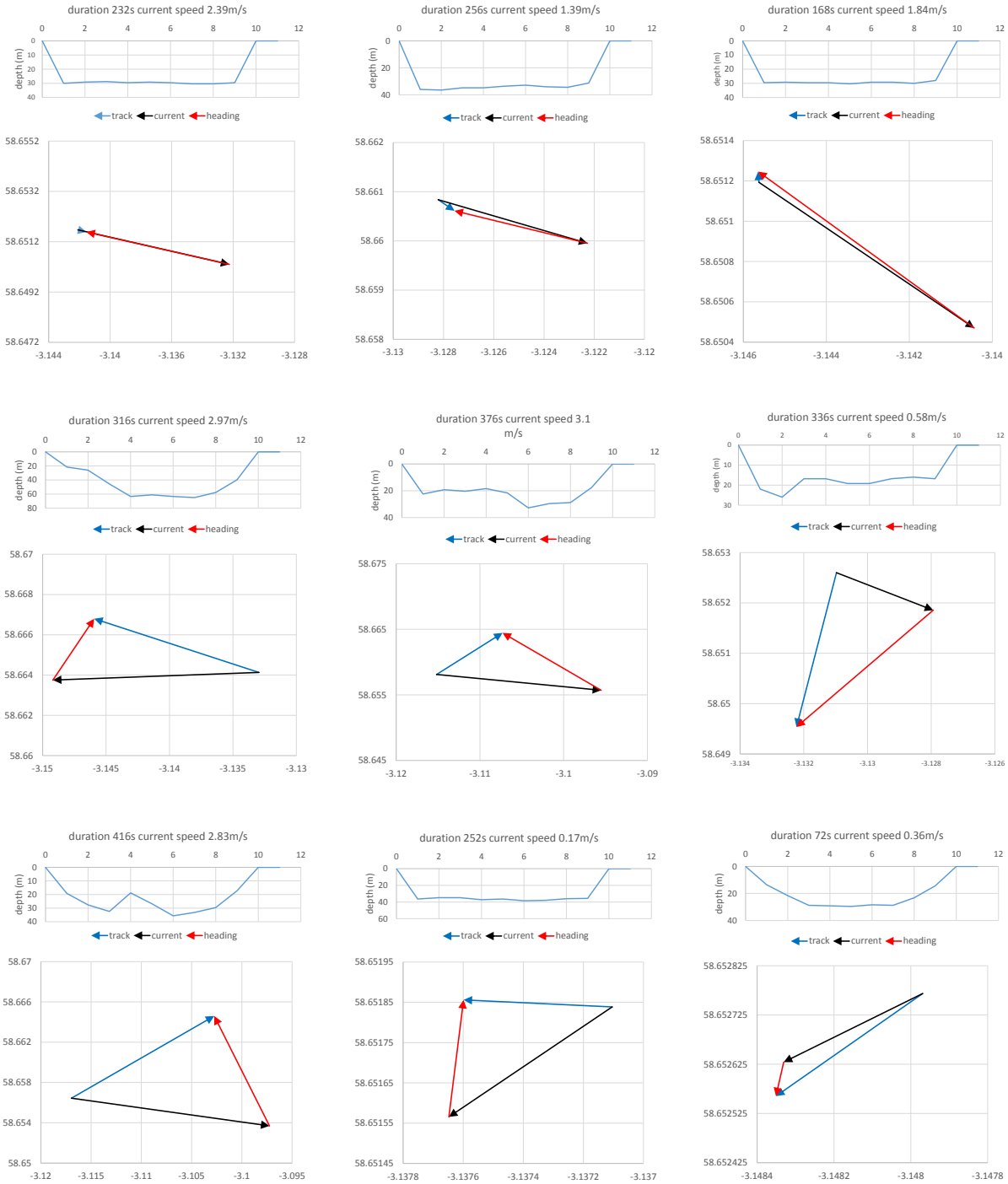

Note: For each dive, the upper pane shows the time depth profile, dive duration and current speed while the lower pane shows the direction of the track or movement over the ground (blue arrow), the direction of flow (black arrow) and the estimated swimming direction (red arrow). In all cases the length of the line is proportional to the speed and therefore also proportional to the distance moved during the dive

Figure 14 Vector diagrams and associated time depth profiles for a sample of individual dives in the vicinity of the tidal array site

6.10 Depth Distribution

A large number of dive profiles collected from harbour seals swimming in tidal rapids exist. As an example, Figure 15 shows the estimated swimming tracks of tagged harbour seals swimming in the Inner Sound with the approximate array location.

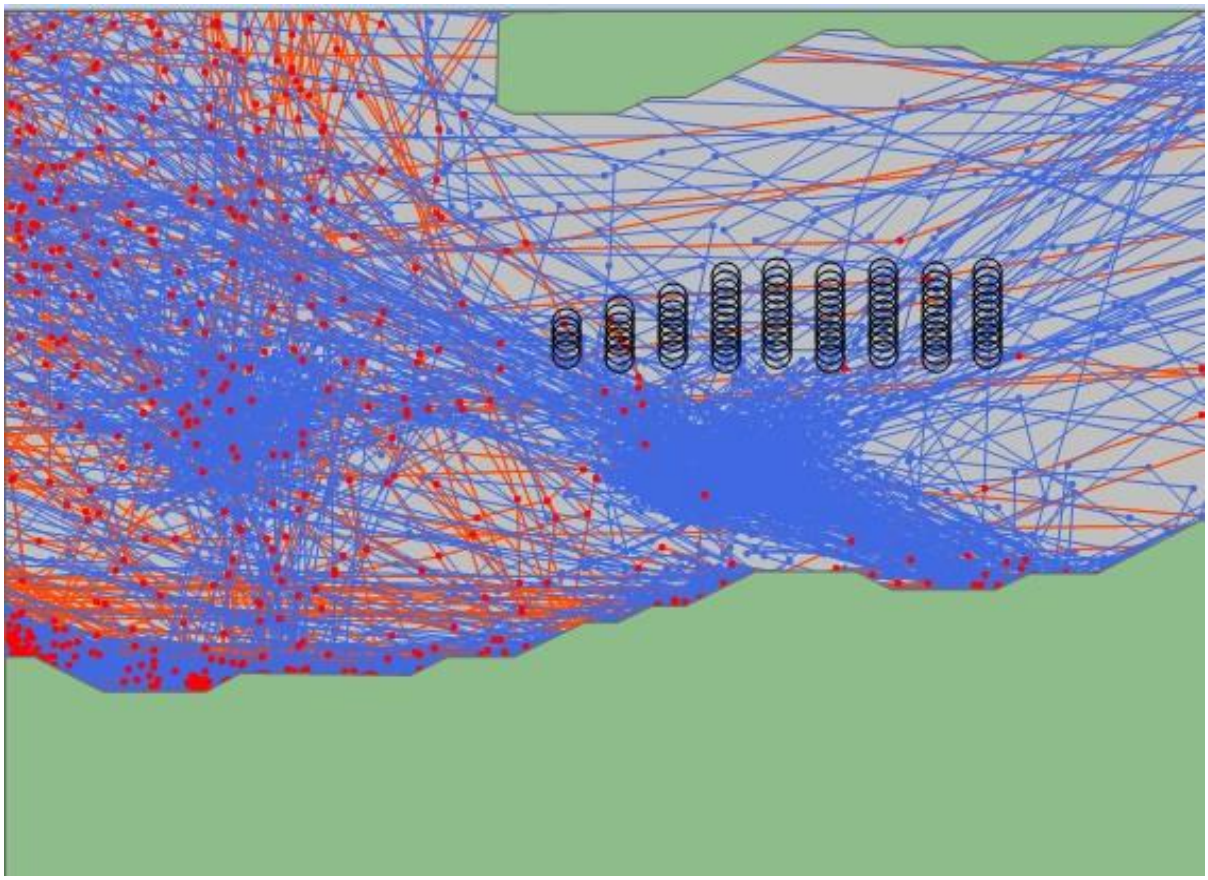

Note: The black circles represent the proposed MeyGen tidal array

Figure 15 Swimming tracks of harbour seals in the Inner Sound, Pentland Firth

The available data comprise a series of GPS locations at approximately 15 minute intervals and a complete set of dive profiles with nine depth estimates evenly spaced through each dive. The XY location of the seal at the start and end of each dive is estimated by linearly interpolating between the location fixes. The water depth at the dive location was extracted from the TruDepth data base.

The locations of the dives are interpolated on the assumption of constant speed and straight line travel between location fixes, leading to some error in the estimate. The variable bathymetry in the areas of interest can also lead to significant error in the estimated water depth for each dive. In previous iterations the depth profiles have been presented as proportions of time spent in depth bins as a proportion of the maximum depth of each dive (Thompson, 2015). For the Inner Sound, this produces a mean proportion of time at depth profile as shown in Figure 16. The majority of time during the dive is spent close to the bottom of the dive. This was assumed to represent the proportion of time spent close to the sea bed. However, in the data for the Inner Sound there appear to be a significant proportion of the dives in mid water. This could lead to an increased probability of seals encountering turbines in mid water and consequently the risk of them colliding.

The data presented below are from harbour seals tagged at Gill's Bay. They are all dives which are estimated to have been within the proposed extended turbine array site.

The major caveats are:

1) The dive locations are estimates. Location quality from the GPS tags is very good, but still has some uncertainty, usually assumed to be ±50 m. A fix is not received for every surfacing, so the locations of dives are linearly interpolated between location fixes.

2) To avoid this interpolation error, only dives that either start or end at the time of a location fix are included. This dramatically reduces the number of useable dive profiles. For this harbour seal study, there are sufficient dives in the vicinity of the proposed array to make such data thinning acceptable. This is unlikely to be the case in most locations for harbour seals and any locations for the more widely ranging grey seals.

There are several alternative ways to use the data to estimate the use of the water column. Figure 16 and Table 3 show the proportion of time spent at different depths during dives, expressed as a percentage of the maximum depth on each dive. Data are shown separately for dives occurring during ebb and flood tides. The profiles for ebb and flood tides are almost identical so the depth distributions were not separated into different tidal states.
.

Table 3 The proportion of time spent at different depths during dives, expressed as a percentage of the maximum depth on each dive

Depth (Prop. Max Depth)	Proportion of Time (Ebb Tide)	Proportion of Time (Flood Tide)
0	0.193	0.147
0.05	0.000	0.001
0.1	0.005	0.008
0.15	0.011	0.014
0.2	0.024	0.025
0.25	0.007	0.011
0.3	0.009	0.017
0.35	0.016	0.023
0.4	0.023	0.029
0.45	0.012	0.018
0.5	0.017	0.022
0.55	0.020	0.022
0.6	0.025	0.030
0.65	0.018	0.021
0.7	0.022	0.022
0.75	0.029	0.028
0.8	0.037	0.038
0.85	0.040	0.038
0.9	0.065	0.059
0.95	0.127	0.118
1	0.300	0.309

Data are shown separately for dives occurring during ebb and flood tides.

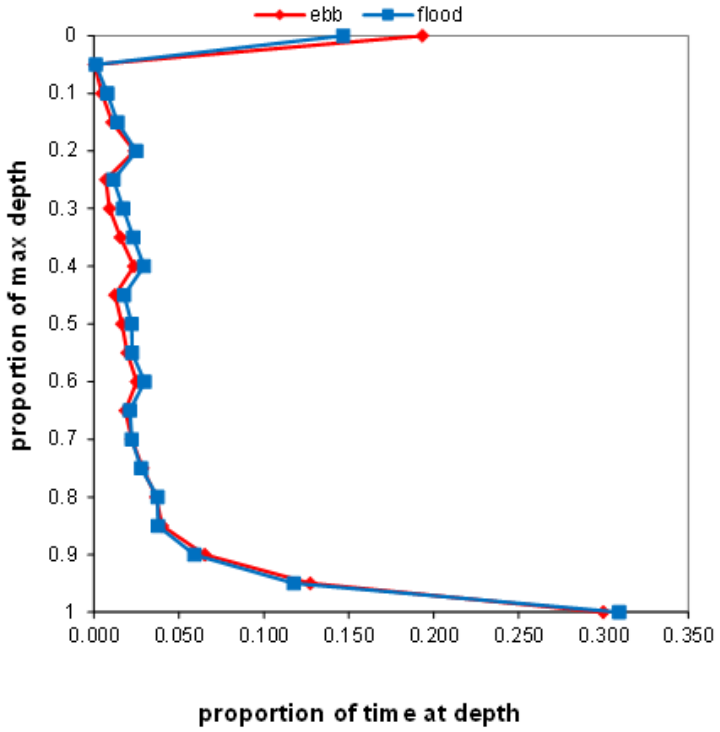

Note: Data are shown separately for dives occurring during ebb and flood tides

Figure 16 The proportion of time spent at different depths during dives, expressed as a percentage of the maximum depth on each dive

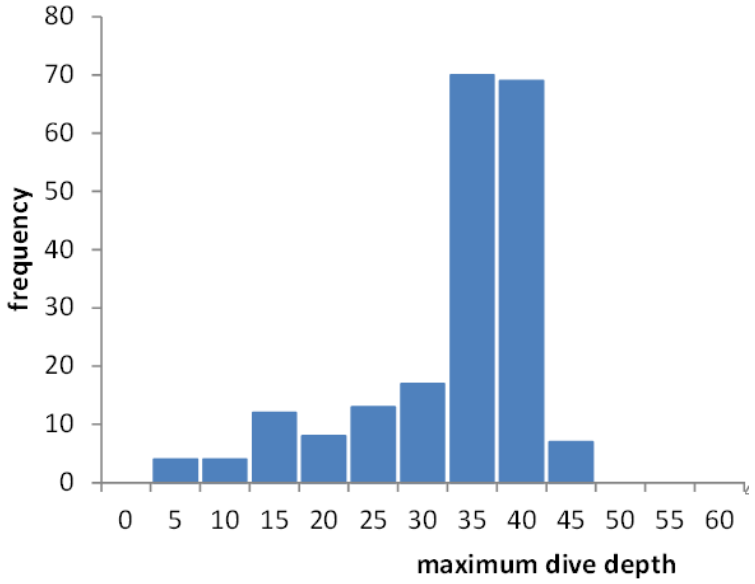

Note: There were 208 dives in the data set

Figure 17 Frequency distribution of dive depths (maximum depth within each dive) within the array site in Inner Sound

As mentioned previously, the assumption that almost all harbour seal dives go to the sea bed does not hold for dives in the Inner Sound. Figure 18 shows the maximum depth of each dive plotted together with the estimated water depth at the estimated dive location. There appears to be a substantial component of mid water diving: in approximately 22% of dives the maximum depth was between 30% and 70% of the estimated water depth. This could have been due to position error leading to over estimates of water depth for some dives. However, restricting the dive sample to those that occurred close in time to a location fix did not remove the mid water dives. Figure 18 shows dives that started or ended within 5 minutes of and 1 minute of a location fix, showing that the intensity of the time filter did not appear to have any effect on the proportion of mid water dives. Thus it can be concluded that the mid water diving is real and not an artefact of the interpolation

.

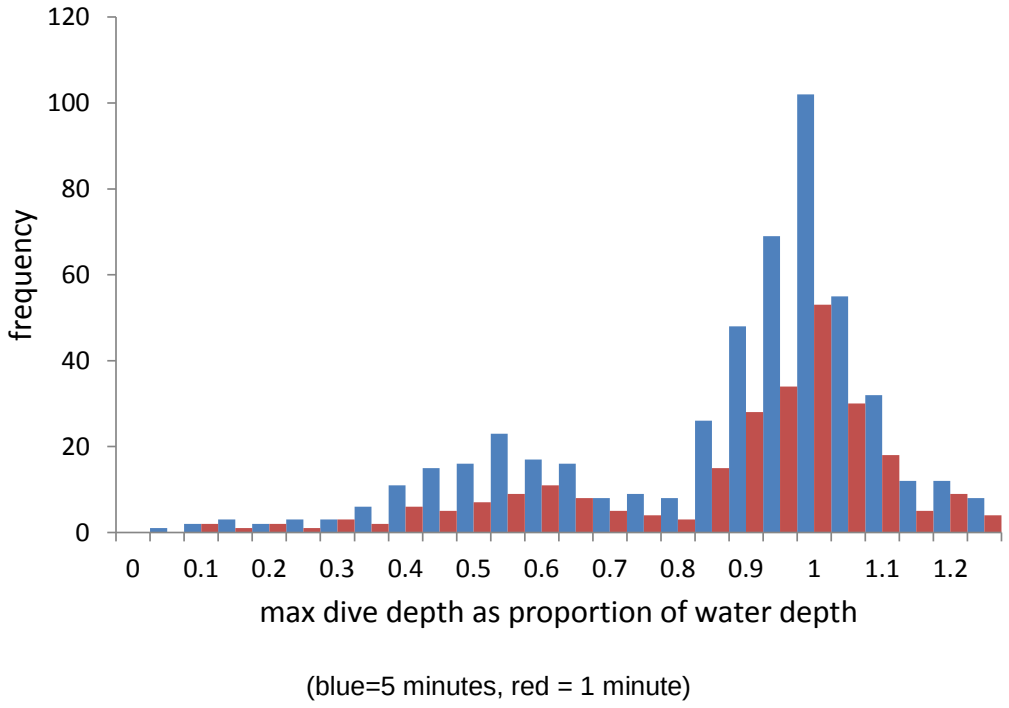

(blue=5 minutes, red = 1 minute)

Figure 18 Maximum dive depth expressed as a percentage of the water depth at the location fix nearest in time to the dive

Figure 19 and Table 4 shows the same depth distribution data shown in Figure 18 but pooled for both flood and ebb tides and stratified by water depth. In shallow water <20 m deep, all of the dives appear to go to close to the sea bed, but in deeper water there are a substantial number of midwater dives

Given the uncertainty about the dive locations, the simplest solution is to assume that the observed distribution of time at depth from the raw dive data provides the

most appropriate descriptor of dive behaviour. As there is a substantial dataset of dives, it is also possible to extract dive depth distributions for different depth ranges.

Table 4 **The proportion of time spent at each depth for dives in 20-30 m and 30-40 m deep water in the Pentland Firth**

Depth (m)	20-30 m	30-40 m
0	0.20	0.22
5	0.06	0.04
10	0.13	0.11
15	0.14	0.14
20	0.11	0.09
25	0.24	0.07
30	0.12	0.19
35		0.12
40		0.02

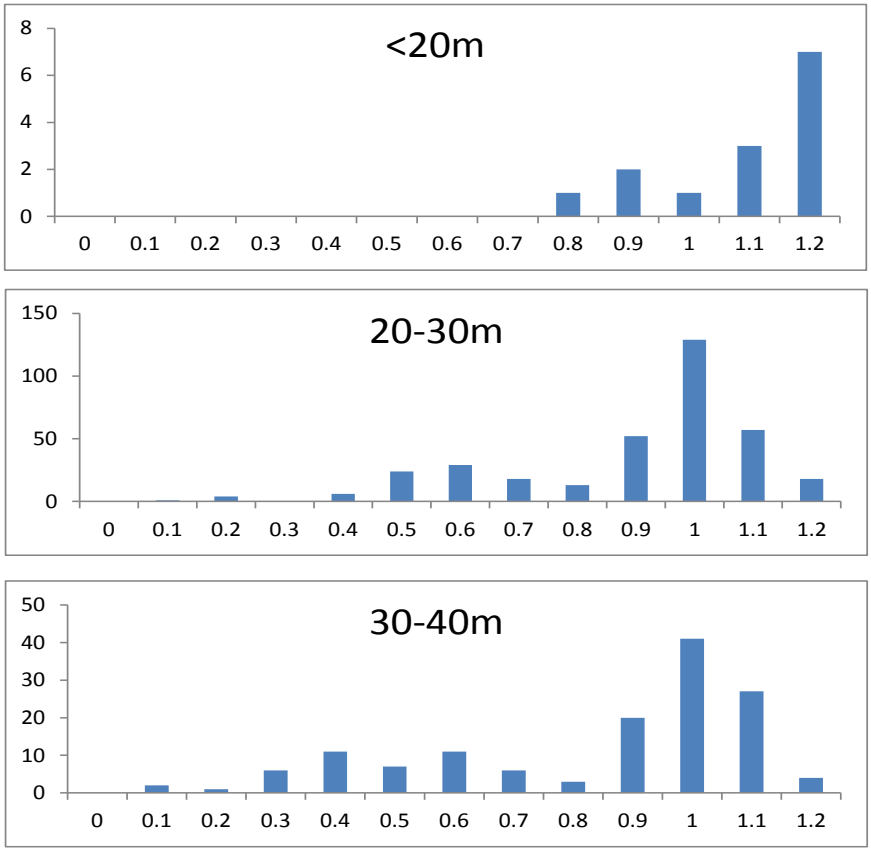

Figure 19 **Maximum dive depth as proportion of water depth in water depth bins 0-20, 20-30 and 30-40 m**

6.11 Effects of Tidal State on Depth Distribution

Both the dive squareness index and proportion of time spent below 80% of the maximum depth attained on that dive showed significant differences between flood and ebb tides (Figure 20, Figure 21) (proportion of time at more than 80% of maximum dive depth t = 4.23; p<0.0001; dive shape t= 6.01; p<0.0001).

Examination of the dive squareness data in Figure 21 suggests that this is due to the presence of a larger number of more V shaped dives during the flood, represented by the small secondary peak at around 0.6 (a higher proportion of time in midwater). Given the large sample size, the observed differences are significant, but, the effect on time spent at different depths in the water column will be small. Although there are statistically significant differences, these do not represent a large physical difference in distribution of time at depth and are likely to have a relatively small effect on CRM estimates. For the purposes of the CRM, dives on flood and ebb tides have been assumed to follow the same depth distribution patterns.

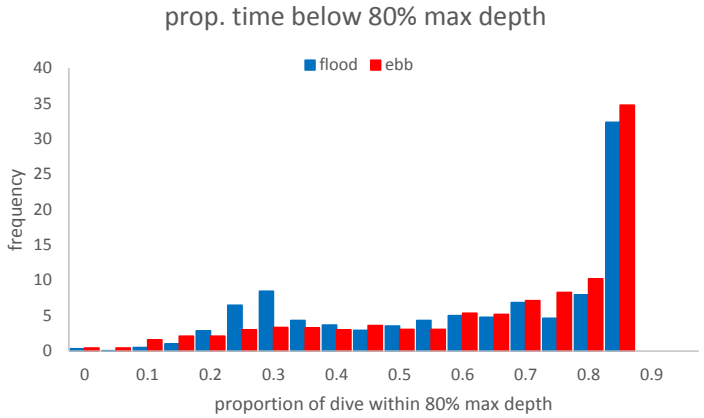

Figure 20 Frequency distribution of dives with different proportions of the dive spent below 80% of the maximum depth

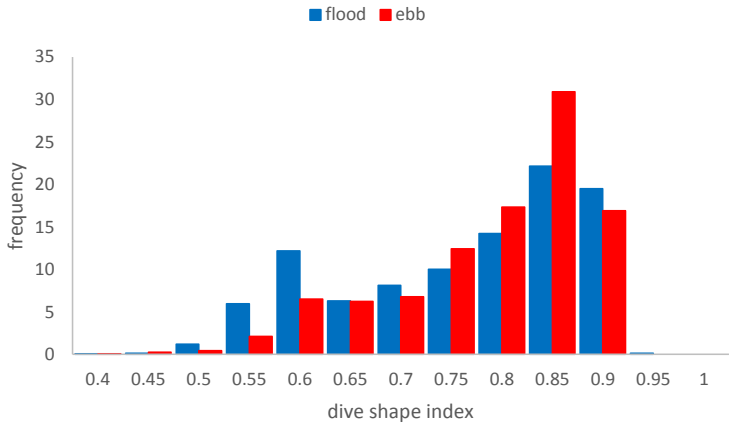

Figure 21 Frequency distribution of dive squareness index

6.12 Effects of Tide State on Transit Speed

Transit speeds were estimated as the rate of movement along a straight line connecting the GPS location fixes before and after a particular dive. Mean transit speeds were 27% higher during ebb tides compared to flood tides at the MeyGen site (Figure 22a) but were not significantly different between ebb and flood tides at the Fall of Warness site (Figure 22b). The difference at MeyGen was significant and is likely to influence the collision rate estimates. This difference was likely to be the consequence of the differences in current speeds encountered during flood and ebb tides at the study site with mean speeds of 1.8 m/s and 1.5 m/s respectively. However, overall there was no clear relationship between current speed and transit speed at the MeyGen site (Figure 23). These transit speed distributions have been used to inform the CRM.

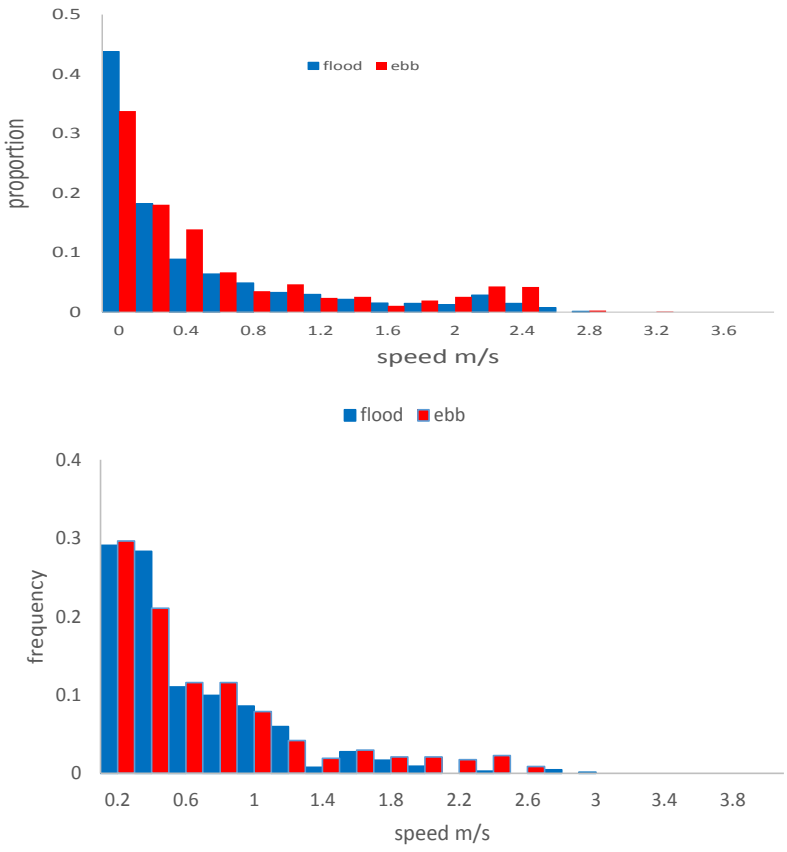

Figure 22 Frequency distribution of transit speeds during flood and ebb tides a) at the MeyGen array site; b) at the Fall of Warness

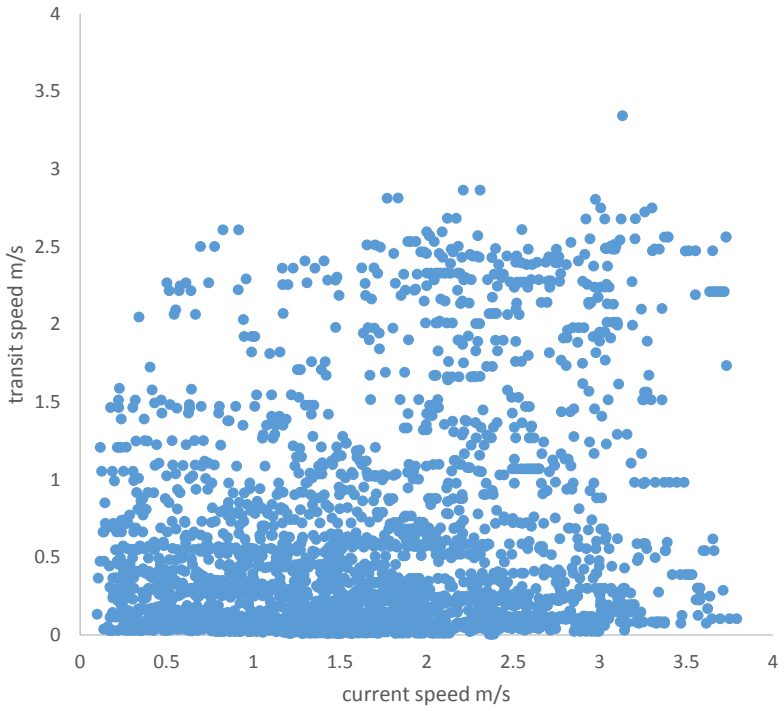

Figure 23 Transit speed against current speed at the MeyGen array site. There was no clear relationship between transit speed and current speed

Estimated swim speeds are higher on the flood than ebb tides, but it is not clear if this is the result of actively swimming faster, or more directed swimming, during dives on ebb tides. It is possible that seals are actively avoiding the current to some extent. The ABPmer model produces a depth averaged flow rates for each location. Currents are likely to be lower close to the seabed and topographical features can produce significant eddies and areas of reduced flow. Seals may be able to exploit such features, which could give rise to an apparent swim speed against the current, and result in low transit speeds.

An important aspect of the movement patterns for collision risk estimates is the direction of transit relative to the flow. For both sites, the transit direction relative to flow was extracted. As before, ebb tide was defined as any current going generally west (i.e. between 180° and 360°) and flood as current going east (i.e. between 0º and 180°). Each dive was then scored positive i.e. going downstream, if the difference between bearing of track over ground and heading of the current was less than or equal to 90° and negative, i.e. going upstream if it was greater than 90°.

At both sites, but particularly at the MeyGen site, there are a cluster of higher speed transits at around 2 m/s when the seals are going with the current (Figure **24**). These could represent active swimming during low flow or passive drifting during downstream swimming.

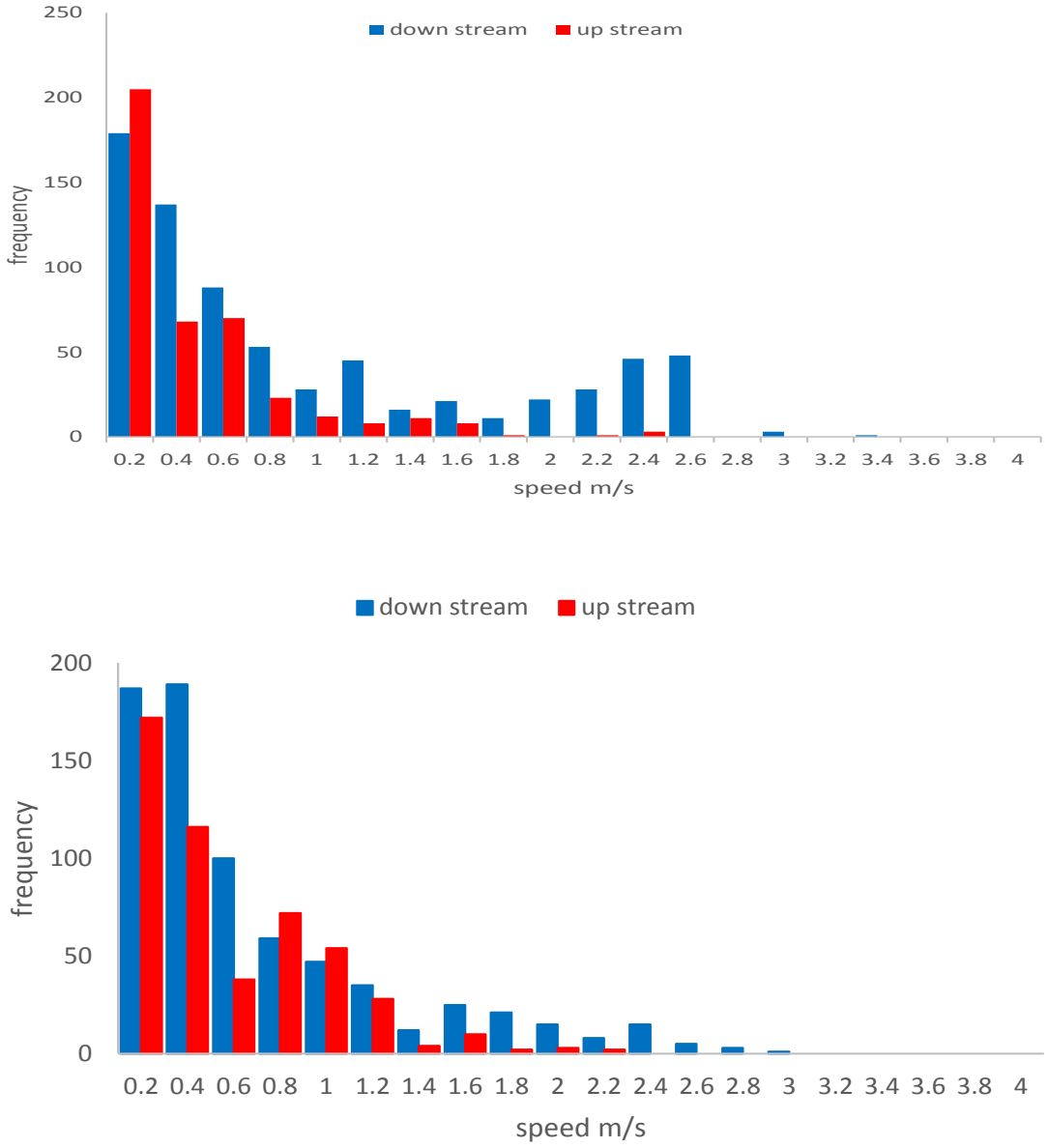

Figure 24 **Frequency distribution of transit speeds going with the flow (downstream) and against the flow (upstream) a) at the MeyGen array site; b) at the Fall of Warness**

6.13 Implications for Assessing Collision Risk in Orkney and the Pentland Firth

In terms of potential effect on CRM estimates, the most striking result is the observation that seals at both locations generally swam against the tide. On most dives, the seal's movement over the ground (transit) was slow, despite the often fast moving currents at those sites. These transit speeds have a direct bearing on the likelihood of being hit by a turbine blade if a seal passes through the swept area. Slow transit speeds will increase that probability. Conversely, slow transit speeds will also reduce the number of times seals will be assessed to pass through the swept areas, and may give approaching seals more time to detect turbines. The transit speeds are presented for each site and divided into flood and ebb tidal phases and further divided into dives with transits going with or against the current (Figure 24). Interestingly the transit speeds do not appear to be related to current speeds (Figure 23).

A corollary of these slow transits over the ground and the high estimated current speeds is that the estimated swim speeds (i.e. speed relative to the water mass rather than speed over the ground) are closely related to current speeds. This may indicate that seals are expending large amounts of energy swimming actively against the current to maintain position or more likely indicates that seals are able to use fine scale flow and turbulence features to minimise the effects of the current.

The distributions of swimming activity at different depths in the water column were estimated from high resolution dive depth profiles (nine depth points per dive) transmitted for each dive by the tags. These were compared to the depth of the water column at the estimated dive locations using depth estimates from a high resolution bathymetry data set (TruDepth).

The data suggest that the seals spend a large proportion of each dive at the bottom of the dive, producing mostly flat bottomed U shaped dives profiles. These patterns do not differ between flood and ebb tides and do not appear to vary with current speed. The dive depth distribution derived from the tags has been used to produce depth usage profiles for seals swimming in different water depths which can be adopted in collision assessments for other sites.

7 Model Refinements

7.1 The ‘Basic’ Collision Risk Model

The Collision Risk Model in its ‘basic’ version, as applied to underwater turbines and marine wildlife, is described in ‘Assessing collision risks between underwater turbines and marine wildlife: Guidance on using three models’ (Scottish Natural Heritage, 2016). A spreadsheet distributed with that guidance facilitates the calculations required.

The CRM calculates the probability of an animal colliding when making a single passage through a rotor. This probability depends on the radius at which the passage through the rotor is made. For modelling purposes, the animal is taken to be a hard object consisting of two equal circular cones stuck base to base, swimming along the direction of the axes of both cones. The blades of the rotor are taken to be laminar, but with a blade width profile which tapers off towards the blade tips, and with a twist along their length, such that the pitch of the blades (the angle between the blade and the rotor plane) increases towards the hub.

By repeating this calculation for each point of the rotor, the basic CRM calculates the average collision risk for a single passage, assuming that animals have an equal likelihood of passage at any point in the rotor. This is then multiplied by the estimated flux of animals passing through the rotor disc, calculated on the basis of the density of animals in the water and their swim speed relative to the rotor. In the basic version, known information on seal behaviour is used to estimate the proportion of animals at risk depth (i.e. between the minimum and maximum depths of the rotor) and the animals are then assumed to be uniformly distributed within this depth range.

The result is an estimated mean collision rate, assuming that animal behaviour is unaffected by the turbines, that is that animals do not avoid the area, navigate between turbines, take effective escape action in response to approaching blades, or indeed are swept clear by the force of water. The result is therefore a ‘no-avoidance collision rate’ and must be qualified by a reasonable view (based on monitoring of existing installations, or expert advice) on the likely levels, if any, of avoidance.

7.2 Possible Refinements

Section 4 outlined the range of possible refinements that were being considered in the course of this review. This section details investigations of these refinements. The following section considers a total of twelve possible refinements to this calculation, taking better account of factors like depth distribution, blade shape, turbine characteristics, and the effect of the current on animal speed through the turbine. One refinement also considers whether a collision is likely to be fatal, by introducing a mortality factor dependent on blade-animal closing speed. Each refinement is described in turn, and its effect demonstrated on a typical collision risk calculation. Unless otherwise stated, the result of applying the refinement is compared with the result of the basic model without any refinements. For the purpose of this section on exploring refinements, models were run for a single rotor, 3 blades, 18 m diameter, 2 m max chord width, standard profile, tip pitch 5 degrees, rotation speed 12 rpm, minimum depth below surface 8 m; animal length 1.6 m, 0.38 m width, speed relative to rotor 1.64 m/s, body ratio 0.5.

7.2.1 Refinement 1: Making Use of a Depth Distribution

If in fact the density of animals varies with depth, then it is quite possible that peaks in animal density may coincide with parts of the rotor which are either more or less risky than average. Figure 25 shows for a typical rotor and marine animal how the probability of collision for a single transit decreases with distance out from the hub; near the hub the probability is limited to 1, meaning collision is certain.

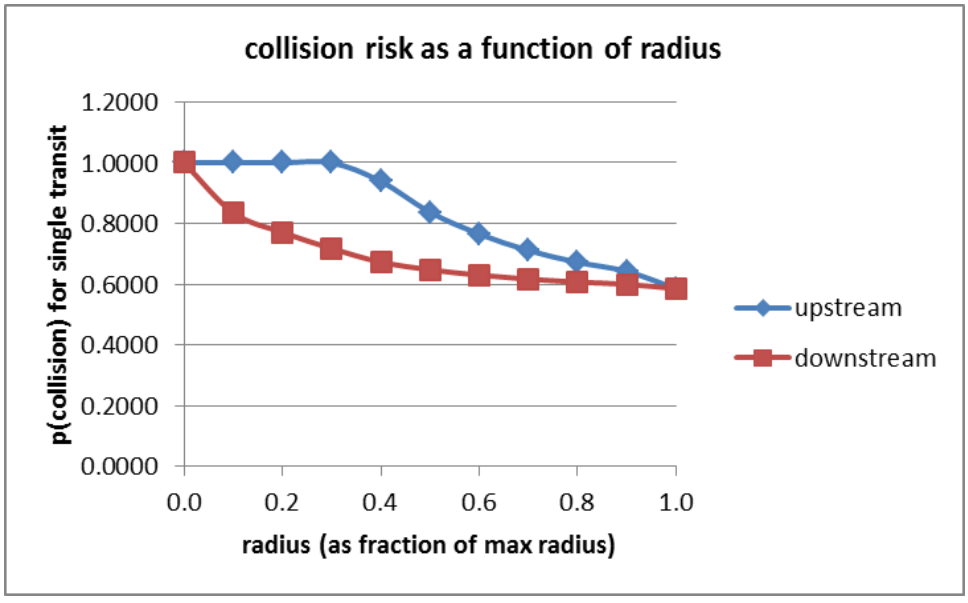

Figure 25 Variation in collision risk with distance from hub

Animals passing through a rotor disc near its maximum depth are therefore exposed to a lower risk than those passing through at or around hub height. In this refinement, the model evaluates the collision rate at each point in the rotor, taking account of both the collision risk and the animal density at each such point, and then sums this over the area of the rotor. This requires knowledge of the likely depth distribution of the animals.

This extension to the model has already been widely used (and termed the 'extended model') in assessing the collision risk between seabirds and offshore wind farm turbines (Band, 2012a). Many seabirds have a flight height distribution concentrated within the first 50 m or so above the sea surface. With turbines in excess of 150 m to the highest rotor tip, and a minimum clearance of the rotor tips from the sea surface of 22.5 m, a majority of those birds flying through the rotor do so through the lowest parts of the rotor, where collision risk is least. For some seabird species, using the flight height distribution in this way has led to estimates of collision rate which are reduced by a factor of 2 or 3 relative to the estimate derived using the basic CRM.

For harbour seals, a distribution of depths has been drawn from telemetry data in the Inner Sound (Thompson, 2015). Clearly the depth distribution is dependent on the depth of the seabed. The data used are those based on seabed depths in the range 30-40 m (see Section 6.10). There is significant uncertainty inherent in the data as seabed depth could only be calculated at the GPS locations where the monitored seals surfaced, which could be many metres away from where the seals spent their time in the water column. Nonetheless, this is the most detailed information available on the use of different water depths in a tidal channel. Figure 26 shows the depth distribution data obtained from the Inner Sound, while the straight line function connecting the midpoints of each histogram bar is the continuous depth distribution used by the CRM spreadsheet. To estimate seal abundance at any given depth, the CRM spreadsheet uses a straight line interpolation based on the underlying histogram data. It is clear that, over the range of depths occupied by a 20 m rotor with a minimum clearance depth of 8 m to the sea surface, the distribution is not uniform but exhibits shallow peaks around 10-15 m and around 25-30 m depth - though the latter may be a product of the uncertainty in water depth noted above.

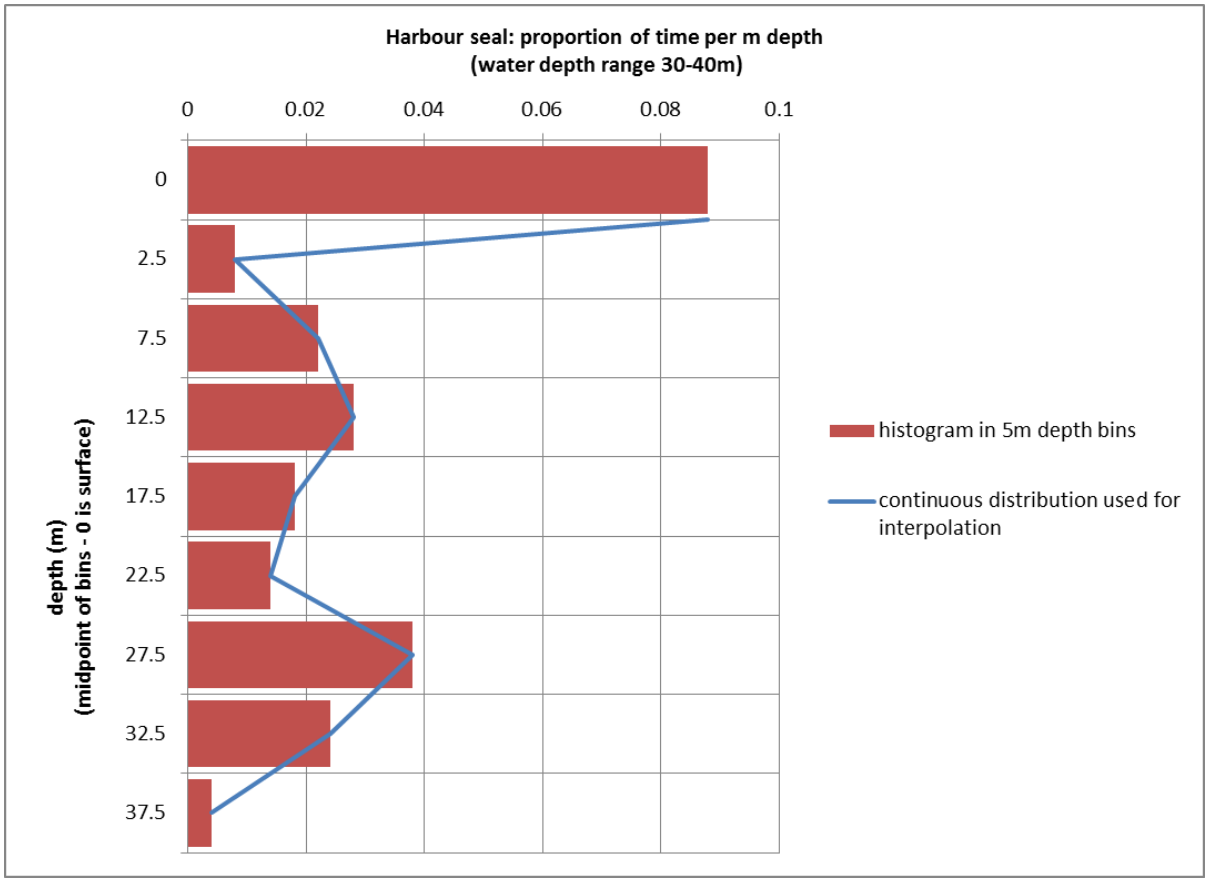

Figure 26 Depth distribution of harbour seals in Inner Sound, Pentland Firth

Table 5 Comparison of mean collision risk for a single transit, as calculated using the basic and extended models

Mean Probability of Collision (%) for a Single Transit						
	Rotor Diameter					
Model	16 m		18 m		20 m	
	Upstream	Downstream	Upstream	Downstream	Upstream	Downstream
Basic	76.4	65.1	75.5	63.6	74.8	62.3
Extended	59.3	50.5	65.1	55.1	73.5	61.9

Table 5 reveals modest differences between the results of the basic and extended models, when applied to rotors spanning different depth ranges. While for a rotor diameter of 16 m, the extended model yields collision rates lower by around 22% than the basic model, the difference is reduced to almost zero for a rotor of diameter 20 m. A 20 m diameter rotor extends down to a depth of 28 m, thus picking out the 25-30 m peak in the depth data. The mean collision risk thus reflects the density of animals at different depths, as well as the risk for each transit (Note that Table 5

should not be taken as illustrative of the effect of different rotor diameters generally – all three rotors in this table use the same rotation speed and blade width, whereas in general larger rotors turn more slowly and have a greater blade width).

7.2.2 Refinement 2: Blade Profile – Width and Twist

The shape of a turbine blade is described in the model by a 'maximum chord width' C, which is the width of the blade at its widest point, and a blade profile factor c/C which is listed in a table for different radii out from the rotor axis. For any given radius, the product of C and c/C is the chord width at that radius.

As included in the spreadsheet accompanying the guidance on the 'basic' version, the CRM makes use of a blade width profile drawn from a wind farm turbine blade. Figure 27 shows blade profiles c/C as a function of radius, both for the basic CRM (i.e. that based on a wind turbine blade) and for a typical tidal turbine design described in detail by Thompson *et al*. (2015b), referred to in this document as the 'exemplar turbine'. The general shape is similar, though the blade root – that part of the blade, usually circular in cross-section - devoted to attachment to the hub - takes up a higher proportion of the radius of the tidal turbine.

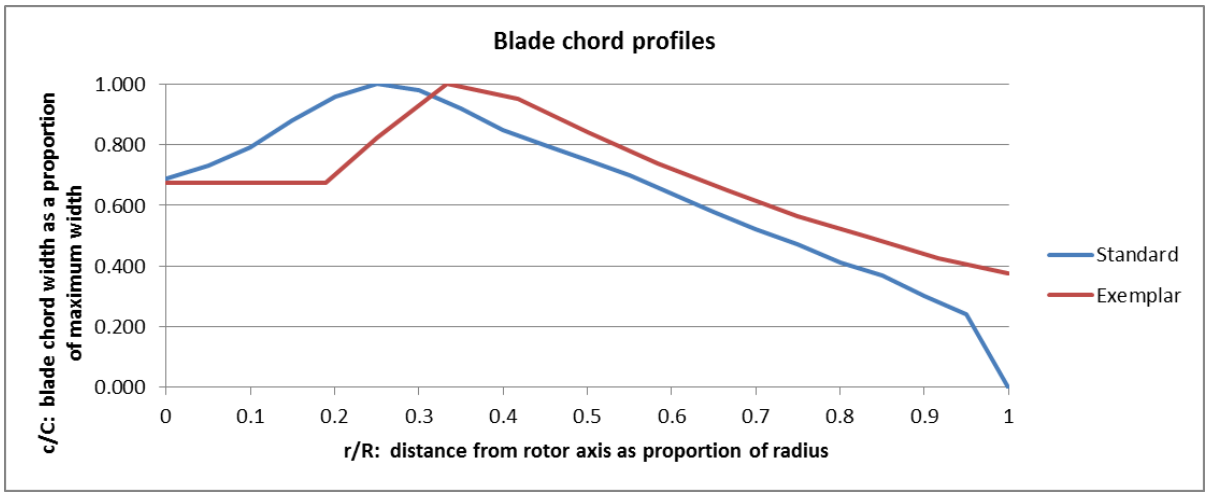

Figure 27 Blade chord profile for exemplar turbine and the standard profile used for wind turbines

The 'basic' CRM uses a calculated pitch angle of the blade at any given radius, given the pitch angle at the blade tips. Imagine that the water is stationary. The rotor blades are rotating and at the same time advancing through the water, making a helical passage. At the tip (at radius R), in a single revolution the blade tip travels a distance $2\pi R$ in the plane of the rotor. If the blade tip has pitch γ_{tip}, then it advances

a distance $2\pi R \tan \gamma_{tip}$. Similarly, at any arbitrary radius r on the blade, where the pitch is γ, the blade advances by $2\pi r \tan \gamma$. But to minimise stress on the blade, all parts of the blade must advance through the water by the same distance. Thus:

$$2\pi r \tan \gamma = 2\pi R \tan \gamma_{tip} \text{ so } \gamma = \tan^{-1} [(R/r) \tan \gamma_{tip}] \quad (9)$$

This formula gives the pitch at intermediate radii, if the pitch at the tip is estimated. It is an approximate formula which takes no account of the loading on the blade or design angle of attack or the aerofoil cross-section of a real blade.

Figure 28 shows the pitch profile using this formula, based on a pitch at the tip of 5°. Also shown is the pitch of the exemplar turbine blade. There is a high degree of similarity between the calculated pitch profile and the one for this exemplar turbine, though close to the blade root the similarity breaks down as the blade cross-section becomes near-circular to enable its attachment at the blade root.

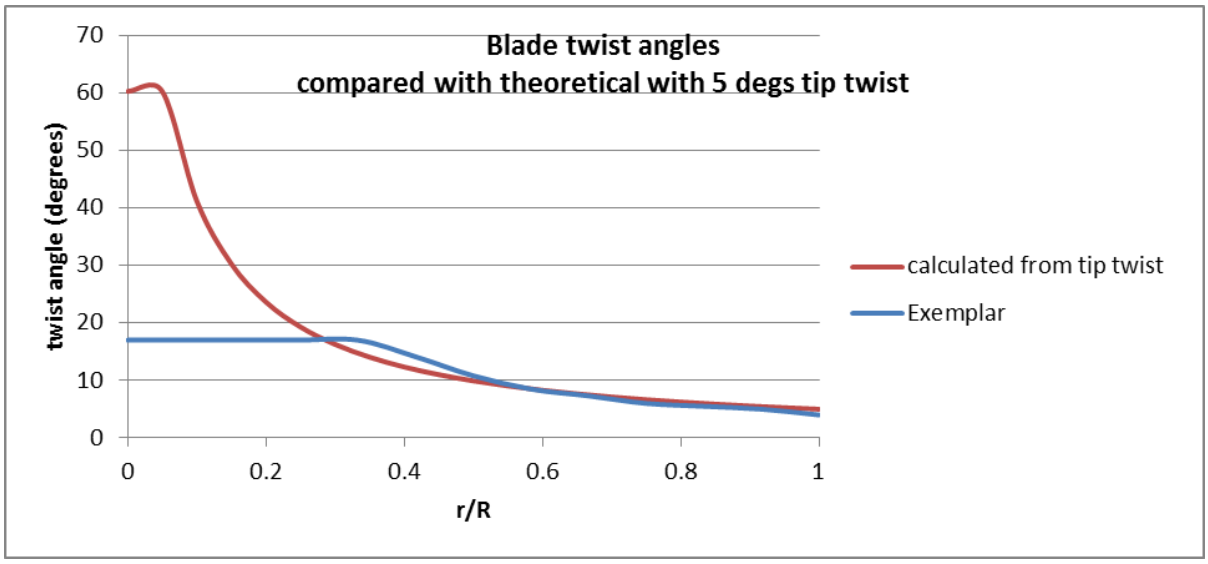

Figure 28 Blade pitch variation from hub to tip, for exemplar turbine and as used in basic CRM spreadsheet

Table 6 compares the mean collision risk for a single transit, using either the blade width and pitch profile as used in the basic CRM spreadsheet, or using the blade width and pitch profile for the exemplar turbine blade. For this table, the results were calculated with refinement 1 (making use of a depth distribution) implemented, as potentially this refinement may be more sensitive than the basic model to effects associated with blade taper. Results were calculated for two rotor rotation speeds: 6 rpm and 12 rpm which are typically close to cut-in speed and full operational speed

respectively. Use of the exemplar blade width and pitch profile increased the mean probability of collision for a single transit by a small amount, typically 1-2%.

Table 6 Comparison of collision risk using standard CRM blade profile with that based on the exemplar turbine

Mean Probability of Collision (%) for a Single Transit				
Rotation Speed	**12 rpm**		**6 rpm**	
	Upstream	**Downstream**	**Upstream**	**Downstream**
Standard CRM blade width and pitch profiles	65.1	55.1	39.0	32.9
Exemplar turbine blade width and pitch profiles	67.3	55.7	40.1	33.7

7.2.3 Refinement 3: Animal Shape

As described above, the basic CRM models the animal as a hard object consisting of two equal circular cones, stuck base-to-base. The cones may be of length and diameter chosen to match the animal concerned. Marine mammals are, in general, not as symmetric as this; their body, towards the front, is the widest part, then their rear portion is long and tapering.

In refinement 3, the model used for the animal is altered to consist still of two base-to-base circular cones, but of different lengths. A 'body ratio' factor μ is introduced, such that the front cone is of length μ L, where L is the overall animal length, and the rear cone is of length (1-μ) L. Hence setting μ=0.5 replicates the basic CRM model.

Table 7 Effect of using a non-symmetric model animal

Mean Probability of Collision (%) for a Single Transit				
Rotation Speed	**12 rpm**		**6 rpm**	
	Upstream	**Downstream**	**Upstream**	**Downstream**
Standard CRM assumption: μ=0.5	65.125	55.046	38.981	32.852
Asymmetric assumption: μ=0.2	65.125	55.080	38.990	32.909

Table 7 shows the effect of changing the body ratio factor from 0.5 to 0.2, representing an animal whose widest cross-section is at a point only one-fifth of the length of the animal, measured from the animal's front. The effect is shown at two rotation speeds, 6 and 12 rpm, typically around cut-in speed and full operational

speed respectively. Calculations are done using the extended model, using the standard blade width and pitch profile. Three points may be noted:

(i) The effect of the change is not significant at either rotation speed: downstream at 6 rpm rotation speed the increase is less than 0.1% in the mean probability of collision;
(ii) The change is greater at lower rotation speeds; and
(iii) The change is greater for downstream transits than upstream.

7.2.4 Refinement 4: Blade Thickness

As described above, the basic CRM models a rotor blade as a twisted lamina of zero thickness. Clearly real blades have a finite thickness, as well as length and width, and that thickness increases towards the hub to secure the necessary strength of the blade.

To test the effect of using a more realistic blade cross-section, aerofoil sections at a radius of 3, 6 and 9 m were obtained for the exemplar rotor of radius 9 m. Each was rotated by the pitch angle appropriate to that radius, so that the rotated aerofoil section then represents properly a cross-section of the blade. Figure 29 shows the NACA 634-421 aerofoil section at 6 m radius out from the hub for the exemplar turbine, rotated as specified to give a pitch angle of 7.3 degrees.

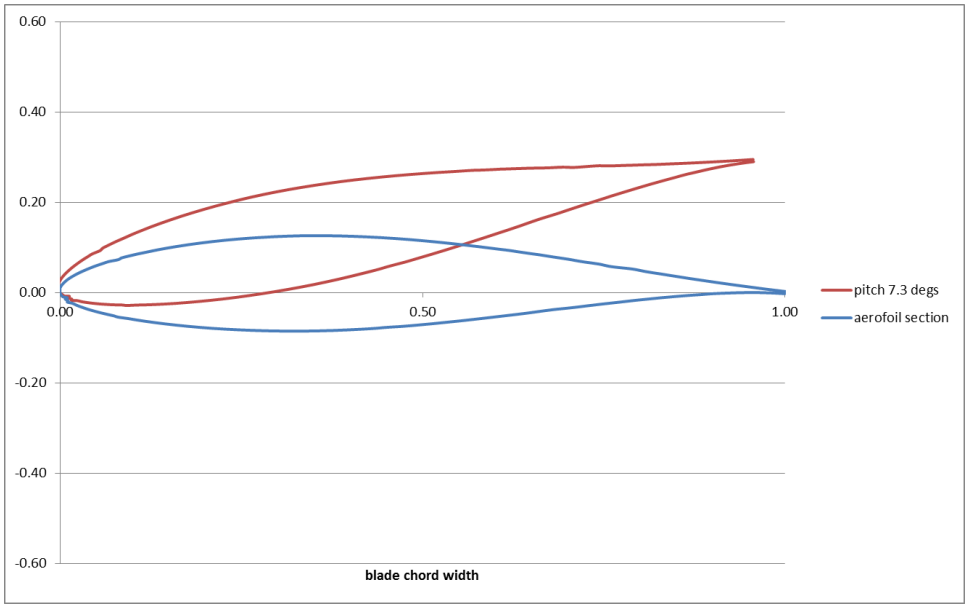

Figure 29 Aerofoil section at radius 6 m for exemplar turbine, showing rotation to pitch 7.3 degrees

Figure 29 shows a blade with aerofoil cross section moving from right to left in a tidal current moving from bottom to top. To consider the effect of blade cross-section, it is easiest to picture the motion of the blade relative to a stationary animal. So for an animal swimming downstream, imagine the animal is stationary and the blade is moving from top to bottom, towards the animal, at the same time as it moves from right to left as the rotor rotates. Each rotor blade rotates with tangential speed r Ω at radius r, meanwhile approaching the animal at speed v parallel to the rotor axis. The swathe carved out by the blade may therefore be drawn at angle $\tan^{-1} \alpha$ to the rotor plane, where $\alpha = v / r \Omega$. Figure 30 shows the blade swathe carved for such a downstream passage; as this is a cross-section of the blade at a radius of 6 m, r = 6 m, Ω = 12 rpm (=12 x 2π/60 radians s^{-1}), and v is the animal speed 1.64 m/s, giving α = 0.218. The two straight lines (green and purple) are then the upper and lower bounds of the rotor swathe, with equations $y=\alpha x + c_{upper}$ and $y=\alpha x + c_{lower}$ if the x-axis is the horizontal axis in Figure 30, y the vertical, and c_{upper} and c_{lower} constants. These lines are drawn so as to be of the correct slope α and to be tangential to the aerofoil section. The width of the rotor swathe as measured perpendicular to the rotor plane (that is, parallel to the rotor axis or parallel to the y-axis in Figure 30) is then $c_{upper} - c_{lower}$.

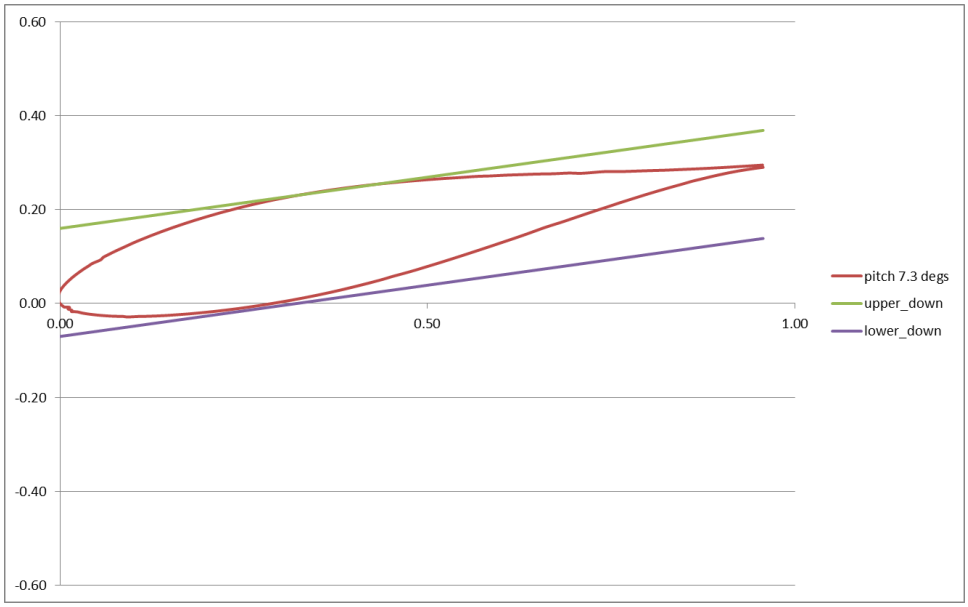

Figure 30 Swathe carved out by blade at radius 6 m (animal passage downstream): in frame in which animal is stationary

This value may be compared with the corresponding distance for a laminar blade (i.e. with a blade cross-section which is a simple straight line), as included in the basic CRM model. The blade swathe width in the CRM for a downstream passage is $c|\alpha \cos \gamma - \sin \gamma|$.

Figure 31 shows the corresponding blade swathe for an upstream transit. Now as the blade moves from right to left, it must also move from bottom to top in this view in which the animal is stationary. As the velocity of the animal is reversed, the sign of α is reversed. As before, the bounds of the rotor swathe may be drawn, of the correct gradient α, whose sign is now reversed as the animal velocity is in the opposite direction. The rotor swathe width is then again calculated as $c_{upper} - c_{lower}$. That may then be compared with the corresponding distance in the basic CRM model for a laminar blade.

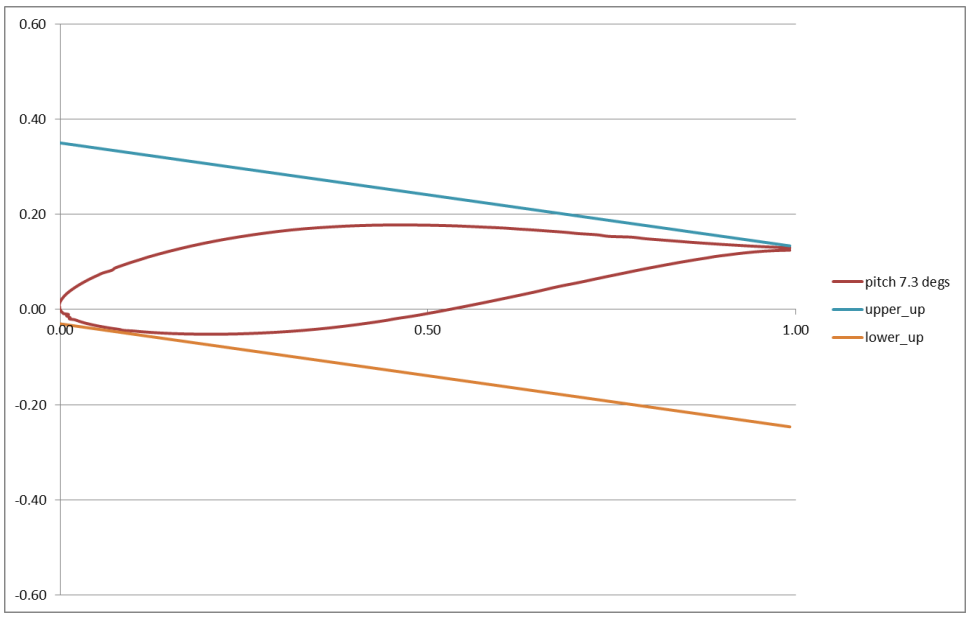

Figure 31 Swathe carved out by blade at radius 6 m (animal passage upstream): in frame in which animal is stationary

Table 8 compares the width of the blade swathe for this exemplar blade, with its aerofoil cross-section, with that assumed in the basic CRM model, for two rotation speeds 6 rpm and 12 rpm.

For an upstream transit, the difference between a blade of real thickness and a blade of zero thickness is significant, but not a major difference, typically adding less than 10% to the CRM estimate. However, for downstream transits, the thickness of the aerofoil section adds a very significant amount to the width of the blade swathe; in one case above (6 m radius, rotation speed 12 rpm), the width of the blade swathe is more than double that calculated by the CRM for a twisted laminar blade. Analysis of sections at radii 3 m and 9 m show a similar trend.

Table 8 Comparison of estimates of blade swathe width, as between the CRM model and use of a real aerofoil section

Width of Blade Swathe (In Units of Blade Width) at 6 m Radius				
Rotation Speed	**12 rpm**		**6 rpm**	
	Upstream	**Downstream**	**Upstream**	**Downstream**
CRM estimate	0.34	0.09	0.56	0.31
Estimate for exemplar blade based on aerofoil section	0.38	0.23	0.59	0.38

In judging whether this change is significant in terms of overall collision risk, however, it should be noted that the CRM formula for collision risk has two main components, representing the risk of leading edge collisions (which depend on animal size), and the risk of trailing blade collisions (which depend on the width of the blade swathe). The above adjustments to take account of blade thickness affect only the latter. For the 18 m diameter turbine rotating at 12 rpm, only 25.9% of the risk for animals passing upstream is due to trailing blade collisions, and only 7.6% of the risk for animals passing downstream. For upstream transits, an increased estimate of less than 10% to the width of the blade swathe will only increase the overall collision risk by around 2.5% (i.e. 10% of 25.9%). For downstream transits, a doubling in the estimate of the width of the blade swathe will make a change of less than 10% to the collision risk.

Furthermore, if the view is taken (see Refinement 6) that mortality due to trailing blade collisions is zero or minimal, then any underestimate in trailing blade collision risk will not affect the overall mortality risk.

Taking Account of Aerofoil Thickness in the Model

Taking rigorous account of the thickness of the aerofoil section within the CRM model would require knowledge of the aerofoil cross-section at all radii from zero to the outer edge of the rotor. The following analysis proposes a simplified adjustment to the model which will make a coarse correction for blade thickness in calculating collision risk for downstream transits.

Figure 32 shows the width of blade swathe (again measured perpendicular to the rotor plane, or parallel to the rotor axis) for both upstream and downstream transits at different rotation speeds, obtained graphically using as above the aerofoil section appropriate to 6 m radius for an 18 m diameter turbine. For upstream transits (green

and purple lines) the graphs show little difference between the swathe width taking account of the real aerofoil cross-section of a blade, and that calculated using the normal CRM calculation of blade swathe width c (α cos γ - sin γ), where c is the chord width at that radius and γ is the blade pitch.

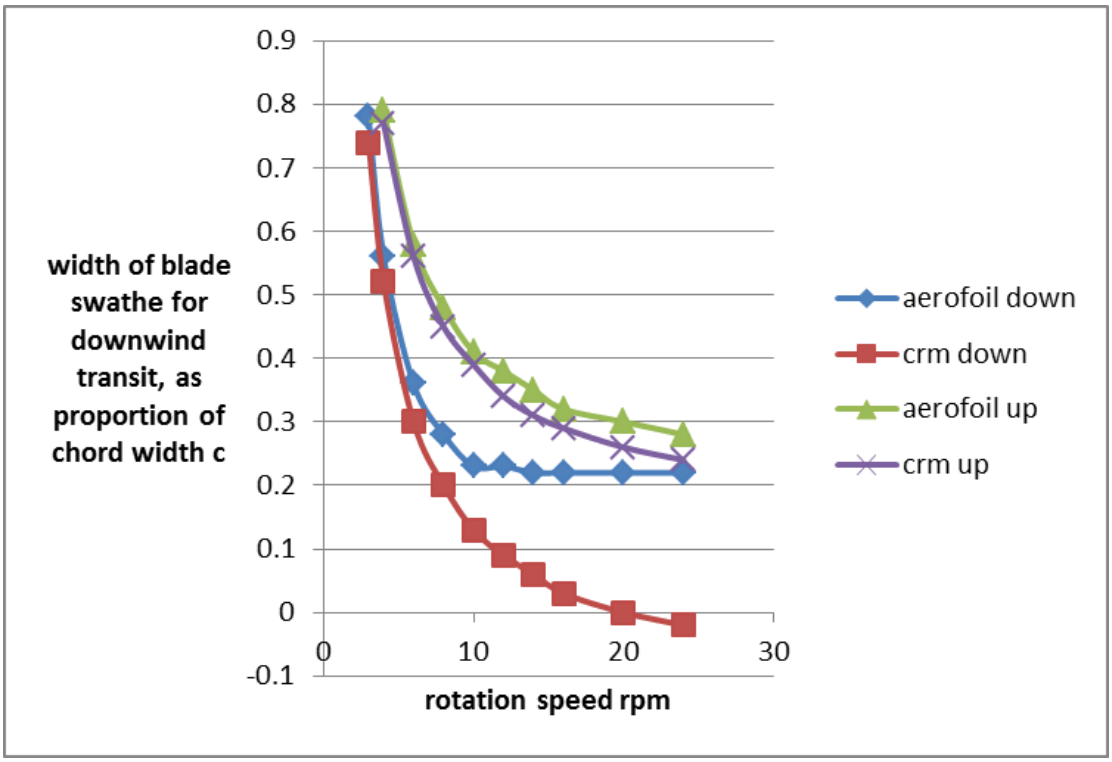

Figure 32 Width of blade swathe using aerofoil shape compared with that calculated from the CRM

For downstream transits (blue and red lines), the swathe width is also close to that of the normal CRM calculation at low rotation speeds, when the blade swathe is at a high angle $\alpha = \tan^{-1}(v/r\Omega)$ to each blade. However at high rotation speeds, the CRM formula for the blade swathe width continues to decrease towards zero (and indeed is zero when α = tan γ), while for a real aerofoil blade, the blade swathe cannot fall below the thickness of the aerofoil. A pragmatic adjustment is thus to allow the aerofoil thickness to take precedence whenever it exceeds the swathe width calculated by the CRM:

$$\text{width of blade swathe} = \max(c\,|\alpha\cos\gamma - \sin\gamma|, \text{aerofoil thickness}) \qquad (10)$$

Aerofoil thickness is not a constant; aerofoil cross-sections are typically thick near the hub (to provide strength to the blade) and thinner towards the tip. Figure 33 (blue line) plots the aspect ratio of the blade (aerofoil thickness as a proportion of

chord width) as a function of radius, showing a steady decrease in aspect ratio at radii greater than the point of maximum chord width. Also plotted is a line at 0.36 times the c/C ratio for each radius. c/C also decreases with radius, as the blade tapers from root to tip. The factor 0.36 is chosen empirically such that the product of 0.36 and c/C matches the decline of aspect ratio with radius.

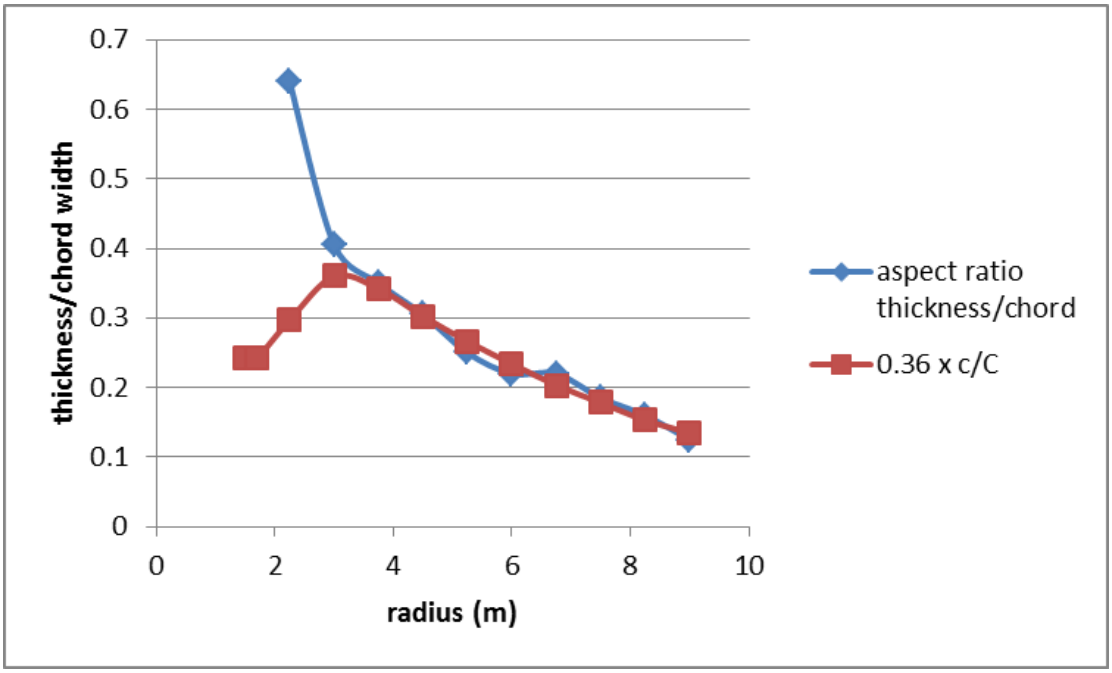

Figure 33 Blade aspect ratio as a function of radius, showing the similarity to changes in c/C with radius

Thus for blade thickness at radius r, as a proportion of chord width c at that radius, the refined CRM spreadsheet uses the function:

$$\text{Max} \{ |\alpha \cos \gamma - \sin \gamma| , 0.36 (c/C) \} \quad (11)$$

where

$\alpha =$ $v / r\Omega$ and c/C is a function of r.

This applies to downstream transits only; for upstream transits no such adjustment is required.

7.2.5 Refinement 5: Mortality

The CRM calculates the probability of a stylised animal colliding with a stylised rotor, assuming no avoiding action is taken by the animal (either by avoiding the area, by

navigating safely through it, or by emergency avoidance). However, not all collisions are likely to lead to the death of the animal. Thompson *et al.* (2015a), using simulated collisions with seal carcasses, showed that slow speed collisions were unlikely to cause death or serious injury to an adult seal and inferred that only collisions at significant impact speeds are likely to cause injury sufficient to be fatal. In this refinement, a mortality function is added to the CRM, mortality being a function of the closing speed between blade and animal. Based on the findings of Thompson *et al*. (2015a) the function used in this refinement is a simple one – a collision is only deemed fatal or would cause serious injury if the closing speed is greater than 5 m/s. This results in a very substantial difference between collision rate and mortality rate, as a high proportion of impacts are below this closing speed.

Table 9 Effect of applying a mortality function

Comparison of Collision Risk with Mortality Risk					
Rotation Speed		**12 rpm**		**6 rpm**	
Direction		**Upstream**	**Downstream**	**Upstream**	**Downstream**
Collision integral	Total	0.283	0.239	0.169	0.143
Mortality integral	Total	0.220	0.192	0.042	0.040
Mortality as a proportion of collisions		77.7%	80.3%	24.9%	28.0%

Table 9 shows the effect of applying a mortality cut-off based on this critical blade-animal closing speed of 5 m/s. Unsurprisingly, the proportion of collisions which are fatal is much lower at low rotation speeds than at higher speeds.

7.2.6 Refinement 6: Distinguishing Between Leading Edge and Trailing Blade Impacts

An animal may be hit by the leading edge of the rotor colliding with some part of the animal; or it may be hit by swimming into some part of the blade other than the leading edge – referred to here as the 'trailing blade'. The leading edge is characterised by a very high curvature, and an impact from the leading edge is far more likely to cause damage to animal tissue than an impact with the gently curved sides of the blade in a trailing blade collision.

In this refinement, the CRM has been modified to calculate the collision risk separately from leading edge and trailing blade collisions. This then opens up the opportunity to apply two separate mortality functions – one for leading edge collisions, one for trailing blade collisions.

A reasonable scenario is to leave the mortality function unchanged for leading edge collisions (i.e. only closing speeds >5 m/s are fatal or would cause serious injury) and set it to zero for trailing blade collisions, which are all assumed non-fatal.

The proportion of all collisions which are trailing blade collisions is very significant for upstream transits, though a relatively small proportion for downstream transits. Setting the mortality function to an impossible high closing speed (100 m/s) for trailing blade collisions ensures there is no contribution to mortality from this class of collision.

Results

Table 10 shows the reduction in mortality risk resulting from the application of these two separate mortality functions for leading edge and trailing blade collisions. The risk is further reduced by 3-13%, in comparison with the mortality calculated in Table 9 on the basis of a single mortality function for all collisions.

Table 10 Comparison of mortality with collision risk, assuming trailing blade collisions are non-fatal

Comparison of Collision Risk with Mortality Risk					
Rotation Speed		**12 rpm**		**6 rpm**	
Direction		**Upstream**	**Downstream**	**Upstream**	**Downstream**
	Leading edge	0.221	0.221	0.111	0.111
Collision integral	Trailing blade	0.073	0.018	0.060	0.032
	Total	**0.283***	**0.239**	**0.169***	**0.143**
	Leading edge	0.183	0.183	0.037	0.037
Mortality integral	Trailing blade	0	0	0	0
	Total	**0.183**	**0.183**	**0.037**	**0.037**
Mortality as a proportion of collisions		64.7%	76.6%	21.9%	25.9%
Compared with proportion based on closing speed alone (see Table 9)		77.7%	80.3%	24.9%	28.0%

* Note that for parts of the rotor close to the hub, an animal may be at risk of both a leading edge and a trailing blade collision; hence the total risk may be less than the sum of leading edge and trailing blade risk.

7.2.7 Refinement 7: Using Rotor Speeds Across the Tidal Cycle Instead of a Single Mean Rotor Speed

The CRM model requires input of the mean rotational speed of the turbine. The rotational speed at any point in time depends on the current velocity, between a cut-in current velocity (below which the turbine is inactive) and a cut-out current velocity (above which the turbine is closed down to prevent excess strain). A rigorous approach to determining a mean rotational speed therefore requires knowledge both of the frequency distribution of current speeds, and of how the rotor rotational speed is expected to vary with current speed:

$$\text{mean rotor speed } \underline{\Omega} = \Sigma\, \Omega(v_c)\, f(v_c) / \Sigma\, f(v_c) \qquad (12)$$

where

$\Omega(v_c)$ = The rotor rotational speed when the current speed is v_c;
$f(v_c)$ = is the frequency distribution of tidal current velocity v_c; and
the summation is over the current speed bins v_c in the distribution.

It is simplest to use a normalised frequency distribution, that is scaling the frequencies $f(v_c)$ such that they add up to 1 – that makes the denominator $\Sigma\, f(v_c) = 1$.

In practice, many users have applied the rotor speed appropriate for the mean current speed, or have opted for an even simpler approach by taking a maximum rotor speed as a 'worst case' and using that within the CRM. For example, in trialling the use of seal tracking data for the MeyGen development, Thompson *et al*. (2015b) used a maximum rotor speed as a worst case scenario.

For the environmental assessment of the same development, in applying the encounter rate model, SRSL (2012) calculated the relative closing speed between blade and animal for a range of tidal current velocities throughout a spring-neap tide cycle. It is likely that this is a broadly parallel process to that above for the CRM, i.e. calculating a time-average of blade-animal closing speed. Mean blade velocity along the blade length, for the entire range of tidal velocities, is given as 3.66 m/s which implies a tip speed around 7.32 m/s. For an 18 m diameter rotor, this implies a rotational speed of around 8 rpm. This is consistent with data elsewhere in the report indicating operational speeds in the range 8-20 rpm. Such an approach goes some way towards taking an average over time of rotor rotational speed, but does not make use of the full information available from manufacturers on the dependence of rotor speed on current velocity.

Refinement 7 makes use of manufacturers' technical data on the dependence of rotor speed on current velocity. These data were provided by MeyGen (2012) for the purpose of the original collision risk assessment, for a 3-bladed 20 m diameter turbine. The data are provided in terms of the tip speed ratio – the ratio of tip speed to current speed, which is an optimum at around 5-6 for a 3-bladed turbine. The rotation speed curve is derived by dividing the tip speed by the radius at the tip (10 m for this 20 m diameter turbine).

Next, predicted tidal current data is input at 15 minute intervals for a full year, using the ABPmer hydrodynamic model, with a total of 35,136 data points. Taking a full year encompasses annual seasonal variations in tides, as well as springs and neap tides following the monthly lunar cycles. For the purpose of exploring this method refinement, the current prediction used is for a point within the Pentland Firth Inner Sound, grid reference ND342750, which is within the area proposed for the MeyGen development.

Analysis of current direction shows a predominantly east-west flow at this location (see Figure 34). Current speed data were therefore classified as either eastwards or westwards, and separate current speed frequency distributions produced for each direction (Figure 35). Both the shape and the magnitude of the two distributions differ significantly between the two directions.

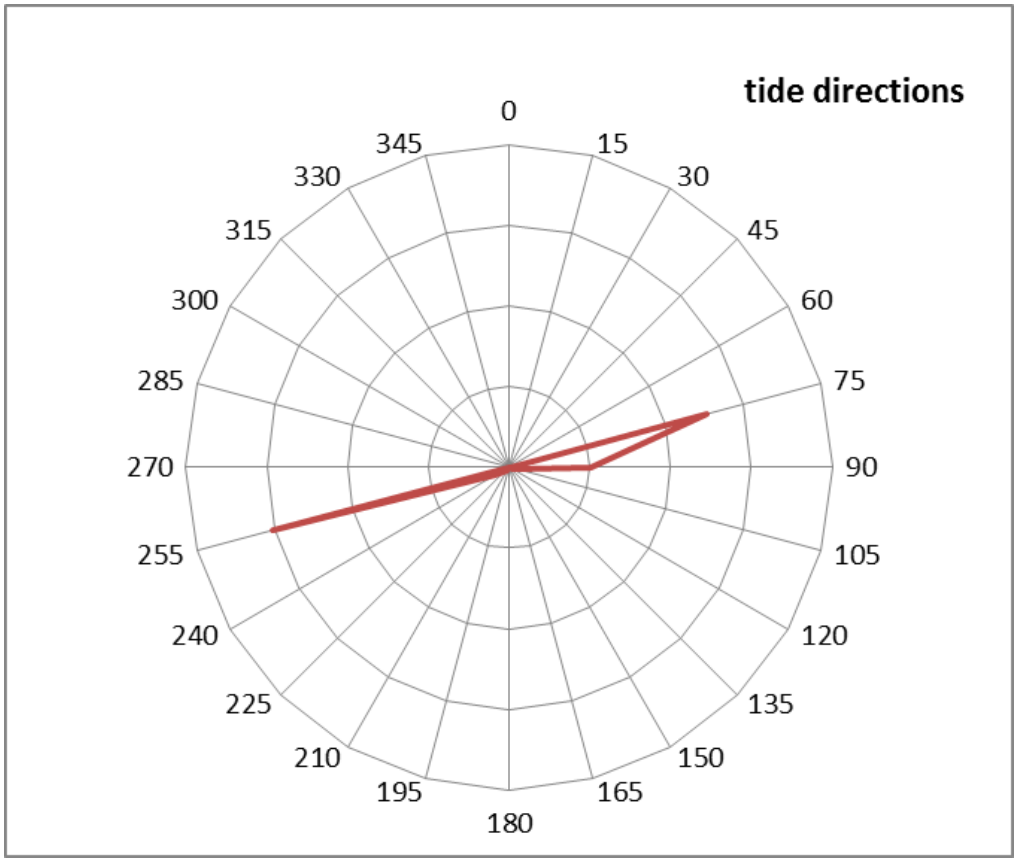

Figure 34 Analysis of current flow directions for location ND 352 750 in 15 degree categories

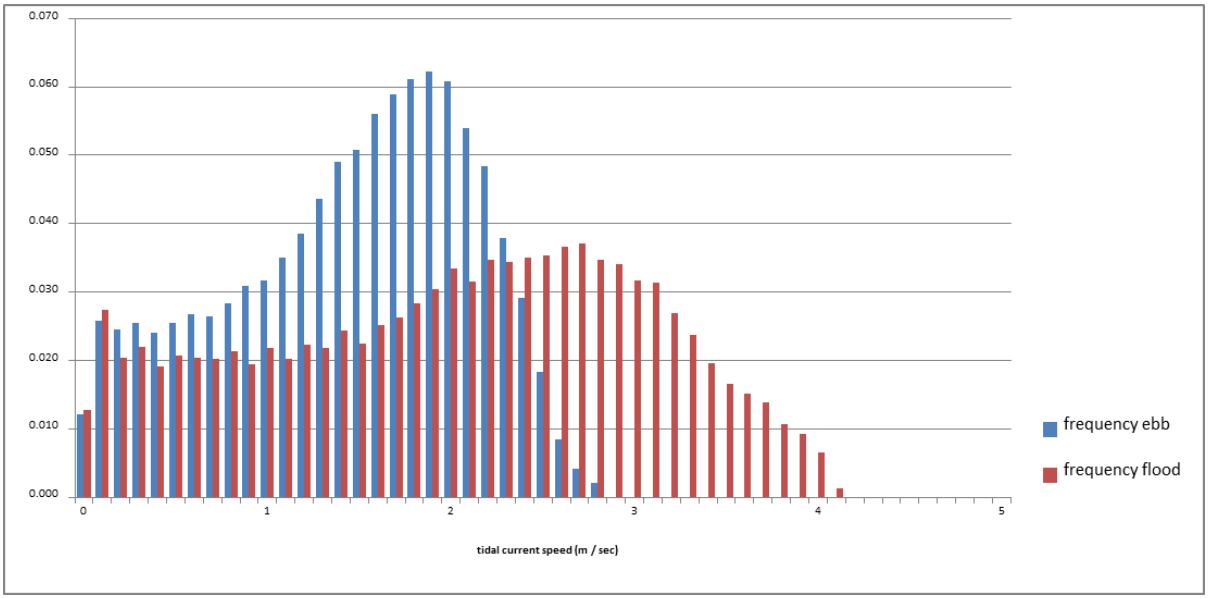

Note: Red is eastwards current (flood), blue is westwards (ebb)

Figure 35 Current speed frequency distributions for location ND 352750

Table 11 Mean current speeds showing differences between ebb and flood currents

	Ebb (Westwards)	Flood (Eastwards)	Average
Mean current speed	1.492	2.051	1.785

This mean current speed could be used to determine a typical rotation rotor speed, using the graph in Figure 35. However the graph is complex, not linear, such that use of a single value corresponding to mean current speed could be misleading. Instead the formula above is used for mean rotor speed:

$$\Omega = \Sigma\, \Omega(v_c)\, f(v_c) / \Sigma\, f(v_c) \qquad (13)$$

Note that advice on use of the CRM for wind farms, when assessing potential bird collisions, has been to use an average of rotor rotational speeds over time *excluding* periods with current velocity below cut-in or above cut-out (Band, 2012b). The proportion of time when the turbine is not operational due to slack water or excessive current speed is then factored in separately. SNH' s guidance on collision risks (Scottish Natural Heritage, 2016) maintains that approach, which gives the most realistic value for mean rotor speed while a turbine is active. The analyses in this document – and the calculations in the associated spreadsheet – depart from that practice: the 'mean rotor speed' and 'mean current speed' are calculated over all time. The mean rotor speed and mean current speed calculated in this way are lower than for turbine-active time only, but the calculated collision rates and mortality rates are not then reduced by a factor to allow for time below cut-in or above cut-out current speeds. The CRM still factors in at the end any non-operational time in respect of downtime for maintenance, at the end of the calculation. There may be a small inaccuracy here, to the extent that these two factors do not exactly balance. However it should be noted that in refinement 8 and other refinements which follow, the need to calculate a mean current and mean rotor speed is obviated, as the mean collision risk is calculated by evaluating the collision risk at each current speed.

$\underline{\Omega}$ has been calculated in two ways for comparison. Firstly it has been calculated directly, reading each 15-minutely data value for v_c then using an interpolation function to estimate Ω for that value of v_c, , and taking an average $\underline{\Omega}$ over all 35,136 data points. The interpolation function is a straight line interpolation from a table of rotor speed against current speed at current speed intervals of 0.1 m/s from 0 to 6 m/s.

Secondly $\underline{\Omega}$ has been calculated using the frequency distribution in Figure 35, giving the frequency of occurrence of each current speed in bins 0-0.1, 0.1-0.2, 0.2-0.3 etc. m/s for 0 to 6 m/s, and multiplying by the appropriate value of rotor speed Ω for each such value. There is little difference in result – see Table 12. The values in Table 12 are a mean rotation speed for use in the CRM, taking the mean across all stages of the tidal current velocity over an entire year at the location in question. These figures (whether obtained directly by averaging over all data points, or derived from the distribution) therefore represent a considerably more reliable basis for a CRM calculation than in the earlier approaches.

Table 12 Mean current speed and turbine rotation speed

		Westwards (Ebb)	Eastwards (Flood)	Overall
Mean current speed	By summing directly from data points	1.486	2.046	1.779
	Using frequency distribution	1.492	2.051	1.785
Mean rotation speed (rads s-1)	By summing directly from data points	0.668	0.653	0.660
	Using frequency distribution	0.669	0.653	

7.2.8 Refinement 8: Calculating Collision Risk for All Stages of the Tidal Cycle

The process can be taken a further stage. Instead of calculating a mean rotor speed across all stages of the tide, and basing an estimate of collision risk on that single mean value for rotor speed, it is possible to apply the CRM calculation for each value of the current speed, thus calculating the collision risk at each stage of the tide, and then taking a mean of collision risk over all stages of the tide:

$$C = \Sigma\, C(\, \Omega(v_c))\, f(v_c \,/\, \Sigma\, f(v_c) \qquad (14)$$

Again for convenience the frequencies are normalised such that $\Sigma\, f(v_c) = 1$.

The method is similar to that used in the previous refinement, except that the value averaged over all stages of the tide is the value of C, the collision risk for each current velocity v_c . The calculation of $C(\, \Omega(v_c))$ for 35,136 data points would be computationally cumbersome, but calculation for the 60 bins in the frequency distribution is quite manageable, so the second method above has been used.

In the remainder of this document, this approach to calculating risk, and also mortality as described in the next refinement, is termed ‘CRM Plus’ to distinguish it from the basic method (‘CRM Basic’), or the extended method (‘CRM Extended’) described in refinement 1.

Results

Table 13 shows how the values for collision risk averaged over all stages of the tidal cycle compare with a value based on using a single mean rotor speed in the CRM. The results are not dissimilar. Risk calculated across all current speeds in the tidal cycle, using the frequency distribution, is typically around 3-4% lower than that estimated on the basis of a single mean rotor speed.

Table 13 Mean collision risk for a single transit

		Westwards (ebb)	Eastwards (flood)
Mean collision risk for single transit using frequency distribution	Upstream transit	0.460	0.454
	Downstream transit	0.379	0.374
Collision risk for single transit based on mean rotation speed	Upstream transit	0.478	0.470
	Downstream transit	0.392	0.386

7.2.9 Refinement 9: Calculating Mortality Risk Across all Stages of the Tidal Cycle

The process can be extended a final stage by calculating mortality across all stages of the tidal cycle, *viz*:

$$M = \Sigma\, M(\, C(\, \Omega(v_c))) \, f(v_c\,) \,/\, \Sigma\, f(v_c) \qquad (15)$$

The method is the same as that used in the previous refinement, except that the value averaged over all stages of the tide is the value of M, the mortality risk for each current velocity v_c. The calculation of $M(C(\Omega(v_c)))$ for 35,136 data points would be computationally cumbersome, but calculation for the 60 bins in the frequency distribution is quite manageable.

As noted above, this approach to calculating potential mortality is termed ‘CRM Plus’ to distinguish it from the CRM Basic or CRM Extended approach.

Results

Table 14 shows how the values for mortality risk averaged over all stages of the tidal cycle compare with a value based on using a single mean rotor speed in the CRM. The results are very similar.

Table 14 Mean mortality risk for a single transit

		Westwards (ebb)	Eastwards (flood)
Mortality risk for single transit	Upstream transit	0.171	0.168
using frequency distribution	Downstream transit	0.158	0.155
Mortality risk for single transit	Upstream transit	0.173	0.170
based on mean rotation speed	Downstream transit	0.160	0.157

7.2.10 Refinement 10: Using Ground Speed Which is the Resultant of Swim Speed and Current Speed

Animals swimming through a current may interact with the current in a variety of ways. They may drift with the current, or they may continue to swim with their usual speed and direction relative to the water body, such that their overall ground speed and direction (or transit vector, in the terminology of Section 6.8) is the resultant sum of a swim vector (swim speed and direction) and a current vector (current speed and direction).

So far the question of how swim speed and direction interacts with current speed and direction has been avoided - the CRM has been based on using a single ground speed, either upstream or downstream. The ground speed has been taken as 1.64 m/s in the examples above. The basic CRM as presented in the draft SNH guidance assumes that all transits are downstream.

In this refinement, there is a test of the effect of using a 'resultant' assumption on seal transit speeds, based on an expectation that if seals swim with a certain foraging speed relative to the water, their ground speed when making downstream transits will be increased by the current speed, while when swimming upstream their ground speed will be decreased by the current speed. A complication is that when they swim upstream, if the current speed is greater than their swim speed, they may have a negative ground speed, that is to say they may be swept backwards through the turbine by the current, thus making a downstream (rather than upstream) transit.

The Collision integral CI is a function of:

- Transit direction (“up” or “down”);
- Rotor speed $\Omega(v_c)$, which in turn is a function of current speed; and
- Animal speed relative to the ground: $v + v_c$ for a downstream transit and $v-v_c$ for an upstream transit.

Thus:

- Downstream: $CI = CI$ (“down”, $\Omega(v_c)$, $(v + v_c)$);
- Upstream: $v \geq v_c$ $CI = CI$ (“up”, $\Omega(v_c)$, $| v-v_c|$); and
  $v < v_c$ $CI = CI$ (“down”, $\Omega(v_c)$, $|v-v_c|$.

Using the standard parameters (3-blade diameter 20 m max chord 2.2 m, animal swim speed 1.64 m/s) gives the results in Table 15.

Table 15 Comparison of collision risk using resultant and fixed ground speeds

		Westwards (ebb)	Eastwards (flood)
Mean collision risk for single transit using resultant ground speed	Upstream transit	0.768	0.651
	Downstream transit	0.242	0.225
Collision risk for single transit using fixed ground speed 1.64 m/s	Upstream transit	0.460	0.454
	Downstream transit	0.379	0.374
Collision risk for single transit assuming animals stationary relative to water	Downstream transit	0.370	0.318

It is clear that when swimming downstream, the collision risk is substantially less than if the fixed ground speed is used; while when swimming upstream, the collision risk is substantially greater.

Mortality risk, too can be calculated in a similar way based on resultant ground speed (Table 16).

Table 16 Collision risk assuming zero swim velocity

		Westwards (ebb)	Eastwards (flood)
Mean mortality risk for single transit using resultant ground speed	Upstream transit	0.298	0.238
	Downstream transit	0.104	0.100
Mortality risk for single transit using fixed ground speed 1.64 m/s	Upstream transit	0.148	0.145
	Downstream transit	0.148	0.145
Mortality risk for single transit assuming animals stationary relative to water	Downstream transit	0.147	0.127

A note of caution - the assumption throughout is that seals are swimming parallel to the rotor axis, an assumption which over-emphasises the effect of resultant ground speed. However, the scenario provides a useful bound to the potential differences in collision risk and mortality due to the differential in speeds as between upstream and downstream transits.

It must be stressed that assuming resultant transit speeds is based on a hypothetical behaviour. In fact, analysis from telemetry studies (see Section 6.8) shows a very different pattern of behaviour, in which seals tend to hold their position against the current, and if they were to pass through turbines while doing so they would pass through at very low transit speeds. The following refinement (11) describes the modelling used to reflect this swim behaviour. Use of the 'resultant' swim speed refinement is therefore not used in the assessment for the MeyGen development, where a strong body of data on seal transit speeds is available. Resultant speeds are used only for the Fall of Warness to indicate an upper bound to the potential collision rate.

An alternative (and also unlikely) scenario is that seals travel with the water body, i.e. with zero swim speed relative to the water. This can be analysed by setting swim speed to zero, and using the 'downstream' columns for computation. The results are reported in the last rows of Tables 15 and 16: they are not hugely different from the results assuming a fixed speed over ground of 1.64 m/s.

7.2.11 Refinement 11: Integrating Over Ground Speed Distribution

The previous option assumes that animals swim as if oblivious to the turbines and sea bed – that is, their usual swim velocity is combined with any current velocity to give a resultant velocity. A study of telemetry data from the Inner Sound, Pentland

Firth (see Section 6.8) indicates a swim behaviour of harbour seals that is very different from that: a higher proportion of seals pass downstream than upstream and in both directions, swim speed is low. The predominant speed is close to zero, i.e. as if the seals were holding position or nearly so with respect to the seabed. Predominant directions of travel (resultant of current and swim velocities) are broadly upstream and downstream, and swim directions are closely so. The pattern is not characterised by a single mean speed of transit through a turbine. Figure 36 shows the ground speed frequency distribution extracted from the telemetry data for the Inner Sound. It reveals the predominance of low ground speeds, both for upstream and downstream movements, which translate into low levels of animal flux through the rotor and hence relatively low collision and mortality rates.

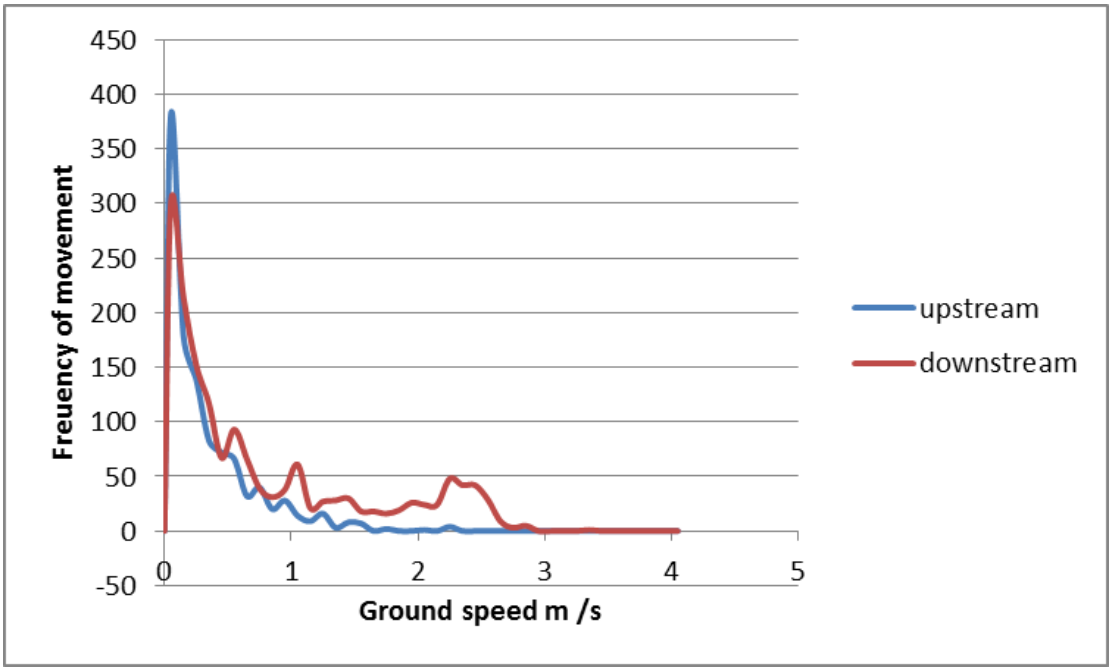

Figure 36 Ground speed frequency of harbour seals diving in an array site.

Refinement 11 is based on the distribution of ground speeds as recorded in the Inner Sound telemetry data. Collision and mortality rates are calculated for each fixed ground speed between 0 and 4.0 m/s in 0.1 m/s intervals. These collision and mortality rates are then multiplied by the (normalised) frequency with which that ground speed occurs in the ground speed frequency distribution. The calculations are done separately for upstream and downstream travel through the turbine, as not only is the collision risk for a single transit different for up and downstream travel, but the ground speed frequency distributions differ too.

$$\text{Collision rate} = \sum f_i \, C(g_i) \qquad (16)$$

$$\text{Mortality rate} = \sum fi \; M(gi) \qquad (17)$$

where

$C(g_i)$ is the collision rate and $M(g_i)$ the mortality rate at ground speed $g_{i;}$ and the summations are over the ground speed bins g_i in the frequency distribution.

The collision and mortality rates for upstream and downstream are then averaged, weighting the average by the total number of transits upstream and downstream respectively (the Inner Sound telemetry data indicated around 40% upstream, 60% downstream movements). For maximum accuracy the calculation has been done making use of the tidal current distribution to calculate collision and mortality risk at each ground speed, that is, using the CRM Plus method outlined in refinements 8 and 9 for each ground speed. Such an approach would not be valid if there was significant degree of correlation between the ground speed and current speed for each dive segment. However no such correlation is evident (Figure 23). Integrating over the ground speed distribution in this way is termed the 'CRM Plus Plus' approach in the remainder of this document, to distinguish it from the CRM Basic, CRM Extended, and CRM Plus approaches described earlier.

Collision rates from this CRM Plus Plus approach - integrating over the ground speed distribution - are significantly lower than estimated using the CRM Basic, CRM Extended or CRM Plus approach above. Figure 37

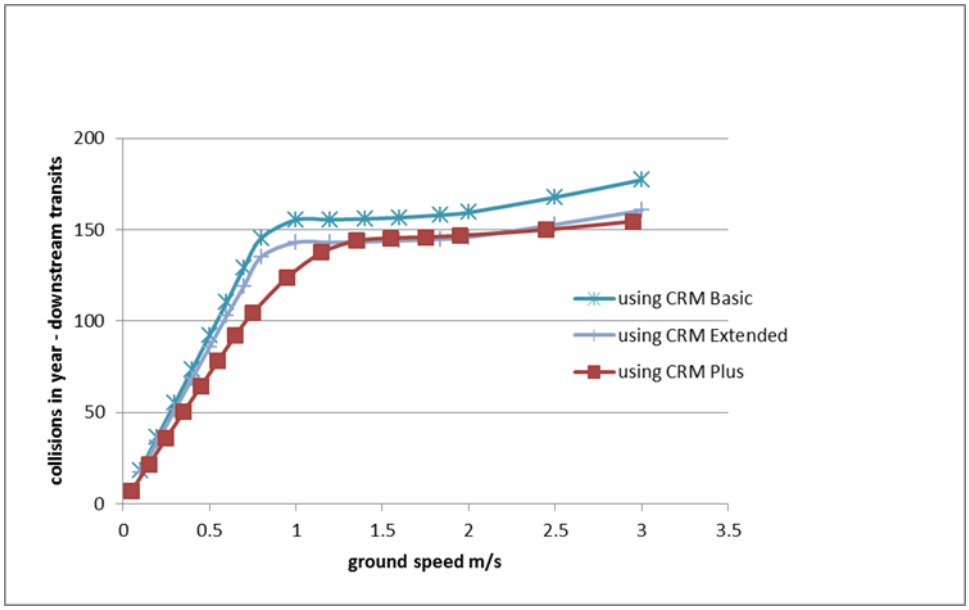

Figure 37 and Figure 38 show how collision rate varies with ground speed for a typical turbine. At low ground speeds, the collision risk for a single transit is 100%, while the flux through a rotor is proportional to the ground speed (Flux = D A v i.e. density x area x speed). At higher speeds of approach, the collision risk for a single transit decreases, offsetting the increase in flux. In Figure 37 and Figure 38, collision rates for each ground speed are shown derived from the Basic, Extended and CRM Plus models, the last making use of the refinements 8 and 9 which integrate over the distribution of tidal current speeds. Using the CRM Plus collision rates, the CRM Plus Plus method then integrates these over ground speed, using the ground speed frequency distribution in Figure 36.

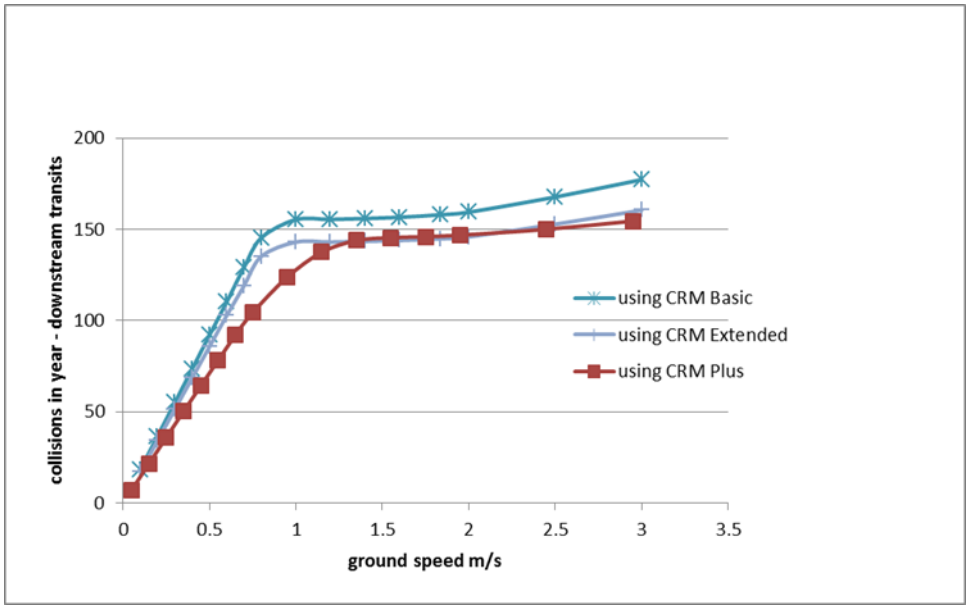

Figure 37 Collision rates as a function of ground speed for downstream movements

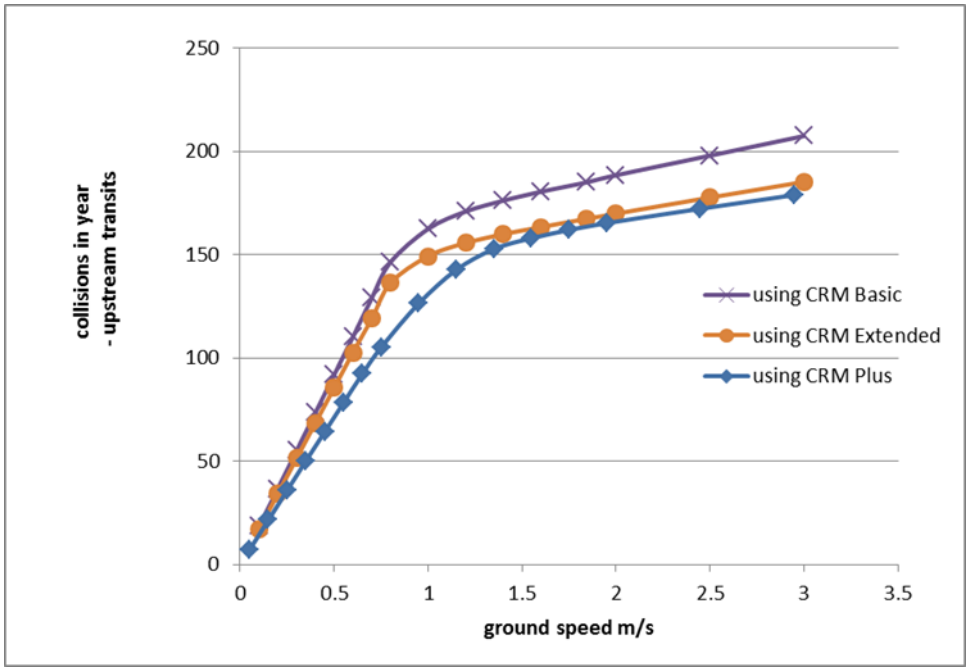

Figure 38 Collision rates as a function of ground speed for upstream movements

The results of the CRM Plus Plus method are shown for two turbines in Figure 39, and compared with the results from use of the Basic, Extended, and CRM Plus methods. For both turbines, the CRM Plus Plus method yields an estimate of around 60% of the CRM Basic method. A caution is that the two turbines used in these calculations are highly similar in specification, so the reduction factor of 60% should not be assumed as a generality at this stage. Table 18 in Section 7.3 summarises the four methods and outlines the refinements incorporated in each these progressively refined methods.

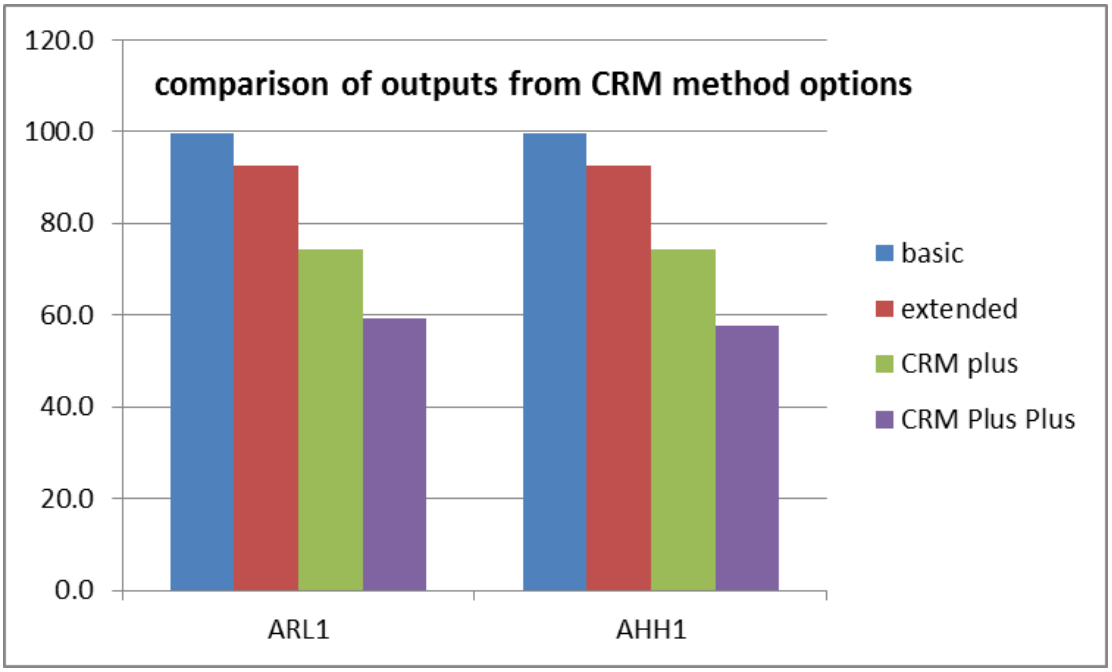

Figure 39 Comparison of collision estimates using progressively refined methods

A downside of the CRM Plus Plus approach is the computational time taken for each calculation. With this approach, a single mean collision rate cumulates over 40 ground speed bins, each of which requires integration over 60 current speed bins, each of which requires integration over 20 radial and 20 angular segments of a turbine disc; and that is repeated for mortality. The number of combinations involved makes this computationally intensive, requiring around 30 minutes of processing time on a typical desktop computer. While there are a number of simple changes which could optimise the process, one such change would be to rely on the basic or extended calculation using mean current and rotor rotation speeds, rather than repeat the full accumulation of risk over the tidal current range for every ground speed; effectively omitting Refinements 8 and 9. The results of Refinement 8 in Table 13 and Refinement 9 in Table 14 suggest that the simplified method would overstate collision risk by at most 3-4%, and mortality by less than 2%. However the results reported in this document, and the calculations performed by the accompanying spreadsheet, implement the full CRM Plus Plus method.

7.2.12 Refinement 12: Seal Density

There are a number of density estimates that could be adopted for a given site assessment. There are a range of different data sources for sites in Orkney and the Pentland Firth including both the EMEC and MeyGen sites considered in this

assessment (Table 17). Estimates can be derived from the seal usage maps produced by SMRU at the resolution of a 5 km by 5 km grid cell (Jones *et al*., 2015). A density for each site was calculated by averaging over the turbine locations. At the MeyGen site, the four turbines are all within a single grid cell therefore the density presented is that of the grid cell containing all the turbine locations. For EMEC, a weighted average is calculated across all cells containing turbines by weighting the cell by the number of turbines present within it. At EMEC, the density estimate used in the previous assessment was based on EMEC's shore based wildlife observations over the grid containing the turbine positions (EMEC, 2014). The calculation of the telemetry derived densities for the MeyGen site is described in Section 6.7. Similar estimates for the EMEC site were not possible due to the difficulty in partitioning usage to specific haul out sites. It is clear that these estimates are very variable. Since the density estimate acts as a direct multiplier in the calculation of collision risk, the choice of density data source makes an extremely significant difference to the resulting collision risk estimates. For the EMEC site, this will lead to an almost 40 fold difference in collision risk estimates, a situation which is clearly undesirable for decision makers. The confidence intervals around these density estimates are generally wide.

Table 17 Range of different seal density estimates available

Density*, Seals per km² (95% Confidence Interval)		
Source Data	**MeyGen**	**EMEC**
5 x 5 km grid scale usage maps (Jones *et al*., 2015)	0.40 (0.17-0.64)	0.60 (0.12-1.00)
Telemetry derived density, small area (This report, Section 6.7)	0.053 (0.004-0.138)	NA
Telemetry derived density, large area (This report, Section 6.7)	0.097 (0.008-0.251)	NA
Site specific visual survey data density (EMEC, 2014)	0.169 (no CI given)	0.01583 (no CI given)
SRSL ERM MeyGen (SRSL, 2012)	0.202 (no CI given)	NA (no CI given)

* See text for details.

7.3 Summary

Table 18 below lists the refinements discussed within the report and offers some assessment as to their significance in altering the estimate of collision risk or mortality risk.

Table 18 Refinements discussed within the report

	Refinement	Assessment
1	Making use of a depth distribution	The 'CRM Extended' method. For harbour seal it is likely to reduce the estimate of collision risk by 15-30% but for other animals which may forage in mid water column the reduction may be less marked.
2	Blade width and twist profile	Substituting a 'real' blade shape for that used in the standard model makes little difference. If the information is available on blade shape, then it may be used, but it should not be expected to change the result much.
3	Animal shape	Changing the model animal shape from two equal circular cones stuck back to back, to two unequal cones, makes very little difference.
4	Blade thickness	Taking account of the thickness of the blade translates to a small but significant addition to risk for upstream transits, and a substantial addition to risk for downstream transits. The analysis required to quantify these additions is however somewhat cumbersome. The addition to risk is all due to trailing blade collisions (i.e. they are not leading edge collisions). If the view is taken that mortality due to trailing blade collisions is zero or minimal, then these additions to collision risk will not affect mortality risk.
5	Mortality	The effect of assuming that collisions with a closing speed < 5 m/s are not fatal is very significant, with reductions in mortality risk ranging from 20% to 75%.
6	Distinguishing between leading edge and trailing blade collisions	Assuming that trailing blade collisions, whether or not with closing speed > 5 m/s, are non-fatal further reduces the risk, by an additional 10% or so.
7	Using mean rotor speed over tidal cycle	This is not so much a refinement as doing with some rigour what is required by the CRM. With tidal prediction data over a complete year, and knowledge of the rotor speed – current speed response curve, a mean rotor speed across the year can be properly calculated.
8	Calculating collision risk over tidal cycle	Even better than Refinement 7 is to average the collision risk arising from each current speed in the tidal cycle. Results may be 3-4% lower than the risk based on a single mean rotor speed. Taken together with refinement 9, this is the 'CRM Plus' method.
9	Calculating mortality risk over tidal cycle	Still better than Refinement 8 is to average the mortality risk arising from each current speed in the tidal cycle. Results are little different from those obtained using a single mean rotor speed.
10	Using a ground speed which is the resultant of swim speed and current	This 'resultant scenario' may not be realised, as animals may swim harder upstream than downstream, but nonetheless it provides a bound to the difference which may be expected between upstream

	Refinement	Assessment
	speed	and downstream speeds.
11	Integrating over ground speed distribution	Using site specific data from telemetry studies in the Inner Sound indicates behaviour very different to that above in refinement 10. Transit speeds are very low and a higher proportion of seals pass downstream than upstream. These low ground speeds translate into low levels of animal flux through the rotor and hence relatively low collision and mortality rates, although for each transit the collision probability is 100%. Integrating collision rates over the ground speed distribution is the 'CRM Plus Plus' method.
12	Refinement of seal density	This highlights the variability of density estimates available for incorporation into collision risk estimates and their considerable influence on resulting estimates.

Each of the refinements adds complexity to the CRM calculation. While some may add to the apparent accuracy of the calculation, it must be borne in mind that none of this takes into account the animals' behavioural response over which there is currently a wide margin of uncertainty. Also, collision rates scale with the density of animals, and at present there is major uncertainty over the density of harbour seals at key project sites.

The refinements which have the potential to make the most significant difference to the CRM collision and mortality estimates, in terms of the percentage change in mortality estimate resulting from the refinement, are judged to be as follows (in descending order of significance):

- Refinement 12: Density;
- Refinement 5: Mortality;
- Refinements 10 and 11: Transit speed;
- Refinement 1: Making use of a depth distribution; and
- Refinement 4: Blade thickness.

It should be noted that the percentage changes reported in each refinement have been evaluated using a single common set of parameters. Results could differ if turbines of markedly different parameters, or animals with different swim parameters, are modelled.

Inclusion of these refinements in the calculation of collision and mortality risk has led to four successively refined methods of calculation, described as 'CRM Basic', 'CRM Extended', 'CRM Plus' and 'CRM Plus Plus'. The spreadsheet developed alongside this document enables calculation using any of these four methods. Table 19

provides a summary of the refinements included in each method. Figure 39 shows the results of all four methods applied to two turbines. It shows a clear trend to reduced estimates of collision risk from use of the progressively refined methods.

Table 19 Summary of progressively refined collision risk modelling methods

Model	Factors Which Successive Models Treat in A More Refined Way		
	Depth Distribution	**Rotational Speed**	**Ground Speed**
CRM Basic See Section 7.1	Assumes uniform depth distribution	Risk based on single mean rotational speed	Uses fixed ground speed or resultant ground speed
CRM Extended See Refinement 1	Uses generic observed depth distribution	Risk based on single mean rotational speed	Uses fixed ground speed or resultant ground speed
CRM Plus See Refinements 8 and 9	Uses generic observed depth distribution	Risk calculated at each current/rotation speed and summed over current speed frequency distribution	Uses fixed ground speed or resultant ground speed
CRM Plus Plus See Refinement 11	Uses generic observed depth distribution	Risk calculated at each current/rotation speed and summed over current speed frequency distribution	Risk summed over observed ground speed frequency distribution
	All four models make use of blade profile and blade pitch information if provided (or use a default profile if not provided), and include a correction to allow for blade thickness (see Refinements 2 and 4). All four models can estimate mortality rate as well as collision rate, based on an assumption that only collisions with a blade leading edge, above a given threshold impact speed, will lead to fatality. As to animal transit speed, the first three models may be calculated for a fixed ground speed or a speed which is the resultant of swim speed and current speed (see Refinement 10). The fourth model requires a known distribution of ground speeds, obtained from studies of animal movement (see Refinement 11).		

8 Updated Assessment for Consented Tidal Energy Projects in Orkney and the Pentland Firth

One of the objectives for this project was to apply the refined collision risk model to the current envelope of consented developments in the Orkney and North Coast seal management unit Orkney and Pentland Firth region. These sites are:

- The MeyGen Phase 1 tidal array development in the Inner Sound, Pentland Firth; and
- EMEC Fall of Warness Tidal Test site (Orkney).

This section outlines the application of the refined model described in the previous section to these projects to provide updated estimates of collision risk.

8.1 MeyGen Phase 1

Four turbines are initially to be installed, comprising one Atlantis turbines (ARL) and three Andritz Hammerfest turbines (AHH), all of rotor diameter 18 m, in an area defined as the Phase 1 development area. Figure 40 shows their approximate locations.

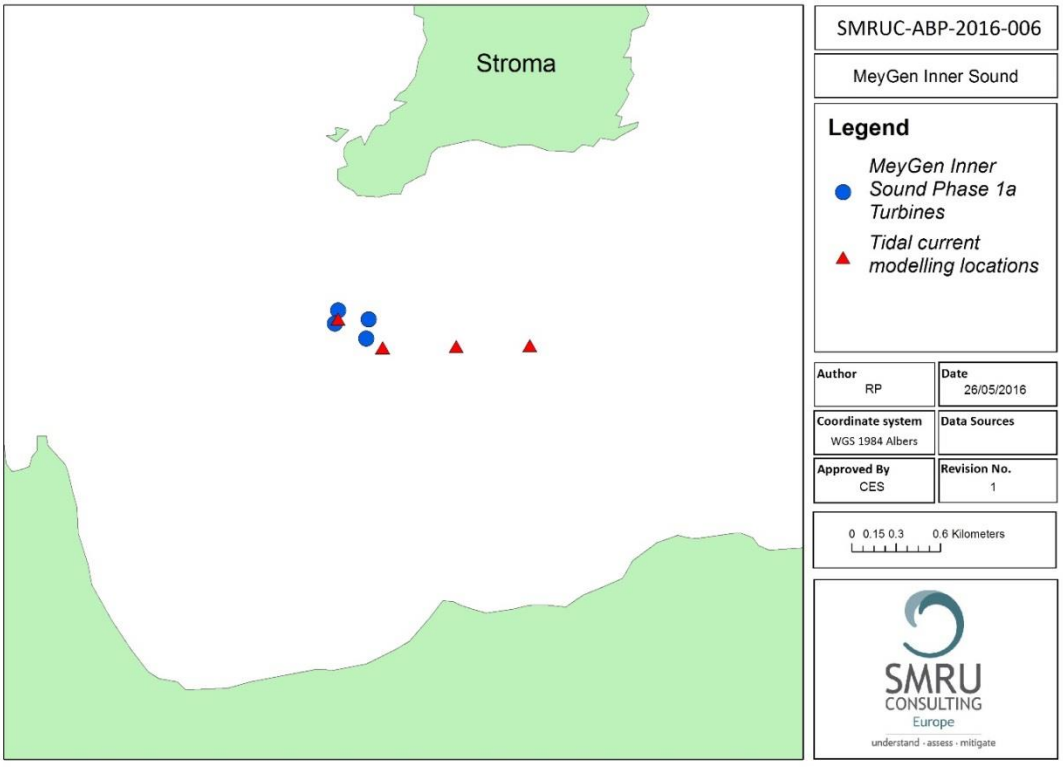

Note: Circles are the turbine positions and triangles are the locations for which detailed tidal information was provided

Figure 40 Location of the MeyGen array

Projected current speed and current direction data were obtained from the ABPmer hydrodynamic model, for a one year period at 15 minute intervals. This data was obtained at four sample locations within the Phase 1 area. Only the two westernmost locations were in fact used as the turbines will all be sited close to the western end of the Phase 1 'box'.

Details of the two turbine types were obtained from the manufacturers of the turbines that will be installed at The MeyGen site (Atlantis, ARL and Andritz Hydro Hammerfest, AHH). The information included the expected rotation speed as a function of current speed, and a blade profile describing the chord width and taper of the individual blades. Information about the pitch profile – including how the blade pitch increases towards the hub – was provided for one turbine type. For the other, the option has been adopted of using the pitch at the blade tip as given by the manufacturer, then calculating twist along the blade length on a simple theoretical basis. Results indicate insignificant difference between these two methods.

The proportion of time unavailable (turbine non-operational) due, for example, to maintenance and repair requirements was quoted as 5% for one type of turbine only, but this figure has been applied across all turbines. The present calculation does not count time below cut-in or over cut-out speed as unavailable, as the rotor speed v current speed mapping already accounts for non-operative time for these reasons. All final figures on collisions or mortality over a period of a year include the 5% deduction of risk for non-availability time due to maintenance or repair requirements.

Harbour seals were assumed to have a body length of 1.41 m and a body width of 0.34 m (Thompson, 2015). The body ratio was set at 0.5, which means that the front and rear taper of a seal's body was assumed to be the same; earlier results have demonstrated that refining this has negligible effects.

It was assumed that collisions with blade leading edges below 5 m/s closing speed would not be fatal or cause serious injury, and that collisions with other, less sharply rounded parts of the blade would not be fatal or cause serious injury; this last was ensured by setting the critical closing speed for the trailing parts of the blade to 100 m/s.

Key information obtained from the analysis of telemetry data from tagged seals in the Inner Sound was used to guide this assessment. In particular the data showed that harbour seals swam predominantly in a direction aligned along the current direction. The distribution of 'ground speeds' – the speed relative to the turbine – peaked at very low speeds, and was not correlated with the current speed. Therefore, the

'CRM Plus Plus' refinement was applied, calculating collision rates at each ground speed from 0 to 4.0 m/s , then multiplying by the frequency at each ground speed to generate a total collision rate. Around 60% of transits were downstream and 40% upstream, and this ratio was then applied to the respective collision and mortality rates for downstream and upstream movement.

Mean speeds of 0.325 m/s (upstream) and 0.778 m/s (downstream) as observed by telemetry were also used as the basis for parallel calculations using the Basic, Extended, and CRM Plus models. Generally, the resulting collision risk estimates reduce in that order, with the CRM Plus Plus results being 70-75% of those from the Basic model.

All model calculations were initially based on a seal density of 1 seal per km². As described in Section 7.2.12, various sources of data on seal density are available. However, the site specific estimates for both sites were not used in these calculations because they are calculated in different ways and are therefore not comparable. Therefore, for the purposes of this assessment, collision estimates were also calculated based on the density derived from the usage maps produced by SMRU (Jones *et al.,* 2015). The overview table (Table 20) shows the collision rate and mortality rate derived from the usage map derived density, including 95% confidence intervals. It is important to note that 100% of the uncertainty in the confidence intervals is attributed to uncertainty in the density estimates, uncertainty in all other parameters has not been included. The rates are shown for the 4-turbine scenario.

Table 20 Collision and mortality rates (per year) across a range of different density estimates for the Phase 1a, four turbine scenario using the CRM Plus Plus method (before any correction for avoidance is added)

Seal Density Data Source Used to Scale From	Seal Density (Seals/km²)	Collisions Per Year	Mortalities Per Year
	1	**235**	**172**
5 x 5 km Grid Scale Usage Maps (Jones *et al*., 2015)	0.40 (0.17-0.64)	93 (40-149)	69 (29-110)

Note: The confidence intervals in the collision and mortality estimates are derived only from the uncertainty in the density estimateS.
Mean and 95% confidence intervals are included

It is stressed that all these figures maintain the assumption of no avoidance, i.e. these are only potential collisions, or potential mortality, if seals did not avoid, navigate through, or escape from the risks imposed by turbines.

8.2 EMEC Fall of Warness

This assessment applies the refined Collision Risk Models (CRM Plus and CRM Plus Plus) described in this report to the EMEC tidal site at the Fall of Warness, Eday, Orkney.

The site currently has eight berths, and plans a ninth, at which tidal energy devices may be installed on a temporary basis for testing and development. The precise location of each machine is not fixed but will lie within a limited radius of the underwater connection points provided at the seabed by EMEC.

The design envelope of the site is envisages up to a maximum occupancy of 12 devices; 6 with a single open rotor of up to 25 m diameter, and 6 with two open rotors of up to 25 m diameter, making a total of 18 rotors.

Figure 41 shows the approximate locations of the eight current berths.

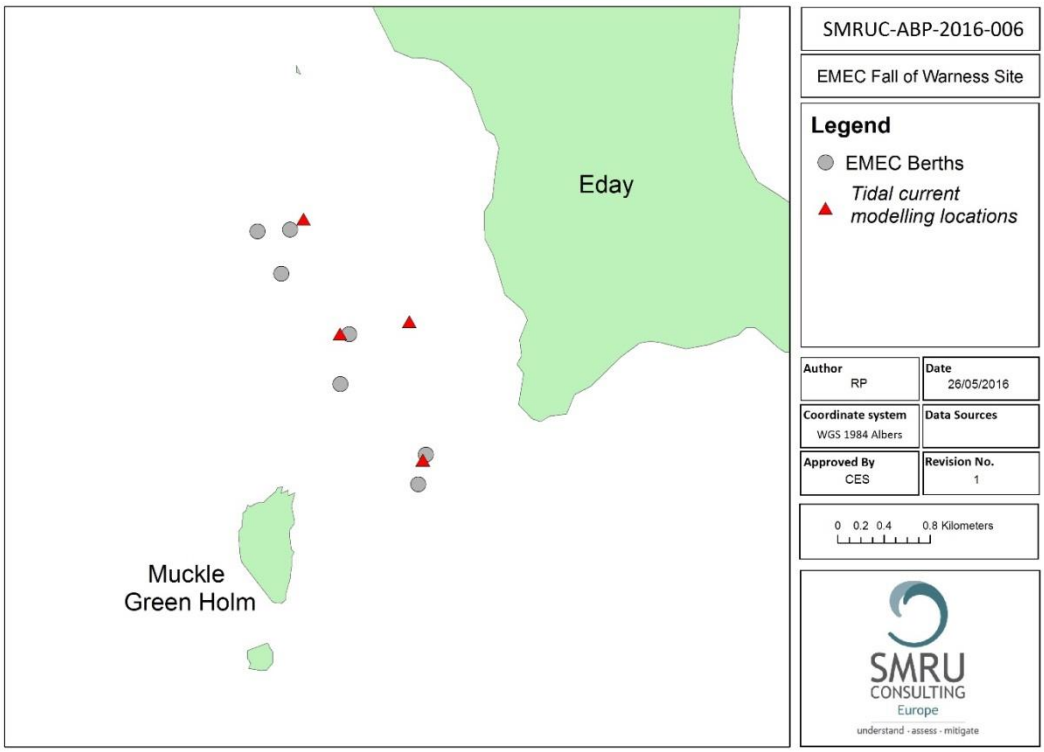

Note: Circles are the turbine positions and triangles are the locations for which detailed tidal information was provided.

Figure 41 Location of the EMEC Fall of Warness tidal test site

Projected current speed and current direction data were obtained from the ABPmer hydrodynamic model, for a one year period at 15 minute intervals. These data were obtained at four sample locations within areas of the eight berths, also shown on the map. Sample locations were deemed to characterise berths according to the following:

- HY 333 290 Berths 1 and 5;
- HY 530 300 Berths 4, 6 and 7;
- HY 539 291 Berth 8; and
- HY 540 279 Berths 2 and 3.

A proposed ninth berth, whose location is not currently known, was deemed to have collision and mortality rates corresponding to the average of all others.

By the nature of EMEC's business, the exact type and dimensions of any machine to be installed for testing are not known, and therefore a collision assessment for the maximum scenario must proceed on some assumptions as to the dimensions, depth, and speed of the turbines. The following has been assumed:

- The turbines are 25 m diameter;
- Specification is as for the Andritz Hammerfest turbines to be installed by MeyGen;
- The blade chord width is scaled up by 25/18 to 2.165 m since the envelope may have 25 m not 18 m diameter turbines;
- Minimum depth is 2.5 m; and
- 5% proportion of time unavailable due to maintenance.

Harbour seals were assumed to have a body length of 1.41 m and a body width of 0.34 m, and a swim speed relative to the water of 1.8 m/s (Thompson, 2015). The body ratio was set at 0.5, which means that the front and rear taper of a seal's body was assumed the same; earlier results have demonstrated that refining this has negligible effects.

It was assumed that collisions with blade leading edges below 5 m/s closing speed would not be fatal or cause serious injury, and that collisions with other, less sharply rounded parts of the blade would not be fatal or cause serious injury; this last was ensured by setting the critical closing speed for the trailing parts of the blade to 100 m/s.

Telemetry data similar to that informing the MeyGen assessment are more limited for the Fall of Warness. It is sufficient however to indicate that the frequency distribution of transit speeds and directions is comparable with that in the Inner Sound. In the absence of better quantitative data, the assessment has been undertaken twice for each of the locations with a tidal current projection:

- Once using the 'ground' model, i.e. assuming that ground speed frequency distribution, and the proportion of animals swimming upstream and downstream is similar to that at the Inner Sound ; and
- Once using the 'resultant' model, i.e. assuming the ground speed is (downstream) the sum of the seal swim speed relative to the water, and the current speed.

The 'resultant' approach is very likely to overestimate collision rate, given that the high resultant speed for animals swimming downstream will translate to a high animal flux in that direction; while the 'ground' model is likely to underestimate collision rate if ground speeds do not peak at low ground speeds as strongly as they do at the Inner Sound. Therefore, it is thought that the two assessments should satisfactorily bracket the 'real' figure.

For the 'ground' model the CRM Plus Plus refinement was applied, calculating collision rates at each ground speed from 0 to 4.0 m/s, then multiplying by the frequency at each ground speed to generate a total collision rate. The ratio of around 60% transits downstream and 40% upstream, as found at Inner Sound, was applied to the respective collision and mortality rates for downstream and upstream movement.

Mean speeds of 0.325 m/s (upstream) and 0.778 m/s (downstream) as observed by telemetry at the Inner Sound were also used as the basis for parallel calculations using the Basic, Extended, and CRM Plus CRM models. Generally the results reduce in that order, with the CRM Plus Plus results being 65-70% of those from the Basic model.

For the 'resultant' model, the swim speed relative to water of 1.8 m/s was adopted, combined with the current speed determined by the current projections at that location. The calculations using the CRM Plus model are the most refined, but again they are paralleled by calculations using the Basic and Extended model, with results showing a reduction from Basic, through Extended, to CRM Plus (there are no results for the CRM Plus Plus model for the 'resultant' model, as ground speed varies across the ground speed frequency distribution.)

All model calculations were initially based on a seal density of 1 seal/km². As noted previously various sources of data on seal density are available, notably that in SMRU seal usage maps (Jones *et al.,* 2015), and that obtained from the EMEC wildlife survey and reported in the Environmental Appraisal collision risk assessment (EMEC, 2014). However, for the purposes of these calculations, collision and mortality estimates have been scaled to the density data sourced from the 5 km by 5 km seal usage maps (Jones *et al.,* 2015).

The overview table (Table 21) shows the collision rate and mortality rates including 95% confidence intervals. It is important to note that 100% of the uncertainty in the confidence intervals is attributed to uncertainty in the density estimates; uncertainty in all other parameters has not been included. The rates are shown both for the maximum scenario of all 18 rotors. It is stressed that all these figures maintain the assumption of no avoidance, i.e. these are only potential collisions, or potential mortality, if seals did not avoid, navigate through, or escape from the risks imposed by turbines.

Table 21 Collision and mortality rates (per year) across a range of different density estimates for the EMEC maximum scenario (before any correction for avoidance is added)

Model	Seal Density Data Source	Seal Density (Seals/km²)	All 18 Rotors	
			Collisions Per Year	Mortalities Per Year
(a) Ground speed model	Used to scale from	1	1627	1149
	5 x 5 km grid scale usage maps (Jones *et al*., 2015)	0.60 (0.12-1.00)	976 (201-1627)	689 (142-1149)
(b) Resultant speed model	Used to scale from	1	2733	1778
	5 x 5 km grid scale usage maps (Jones *et al*., 2015)	0.60 (0.12-1.00)	1960 (337-2733)	1067 (219-1778)

(a) Details results using the ground speed model,
(b) Details results using the resultant speed model.
( ) 95% confidence intervals are included in brackets
Note The confidence intervals around the collision and mortality estimates are derived only from uncertainty in the density estimates

9 Population Consequences of Predicted Mortality Rates

9.1 Introduction

In order to provide context for the collision risk modelling exercise, a basic assessment of the potential population consequences of a range of mortality rates were carried out.

Differences in predicted trajectories between a simulated population with no collision related mortality and populations experiencing a range of annual collision related mortality were explored using a publicly available stochastic population modelling tool (a version of the Interim Population consequences of Disturbance framework modified to model the population consequences of collisions). The Interim Population Consequences of Disturbance (PCoD) framework was developed primarily to investigate the sub-lethal and cumulative effects of exposure to noise, primarily from piling activity as a result of offshore wind farm construction and provide predictions of how such exposures would be manifested at a population level over the short, medium and long term. The model framework also has the facility to model the additional effects of animals being removed from the population as a result of collision, which is actually a simpler proposition than trying to model the sub lethal effects of disturbance.

The interim PCoD approach can accept, as an input, the predicted number of collision related mortalities from a given project (or range of projects). In the current implementation, it is assumed that adult and juvenile animals are equally likely to be involved in collisions. This assumption can easily be modified if evidence emerges that certain age classes are more vulnerable than others.

One of the potential limitations of the interim PCoD framework is that it does not include any form of density dependence. That is, the process whereby demographic rates change in response to changes in population density, resulting in an increase in the population growth rate when density decreases and a decrease in that growth rate when density increases. With the exception of grey seals, there is no published evidence for density dependence in UK populations of marine mammals. For most species, there are insufficient data. The general effect of not including density dependence will be to overestimate the long term impact, since the model does not include any increase in fecundity or decrease in survival that may result from decreased density of an impacted population which has been reduced in size. However, because the Orkney and North coast harbour seal management unit

population has been declining recently, with no sign of recovery, it is unlikely that density dependence is operating within this population.

One of the benefits of the PCoD model framework is that it makes it possible to incorporate many of the uncertainties in the input parameters into the predictions of effect. This means that the interim PCoD framework provides a range of plausible values (i.e. with confidence intervals) as opposed to a single best estimate. In the context of collision assessment, this could include uncertainty about the size of the population in a particular management unit, uncertainty about the size of any vulnerable sub-population, uncertainty in the number of animals that will collide with a particular development, uncertainty about the probability of death following a collision, and in the effects of demographic stochasticity and environmental variation.

This approach of using the comparison between impacted and un-impacted populations (so called counterfactual analysis) does not rely on acceptance that the population trajectories are close to reality, but simply that given the same set of assumptions underlying the baseline population dynamics applied across both populations, any difference in predicted population trajectory can be attributed to the impact.

9.2 Method and Results

A range of mortality rates were defined covering the range of results in the collision risk assessments detailed in the previous section, although extending the lower end of the range to a minimum of 1 collision. (ranging from 1 to 2123). Table 22 provides the population parameters used in the modelling which are based on the values provided in Harwood and King (2013). The total count of 1938 (SCOS, 2015) was scaled to the population estimate based on a correction factor of 1.388 to account for animals at sea during the time of the count, giving a population estimate of 2691 harbour seals. Each population was simulated 1000 times. Simulations were set to run for 25 years but because even baseline scenarios were predicted to decline over time, most simulations crashed before reaching 25 years. Many 'impact' scenarios crashed much earlier than this.

The interim PCoD framework provides as outputs, the probability of a 1%, 2% and 5% decline in each of the un-impacted and impacted populations after each year of the simulation, and the additional risk therefore presented by that level of impact presented as the difference between the two.

Table 22 Parameters used in PCoD model for the Orkney and North Coast harbour seal population

Parameter	Value
Population count	1938
Scaled population estimate	2691
Age at first breeding	4
Age at independence	1
Pup survival	0.6
Juvenile survival	0.56
Adult survival	0.86
Fecundity	0.88

Table 23 presents the probability of a 5% decline after 5 years of simulation over a range of mortality rates. This particular combination was chosen for presentation because the probability of smaller declines and over longer periods were close to 1 for most of the simulations. Mortality of between 1 and 15 harbour seals per year as a result of anthropogenic activities increases the risk of a 5% decline over five years, compared with a scenario with no anthropogenic mortality by 1-3%. As the number of harbour seals suffering mortality per year increases, so does the risk of a 5% decline over five years, up to 9% if 150 seals were killed per year. Although greater numbers of seals killed have been modelled, the results in Table 23 show that the percentage difference declines. This is because the probability of a 5% decline over five years is already very high in the un-impacted scenario; additional mortality leads to a probability of 1 that there will be a 5% decline, at values of seals mortality above 60 per year. The fluctuation in un-impacted values is as a result of the stochasticity in the model and uncertainty around parameter values.

Table 23 **Interim PCoD framework results: the probability of a 5% population decline after 5 years from simulations over a range of collision related mortality rates**

# Annual Collision Related Mortalities	Probability of a 5% Decline After 5 Years		
	Impacted	Un-impacted	Increase
1	0.94	0.93	1%
5	0.961	0.948	1%
12	0.95	0.921	3%
15	0.973	0.949	2%
20	0.977	0.922	5%
40	0.99	0.92	7%
60	0.997	0.915	8%
90	1	0.941	6%
150	1	0.911	9%
180	1	0.934	7%
220	1	0.927	7%
300	1	0.929	7%
426	1	0.935	6%
617	NA	NA	NA
850	NA	NA	NA
1083	NA	NA	NA
1235	NA	NA	NA
2123	NA	NA	NA

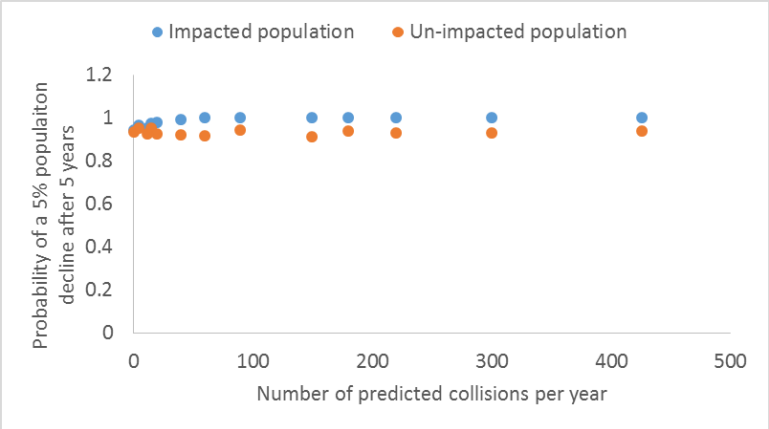

Note: The probability of a 5% population decline after 5 years from simulations over a range of collision related mortality rates, paired simulations from impacted and un-impacted populations are shown.

Figure 42 **Interim PCoD framework results**

9.3 Summary

This analysis demonstrates the current unfavourable status of the Orkney and North coast harbour seal management unit. Even the un-impacted population is predicted to decline significantly in future. This analysis has also shown that the addition of collision-related mortalities increases the probability of decline and increases the magnitude of decline. Mortality rates of 15 animals per year present an additional risk of a 5% decline over 5 years of 1-3%. The risk of a 5% decline increases by 9% at an annual mortality rate of 150. This does not seem very high given the current status of the population. However, this is constrained by the fact that the probability of a 5% decline is already high and the probability of a 5% decline cannot increase beyond one. Further adaptation of the PCoD code would be required to explore this further.

It is important to note that these simulations can only be carried out based on current and recent population trends and therefore any future changes in vital rates (e.g. recovery or stabilisation of the population from current declines) cannot be incorporated. However, this analysis does provide a way of presenting a probabilistic assessment of the potential population consequences of a range of collision rates. This approach could be used as the basis for comparison with a PBR approach for decision making and additionally the outputs from the interim PCoD framework could be adapted in future to produce metrics specifically designed for this application and for this population. It may also be worthwhile repeating this exercise for a range of estimates which incorporate estimates of avoidance.

10 Summary and Conclusions

This study has identified, tested and implemented a range of refinements to an existing Collision Risk Model (Band, 2015). This section of the report provides a brief summary of the main refinements and considers the areas of remaining uncertainty in predictions and the application of this revised CRM to other sites and projects.

The refinements considered covered a range of areas, falling into four main categories:

- More detailed and device specific information from turbine manufacturers (shape of rotors and relationships between current and rotor speed);
- More detailed understanding of tidal currents;
- A better understanding of seal behaviour in tidal areas in relation to tide; and
- A developing understanding of the consequences of collisions between seals and rotors and the likelihood of mortality.

As detailed in Section 7.3, the parameters most influencing the magnitude of predicted collision rates are (in descending order):

- Seal density;
- incorporation of a minimum speed for mortality;
- incorporation of telemetry derived estimates of transit speed;
- incorporation of telemetry derived depth distribution; and
- incorporation of a blade thickness parameter.

All other modifications had relatively minor effects on the resulting collision risk estimates. However it is important to note that the majority of the comparisons have been undertaken with a common set of parameters and therefore results could differ if turbines of markedly different parameters are modelled.

The refined model assumed that leading blade collisions would only be fatal at closing speeds above 5.2 m/s. This is based on trials carried out by Thompson *et al.* (2015a) and there are a number of uncertainties associated with this. For example, the mortality threshold taken from this investigation was based on simulated collisions with an impact angle more acute than that of the interactions simulated in the model. While correction factors were employed to estimate the true collision speeds seen in the trials, there remains some uncertainty about perpendicular collisions. Further collision trials are planned for 2016 to reduce uncertainties and

resulting thresholds will be factored into future models to gain a more confident estimate of mortality rates at these sites.

Seal behaviour was remarkably similar between the two sites considered in these investigations. At both sites, transit speeds were low and there was an approximate 40/60 split between upstream and downstream transits. Analyses from tagged harbour seals at Strangford Lough demonstrate similar patterns in terms of slow transit rates and transits oriented largely in line with the current in the tidal stream associated with Strangford Narrows (Wood *et al*., 2016). SMRU are currently investigating data from a number of other sites with a view to assessing the generalities of these findings and how they should be applied in future assessments.

This assessment has not included the application of avoidance/evasion rates, primarily because there is currently not enough empirical evidence on which to base the quantification of these. However, a range of potential collision and mortality rates can be expressed assuming a range of potential avoidance rates. An illustration of this is provided in Table 24. Purely for purposes of comparison the density estimates presented are equivalent to those presented in the original assessments for these sites (SRSL, 2012; EMEC, 2014).

Table 24 Mortality rates incorporating a range of avoidance rates

Estimate		0% Avoidance	50% Avoidance	95% Avoidance
MeyGen Phase 1: 4 turbines	(0.202 seals/km²)	37	18.5	1.85
EMEC max scenario: 18 rotors	(0.01583 seals/km²)	31	15.5	1.55

The refined model presented here uses site specific and turbine specific data. It is therefore not likely to be generally applicable and will need to be revised for use in other locations and with different turbines.

11 References

ABPmer 2012. Pentland Firth and Orkney Waters Hydrodynamic Modelling: Model Calibration. Report R.1935 for The Crown Estate. March 2012.

Band, B. 2000. Windfarms and birds: calculating a theoretical collision risk assuming no avoiding action. Scottish Natural Heritage Guidance Note.

Band, B. 2012a. Using a collision risk model to assess bird collision risks for offshore windfarms. The Crown Estate Strategic Ornithological Support Services (SOSS) report SOSS-02. SOSS Website. www.bto.org/science/wetland-and-marine/soss/projects

Band, B. 2012b. MeyGen tidal-stream turbine array comments on marine mammal collision risk assessment. Unpubl Rep to Scottish Nat Heritage, 17/09/2012, Commercial in confidence.

Band, B. 2014. Detailed Collision Risk Assessment: Marine mammals, Basking shark, and Diving Birds. In Fall of Warness test site Environmental Appraisal: Annex 7. EMEC.

Bauduin, S., Martin, J., Edwards, H.H., Gimenez, O., Koslovsky, S.M. and Fagan, D.E. 2013. An index of risk of co-occurrence between marine mammals and watercraft: Example of the Florida manatee. Biological Conservation, **159**, 127–136.

Batty, R., Benjamins, S. and Wilson, B. 2012. MeyGen tidal-stream turbine array environmental impact assessment: modelling encounter rate between turbines and animals. SAMS Research Services Limited, Commercial in confidence.

Batty, R.S. and Wilson, B. 2010. Predicting the abilities of marine vertebrates to evade collision with tidal stream turbines. Third International Conference on Ocean Energy, 6 October, Bilbao, 3–6.

Benjamins, S., Dale, A., Hastie, G., Waggitt, J.J., Lea, M-A, Scott, B.E. and Wilson, B. 2015. Confusion reigns? A review of marine megafauna interactions with tidal-stream environments. Oceanography and Marine Biology An Annual Review, **53**, 1-54.

Broadhurst, M., Barr, S. and Orme, D. 2014. *In situ* ecological interactions with a deployed tidal energy device; an observational pilot study. Ocean and Coastal Management, **99**, 31-38.

Carlson, T., Grear, M., Copping, A., Halvorsen, M., Jepsen, R. and Metzinger, K. 2014. Assessment of Strike of Adult Killer Whales by an OpenHydro Tidal Turbine Blade. Prepared for the US Department of Energy by Pacific Northwest National Laboratories.

Cook, A.S.C.P., Humphreys, L., Masden, E.M. and Burton, N.H.K. 2014. The avoidance rates of collision between birds and offshore turbines. Scottish Marine and Freshwater Science Volume 5 Number 16. Published by Marine Scotland Science.

Davies, I. and Thompson, F. 2011. Assessment of collision risk for seals and tidal stream turbines. International Council for the Exploration of the Seas (ICES), Report no C 2011/S11.

EMEC 2014. Fall of Warness Environmental Impact Appraisal. REP443-04-01-20141120.

Feldkamp, S.D. 1987. Swimming in the California sea lion: morphometrics, drag and energetics. Journal of Experimental Biology, **131**, 117–135.

Gerritsen, J. and Strickler, J.R. 1977. Encounter Probabilities and Community Structure in Zooplankton: a Mathematical Model. Journal of the Fisheries Research Board of Canada, **34**, 73–82.

Grant, M., Trinder, M. and Harding, N. 2014. A diving bird collision risk assessment framework for tidal turbines. Scottish Natural Heritage Commissioned Report No 773.

Hanke, W., Wieskotten, S., Marshall, C. and Dehnhardt, G. 2013. Hydrodynamic perception in true seals (*Phocidae*) and eared seals (*Otariidae*). Journal of Comparative Physiology A, **199**, 421–440.

Hastie, G.D., Benjamins, S., Moss, S., Russell, D.J.F., Wilson, B. and Thompson, D. In review. Dynamic habitat corridors for marine predators; intensive use of a coastal channel by harbour seals is modulated by tidal currents. Behavioural Ecology and Sociobiology.

Hindell, M.A. and Lea, M.A. 1998. Heart rate, swimming speed, and estimated oxygen consumption of a free-ranging southern elephant seal. Physiological Zoology, **71**, 74–84.

Jones, E.L., McConnell, B.J., Smout, S., Hammond, P.S., Duck, C.D., Morris, C.D., Thompson, D., Russell, D.J.F., Vincent, C., Cronin, M., Sharples, R.J. and Matthiopoulos, J. 2015. Patterns of space use in sympatric marine colonial predators reveal scales of spatial partitioning. Marine Ecology Progress Series, **534**, 235–249.

King, S.L., Schick, R.S., Donovan, C., Booth, C.G., Burgman, M., Thomas, L. and Harwood, J. 2015. An interim framework for assessing the population consequences of disturbance. Methods in Ecology and Evolution, **6**, 1150–1158. doi:10.1111/2041-210X.12411.

Lonergan, M. and Thompson, D. 2015. Collision risk and impact study: Examination of models for estimating the risk of collisions between seals and tidal turbines. Sea Mammal Research Unit, University of St Andrews, Report to Scottish Government no MR 722, St Andrews.

MeyGen 2012. Marine Mammal Encounter Modelling - Turbine data. Commercial in confidence.

Nicholson, A.J., Bailey, V.A. 1935. The Balance of Animal Populations. Proceedings of the Zoological Society of London, **105**, 551–598.

Parrott, L., Chion, C., Martins, C.C.A., Lamontagne, P., Turgeon, S., Landry, J.A., Zhens, B., Marceau, D., Michaud, R., Cantin, G., Menard, N. and Dionne, S. 2010. 3MT Sim: An agent based model of marine mammals and maritime traffic to assist management of human activities in the Saint Lawrence Estuary, Canada. Report submitted to the Scientific Committee of the International Whaling Commission 62nd Annual Meeting, Agadir, Morocco, 30 May – 11 June.

Russell, D.J.F., Brasseur, S.M.J.M., Thompson, D., Hastie, G.D., Janik, V.M., Aarts, G., McClintock, B.T., Matthiopoulos, J., Moss, S.E.W., McConnell, B. 2014. Marine mammals trace anthropogenic structures at sea. Current Biology, **24**, R638–R639.

Savidge, G., Ainsworth, D., Bearhop, S., Christen, N., Elsaesser, B., Fortune, F., Inger, R., Kennedy, R., McRobert, A., Plummer, K.E., Pritchard, D.W., Sparling, C.E. and Whittaker, T.J.T. 2014. Strangford Lough and the SeaGen Tidal Turbine. In: Shields MA, Payne AIL (eds) Marine Renewable Energy Technology and Environmental Interactions SE - 12. Springer Netherlands, 153–172.

SCOS 2015. Scientific Advice on Matters Related to the Management of Seal Populations: 2015. Sea Mammal Research Unit. http://www.smru.st-andrews.ac.uk/documents/scos/SCOS_2015.pdf

Scottish Natural Heritage 2016. Assessing collision risk between underwater turbines and marine wildlife. SNH Guidance Note. http://www.snh.gov.uk/planning-and-development/renewable-energy/offshore-renewables/marine/

Sparling., C., Gillespie, D., Hastie, G., Gordon, J., Macaulay, J., Malinka, C., Wu, M. and McConnell, B. 2016. Scottish Government Demonstration Strategy: Trialling Methods for Tracking the Fine Scale Underwater Movements of Marine Mammals in Areas of Marine Renewable Energy Development Scottish Marine and Freshwater Science Vol 7 No 14.

SRSL 2012. MeyGen Tidal steam turbine array environmental impact assessment: modelling encounter rate between turbines and marine mammals. Report to MeyGen.

Stantec 2015. Quantitative Assessment of Increased Potential for Marine Mammal-Vessel Interactions from the Trans Mountain Expansion Project.

Thompson, D. 2015. Parameters for collision risk models. Report by Sea Mammal Research Unit, Univ St Andrews, Scottish Natural Heritage.

Thompson, D., Brownlow, A., Onoufriou, J., Moss, S. 2015a. Collision Risk and Impact Study: Field tests of turbine blade-seal carcass collisions. Sea Mammal Research Unit Report to Scottish Government. St Andrews.

Thompson, D., Onoufriou, J., Brownlow, A., Morris, C. 2015b. Data based estimates of collision risk: an example based on harbour seal tracking data around a proposed tidal turbine array in the Pentland Firth. Sea Mammal Research Unit Report to Scottish Government. St Andrews.

Turnpenny, A.W.H., Clough, S., Hanson, K.P., Ramsay, R. and McEwan, D. 2000. Risk assessment for fish passage through small, low-head turbines. Fawley Aquatic Research Laboratories Ltd, report to the Energy Technology Support Unit (ETSU), Harwell, Didcot, Oxfordshire, OX11-ORA, Contractor's Report No. ETSU H/06/00054/REP.

Wilson, B., Batty, R., Daunt, F., Carter, C. 2007. Collision risks between marine renewable energy devices and mammals, fish and diving birds. Report to the Scottish Executive Scottish Association for Marine Science.

Wood, J., Joy, R. and Sparling, C. 2016. Harbor Seal – Tidal Turbine Collision Risk Models. An Assessment of Sensitivities. Report prepared for The US Department of Energy by SMRU Consulting.

Zamon, J. 2003. Mixed species aggregations feeding upon herring and sandlance schools in a nearshore archipelago depend on flooding tidal currents. Marine Ecology Progress Series, **261**, 243–255.

12 Abbreviations

3-D	Three-dimension(al)
ABPmer	ABP Marine Environmental Research Ltd
AHH	Andritz Hydro Hammerfest turbines
ARL	Atlantis Resources Limited
CI	Collision Integral
CRM	Collision Risk Model
º	Degree(s)
EIA	Environmental Impact Assessment
EMEC	European Marine Energy Centre
ERM	Exposure Risk Model
ETSU	Energy Technology Support Unit
GIS	Geographic Information System
GPS	Global Positioning System
GSM	Global System for Mobile
ID	Identity
iPCoD	Interim Population Consequences of Disturbance
Juv	Juvenile
MSI	Marine Scotland interactive
NA	Not Applicable
NACA	National Advisory Committee for Aeronautics
NERC	Natural Environment Research Council
NI	Northern Ireland
PBR	Potential Biological Removal
PCoD	Population Consequences of Disturbance
POL	Proudman Oceanographic Laboratory
POLTIPS	Proudman Oceanographic Laboratory Tidal Prediction Software
rpm	Revolutions per Minute
SAMS	Scottish Association for Marine Science
SCOS	Special Committee on Seals
SMRU	Sea Mammal Research Unit
SNH	Scottish Natural Heritage
SRSL	SAMS Research Services Limited
UK	United Kingdom
USA	United States of America
WA	Washington
WCS	Worst Case Scenario

13 Acknowledgements

This project was funded by the Scottish Government and Scottish Natural Heritage. Valuable input and review was provided by the project steering group which included representatives from Marine Scotland, Marine Scotland Science, MeyGen and Scottish Natural Heritage. We would also like to thank MeyGen for providing information on turbine parameters for use in the modelling.

Appendix 1 Seal Densities, Confidence Intervals and CRM Estimates

Seal Density Estimates From a Range of Sources Including Confidence Intervals as Inputs Into Collision Risk Models (Carol Sparling and Dave Thompson, May 2016)

This briefing note is to inform discussions regarding reporting of collision risk estimates on the Marine Scotland project on collision risk estimation for harbour seals and tidal turbines.

In undertaking this work a review was carried out of the available density estimates and initial exploration revealed that there was a wide variation in the range of available estimates. This note compares these estimates further and includes estimates of upper and lower confidence limits.

Density estimates were available from the EMEC site from:

- SMRU usage maps at 5 x 5 km grid cell resolution (version uploaded on MSI in 2013); and
- A density estimate derived from the wildlife survey data collected at EMEC and presented in the EMEC environmental appraisal (EMEC, 2014).

Density estimates were available from the MeyGen site from:

- SMRU usage maps at 5 x 5 km grid cell resolution (version uploaded on MSI in 2013);
- a density estimate used in the original ES collision risk predictions based on seal haul out count ‘spread’ out uniformly over an area constrained by typical seal foraging distances (SRSL, 2012); and
- Two estimates at different scales achieved by scaling up the seal usage that is represented by the telemetry information from the seals tagged in Gills Bay in 2011/2012 and scaled up to the total local population.

As part of this exploration it has become apparent that the 5 x 5 km maps available on the Marine Scotland Interactive website are considerably out of date and contain much less data than available in the set of 5 x 5 km maps from a recent update (Jones *et al*., 2015) therefore these were also compared with those presented in the main report.

These density estimates for each of the tidal energy projects are given in Table 1.1. Associated collision and mortality rate estimates are given in Table 1.2 and Table 1.3 respectively.

A number of features are apparent when viewing these summaries:

1) The different density estimation methods produce widely differing population densities for the same sites.

2) There are considerable differences between the site based survey estimate for EMEC and the usage map estimates (a difference of approximately 44 times). These calculations have been checked and verified and we consider that there are no errors in calculation. Although there are a number of reasons why the survey data may underestimate density (e.g. non-correction for detection bias with distance, incomplete correction for availability bias and assumption that all seals available at the surface were detected) it is difficult to imagine that these corrections would account for the observed magnitude of difference unless the probability of detection was extremely low. Further work using mark-recapture techniques would be necessary to investigate this.

3) There are considerable differences between the usage map estimates and the 'telemetry derived estimates' for the MeyGen site (a difference of approximately 13 times if using the 'large' area, a difference of approximately 25 times if using the small area). However, as noted in the CRM report, the density of locations in the raw telemetry data varies widely over relatively short distances. E.g. moving the study site by 1 km to the south led to a factor of 12 increase in the density estimate. Estimating a usage surface representative of the population distribution entails a component of smoothing of the raw telemetry data. In areas with wide local variations in telemetry based densities it is likely that smoothing would increase low density site estimates and decrease high density site estimates.

4) The wide confidence intervals on the density estimates result in very wide confidence intervals around the point estimates of collision and mortality rates. This indicates the level of uncertainty around the point estimates and cautions against over-reliance on the point estimates.

5) The highest point estimates for collision rates are implausible given that they are considerably higher than the total harbour seal population estimate of approximately 2700 for the Orkney and North Coast management unit (SCOS, 2015). This indicates a limitation of the current mathematical approach to collision risk estimation that treats every encounter as an independent event and 'samples with replacement' so that the population of vulnerable animals does not reduce through time. The methodology does not include any response by the seals to the presence of turbines, so does not explicitly model avoidance or evasion nor any form of learning from past encounter experiences. A more 'simulation-based' approach would be required to incorporate removals and assumptions of learning and animal turnover to provide plausible bounds to these estimates.

As a result of these features, the resulting variation in collision and mortality estimates is very large – both within and between different sources of density. Across all these estimates of density the point estimates of total annual mortalities range from 9 to 216 seals per year for the MeyGen site and between 18 and 824 per year for the EMEC site. Including the confidence intervals for all estimates expands these ranges from 0 to 522 for the MeyGen site and 0 to 1824 for the EMEC site.

Table 1.1 Mean densities and upper and lower confidence intervals for each density estimate from both EMEC and MeyGen sites

Source of Density Estimate	Density (Seals/km² (95% CI))	
	Inner Sound (MeyGen)	**Fall of Warness (EMEC)**
5 km x 5 km Usage map (Previous MSi version)	1.26[1] (0.00-3.22)	0.71[2] (0.00-1.58)
5 km x 5 km Usage map (Jones *et al*., 2015 version)	0.40[1] (0.17-0.64)	0.60[2] (0.12-1.00)
Inner Sound telemetry data (Transits through turbine array scaled up to population using local haul out count, large area: whole array +500 m buffer)	0.10 (0.008-0.251)	NA
Inner Sound telemetry data (Transits through turbine array scaled up to population using local haul out count, small area: phase 1 +250 m buffer)	0.05 (0.004-0.138)	NA
Site specific estimate used in previous assessments	0.202[3] (no CI given)	0.016[4] (no CI given)

Note: Also displayed are the densities calculated using the sample of telemetry data collected in the Inner Sound in 2012

[1] At the MeyGen site the four turbines are all within a single grid cell therefore the density presented is that of the grid cell containing all the turbine locations.

[2] At EMEC, a weighted average was calculated across all cells containing turbines by weighting the cell by the number of turbines present within it.

[3] From the original ERM carried out for MeyGen ES – based on haul out count and estimated foraging area (SRSL, 2012)

[4] EMEC Wildlife Observation Survey Data – presented in EMEC (2014).

Table 1.2 Collision rate estimates (per year) based on the different density estimates and associated confidence intervals for each site

Source of Density Estimate	# of Collisions Predicted Per Year (95% CI)	
	Inner Sound (MeyGen) – 4 Turbines.	**Fall of Warness (EMEC) – WCS – 18 Turbines**
5 km x 5 km Usage map (Previous MSi version)	294 (0-751)	1167 (0-2582)
5 km x 5 km Usage map (Jones *et al*., 2015 version)	93 (40-149)	976 (201-1634)
Inner Sound telemetry data (Transits through turbine array scaled up to population using local haul out count, large area: whole array +500 m buffer)	23 (2-59)	NA
Inner Sound telemetry data (Transits through turbine array scaled up to population using local haul out count, small area: phase 1 +250 m buffer)	12 (1-32)	NA
Site specific estimate used in previous assessment	47	26

Note: The estimates provided are those from the CRM Plus Plus model as presented in the main draft report (i.e. using the distribution of ground speeds as determined by telemetry data in the Inner Sound)

Table 1.3 Mortality rate estimates based on the different density estimates and upper and lower confidence intervals for each usage map grid scale and each site

Source of Density Estimate	# of Mortalities Predicted Per Year (95% CI)	
	Inner Sound (MeyGen) – 4 Turbines.	**Fall of Warness (EMEC) – WCS – 18 Turbines**
5 km x 5 km Usage map (Previous MSi version)	216 (0-522)	824 (0-1824)
5 km x 5 km Usage map (Jones *et al*., 2015 version)	69 (29-110)	689 (142-1154)
Inner Sound telemetry data (transits through turbine array scaled up to population using local haul out count, large area: whole array +500 m buffer)	17 (1-43)	NA
Inner Sound telemetry data (transits through turbine array scaled up to population using local haul out count, small area: phase 1 +250 m buffer)	9 (1-24)	NA
Site specific estimate used in previous assessment	35	18

References

EMEC 2014. Fall of Warness Environmental Impact Appraisal. REP443-04-01-20141120.

Jones, E.L., McConnell, B.J., Smout, S., Hammond, P.S., Duck, C.D., Morris, C.D., Thompson, D., Russell, D.J.F., Vincent, C., Cronin, M., Sharples, R.J. and Matthiopoulos, J. 2015. Patterns of space use in sympatric marine colonial predators reveal scales of spatial partitioning. Marine Ecology Progress Series, **534**, 235–249.

SCOS 2015. Scientific Advice on Matters Related to the Management of Seal Populations: 2015. Sea Mammal Research Unit. http://www.smru.st-andrews.ac.uk/documents/scos/SCOS_2015.pdf

SRSL 2012. MeyGen Tidal steam turbine array environmental impact assessment: modelling encounter rate between turbines and marine mammals. Report to MeyGen.

Appendix 2 Detailed CRM Results for MeyGen

MeyGen harbour seal collision risk assessment (before avoidance) using the 'ground speed' model which used the telemetry derived ground speed frequency distribution, and the proportion of animals swimming upstream.

Table 2.1 Collision and mortality rates per annum per turbine at seal density 1/km² (MeyGen)

Turbine	CRM Plus Plus Model		Basic Model		Extended Model		CRM Plus Model	
	Per Annum							
	Collisions	Mortality	Collisions	Mortality	Collisions	Mortality	Collisions	Mortality
ARL1	59.4	44.1	99.6	61.3	92.7	62.7	74.3	58.1
AHH1	57.7	42.2	94.7	58.8	88.7	59.3	73.9	56.0
AHH2	58.6	43.5	97.3	60.4	90.2	61.5	75.1	57.8
AHH3	57.7	42.2	94.7	58.8	88.7	59.3	73.9	56.0
Total 4-turbine scenario	**233**	**172**	**386**	**239**	**360**	**243**	**297**	**228**

Based on density of 1 harbour seal / km² To be scaled in proportion to actual density

ARL 1 Atlantis

AHH1, 2 and 3 Hammerfest

Seal Density km^{-2}	4-Turbine Scenario		
	Collisions	Mortality	
1	233	172	Density as used for above calculations

Appendix 3 Detailed CRM Results for EMEC Fall of Warness

Fall of Warness - EMEC tidal site - maximum scenario using both the ground speed model, (assuming behaviour the same as at the Inner Sound using the ground speed frequency distribution, and the proportion of animals swimming upstream and downstream from the Inner Sound telemetry data) and the resultant model.

Table 3.1 Collision and mortality rates per annum per turbine at seal density 1/km² (EMEC)

Using Ground Speed Model

	CRM Plus Plus		Basic		Extended		CRM Plus	
	Collisions	**Mortality**	**Collisions**	**Mortality**	**Collisions**	**Mortality**	**Collisions**	**Mortality**
HY 333 290	92.8	66.1	145.7	90.4	146.3	88.8	124.2	91.7
HY 530 300	92.8	65.7	145.1	85.8	145.7	84.3	124.7	91.2
HY 539 291	63.7	38.8	109.4	13.6	109.9	13.6	87.2	53.2
HY 540 279	99.4	72.8	155.3	106.2	155.9	104.5	130.9	100.3
Average	**87.2**	**60.9**						

Using Resultant Model

	Basic		Extended		CRM plus	
	Collisions	**Mortality**	**Collisions**	**Mortality**	**Collisions**	**Mortality**
HY 333 290	191.3	112.7	193.0	110.9	152.8	100.1
HY 530 300	191.1	112.5	192.9	110.7	151.8	98.5
HY 539 291	153.6	29.7	155.8	29.5	119.4	67.6
HY 540 279	178.6	113.7	180.4	112.2	169.0	115.2
Average					**148.3**	**95.4**

18 Rotors Distributed Two to Each of Nine Berths

		Berth	Rotors	Weighting
HY 333 290	characterises	Berths 1,5	4	0.222

HY 530 300	Berths 4,6,7	6	0.333
HY 539 291	Berth 8	2	0.111
HY 540 279	Berths 2,3	4	0.222
Average of all four	**Berth 9**	**2**	**0.111**
Total		**18**	**1**

Collision and Mortality Rate Per Turbine:				**Collision and Mortality Rate**	
Seal Density km^{-2}	**Using Ground Speed Model**			**For All 18 Turbines:**	
	CRM Plus Plus			**CRM Plus Plus**	
	Collisions	**Mortality**		**Collisions**	**Mortality**
1	90.4	63.8	Used for above calculations	1627	1149
Seal Density km^{-2}	**Using Resultant Speed Model**			**For all 18 Turbines**	
	CRM Plus			**CRM Plus**	
	Collisions	**Mortality**		**Collisions**	**Mortality**
1	151.9	98.8	Used for above calculations	2733	1778